NEUTRON IRRADIATION OF SYNTHETIC MORDENITE

by

MUHAMMAD SALIM KHALID

A thesis submitted for the
Degree of Doctor of Philosophy of
London University

Chemistry Department,
Royal College of Science,
Imperial College of Science and Technology,
London S.W.7.

September 1966.

ABSTRACT

Na-mordenite, also known as "Zeolon" is a synthetic zeolite. It possesses stable, crystalline and open lattice, and can therefore function as an excellent gas sorbent and cation exchanger. Na-mordenite was chosen for the neutron irradiation studies to compare its properties with those already found in a previous study, Linde Sieve 13X. Na-mordenite is a more compact structure and has a higher silica to alumina contents than NaX, and these properties have been shown to be important in determining its resistance to radiation damage.

A volumetric apparatus was constructed to study the sorption of argon and krypton by Na-mordenite, over a wide range of temperatures. The krypton isotherms measured at low temperature were analyzed by applying them to various limiting isotherm models from which the corresponding entropy functions were obtained. The model based on localized sorption was found to provide the best fit to the experimental data.

The neutron dose of 5.0×10^{17} n/cm^2 resulted in no observable change in the sorbent properties of Na-mordenite and the zeolite still retained excellent sorbent properties even at a dose of 1.6×10^{19} n/cm^2. However, a neutron dose of 2.8×10^{19} n/cm^2 was found to have changed the sorption and cation exchange properties of Na-mordenite. The sample receiving a neutron dose of 5.0×10^{19} n/cm^2 was found to sorb no argon at $90K^{\circ}$ and when tested for its crystallinity by x-ray analysis was found to be completely amorphous.

Therefore, it can be concluded from the gas sorption

and cation exchange results that Na-mordenite can withstand very high neutron dose. The x-ray analysis of the samples receiving a neutron dose of 2.8×10^{19} n/cm^2, and 3.3×10^{19} n/cm^2, suggested that the lattice of Na-mordenite had contracted, and this was confirmed from the observed changes in the sorption properties of Na-mordenite.

ACKNOWLEDGEMENTS

I wish to express my sincere thanks to Dr. L.V.C. Rees for his supervision and encouragement during the course of this work.

I should also like to thank the technical staff of the Chemistry Department of Imperial College for their assistance, and my fellow students for the many interesting discussions and practical suggestions.

Finally I wish to express my gratitude to the Pakistan Atomic Energy Commission for the award of Colombo Plan Scholarship.

CONTENTS

CHAPTER 1

1.1. General Introduction

1.2. Zeolites

1.3. Gas Adsorption

1.4. Neutron Irradiation

1.1. General Introduction:-

When a crystal is treated with energetic radiations, defects and imperfections are created. The spatial arrangement of defects which remains after the irradiation has ceased is generally described as "radiation damage".

In many respects this term is misleading since the physical properties of solids exposed to energetic radiations are not always adversly affected, e.g. hardness in metals is definitely enhanced, consequently there has been a tendency recently to use the term "radiation effect" to describe the radiation induced changes.

This work presents the effects of neutron irradiation of an alumino silicate material. The method employed was to study the change in its adsorption properties. Sorption of krypton over a wide range of temperature and surface coverage has been studied.

The framework of certain zeolites is far more rigid, stable and well defined than the polymeric structures of organic ion exchange materials such as sulphonated polystyrenes and phenolic resins. Although both zeolites and resins are well known for their efficiency as ion exchangers, it appears strange that comparatively little work has been done with inorganic exchange materials, whereas the effect of irradiation of resins has been widely studied.

Rees and Williams (1) have studied the effect of fast neutron irradiation of Linde molecular sieve 13-X, using sorption of argon at 90K^{o} as a measure of the damage. They established that the damage was first

observed at an integrated fast neutron dose of 6.2×10^{17} neutrons cm^{-2} and collapse of lattice occurred when the dose was 7.0×10^{19} neutrons cm^{-2}. These samples were also subjected to an accompanying dose of y - radiation, which amounted to $\backsim 10^{10}$ rads in the first sample and $\backsim 10^{12}$ rads in the second. A neutron dose of 1.9×10^{19} neutrons cm^{-2} accompanied by a y dose of 10^{12} rads, did not change the ion exchange capacity of the zeolite and it still functioned as an excellent gas adsorbent. It can thus be concluded that the zeolite is far more resistant towards the damaging effects of radiation than its organic counterparts, since resins have been found to be destroyed after being subjected to doses of around $\backsim 10^{10}$ rads of y - radiation (63).

The work reported in this thesis is a continuation of the studies carried out by Rees and Williams, however, the effect of irradiation on zeolites has been considered. Interest was directed towards the thermodynamics of sorption of inert gases in order to determine which, if any, of the sorption sites were affected by the radiation.

Choice of Material:- Synthetic mordenite was chosen for its high silica to alumina (10:1) content. This zeolite because of its high Si/Al ratio is very resistant to acid solutions, a property not possessed by NaX. However, silicon has a larger cross-section for fast neutron than aluminium and this material may not be so resistant to neutron irradiation.

The open lattice structure of synthetic mordenite made it possible to study in some detail the thermodynamic of physical adsorption. The channels in synthetic mordenite are smaller than those in NaX (1),

therefore, any changes occurring in the channels due to neutron irradiation should be easier to detect in synthetic mordenite than in NaX.

Synthetic mordenite was therefore chosen as a suitable zeolite for carrying out sorption experiments on over a wide range of θ and temperature, in order to determine the changes in thermodynamic properties with neutron irradiation.

1.2. Zeolites:-

1.2.1. Alumino - Silicate Structure:-

Crystalline alumino - silicates are all built from tetrahedral SiO_4^{4-} and AlO_4^{5-} units. These units can be bonded together through common oxygen atoms and it is possible for one SiO_4^{4-} unit to join directly with from one to four other silica or alumina units yielding various structures. If silica units are linked by tetrahedral co-ordination a three dimensional framework of composition $(SiO2)_n$ results with no residual charge. However, the inclusion of alumina tetrahedra in replacement of silica units leaves the framework with a negative charge which requires cations to be also present in the interstices of the structure to achieve net electro-neutrality. The extent of substitution of AlO_4^{5-} for SiO_4^{4-} is limited by Loewenstein's rule (2) and the maximum alumina content occurs when alternation between alumina and silica units is present. This is because it is not possible for any two AlO_4^{5-} tetrahedra to exist adjacent to each other.

The group of alumino silicates classified as zeolites have very open frameworks, the large channels existing in the lattice being filled with water. Three types of zeolite frameworks exist:-

1) Three dimensional framework zeolites, e.g. Faujasite, NaA, and Mordenite.
2) Lamellar zeolites, e.g. Stilbite and heulandite.
3) Fibrous zeolites, e.g. Thomsonite and natrolite.

The first group is the most important and stable. They can be dehydrated by heating up to temperatures as high as 700°C under vacuum without any appreciable shrinkage of the lattice. Due to the open structure, the cations can be easily and often rapidly exchanged for others by contact

with the appropriate salt solution. When dehydrated the crystals develop great sorptive capacities for various sorbates. However, this sorption is selective as molecules of a greater diameter than the smallest "windows" controlling excess to the channels will be unable to penetrate into the channels. This "molecular sieve" property is very important, leading to the possible separation of molecules of different diameter by choosing a zeolite with the correct pore size. The zeolite water may occupy definite sites in the lattice as with hydrates, forming a series of solid solutions during dehydration, alternatively, it may be completely mobile occupying no definite positions, and thirdly, it may be held interstitially by physical adsorption. It differs from water of crystallization and chemisorbed water. Electrical conductivity is occasionally attributed to zeolite water which infers that it is mobile.

The "mesh" of a zeolite sieve is determined not by the volume of the intercrystalline cavities but by the free dimensions of the apertures which link them together. Whether or not a given molecule may enter the pore structure of a zeolite, is decided by its size and shape relative to the aperture dimensions of the zeolite; chabazite sorbs water freely but iso-butane, a large molecule is not sorbed. The free diameter of the largest aperture in the zeolite acts as a rough guide, Breck and Smith (6) have found that due to bond vibrations, in general molecules of diameter up to 0.5A^{o} greater than the "free diameter" of the aperture can pass through easily. Large molecules enter the crystal with greater and greater difficulty; molecules 1A^{o} wider than the free diameter cannot enter at all. It should be remembered that many molecules possess two different diameters, the diameter of nitrogen measured normal to its longitudinal axis is

3.0A°, while its longitudinal diameter is 4.1A°. For such a molecule, the rate of sorption might be diminished because the molecules might have to re-orientate themselves in a favourable direction for diffusion through the lattice.

The sorptive properties of a zeolite also depend on the type and number of cations present. Linde sieve (NaA), (Breck et al 1956) is capable of sorbing molecules up to 4A° in diameter; molecules up to 5A° in diameter are readily adsorbed when approximately one-third of the Na^+ ions are exchanged for Ca^{2+}. This increase in sorption was due to a difference in cations size, Na^+ and Ca^{2+} have nearly same radii, it was due to the removal of Na^+ ions which were obstructing the entrance to the adsorptive cavities. Replacement of the Na^+ ions by large K^+ effectively reduces the pore size even further.

Molecular sieve properties of zeolites can also be affected by pre-adsorption of polar molecules. Small amounts of water or ammonia present in the pores of NaA drastically reduce oxygen sorption. Barrer and Rees (8) investigated the effect of pre-adsorbed polar molecules on the sorptive properties of mordenite and chabazite. Breck considers that the polar molecules cluster about the cations thus blocking the channels and reducing the pore size.

1.2.2. Na-Mordenite:-

Na-mordenite is a synthetic form of the natural mineral mordenite. It contains only Na^+ ions in contrast to the natural species which contain Na^+, K^+ and Ca^{2+} ions. It is synthesized by the Norton Company Ltd. of America and is commercially known as "Zeolon".

Detailed x-ray analysis has been carried out by Meier (3) on the natural zeolite. The sample was calcium rich and he percolated it with concentrated sodium nitrate

solutions to exchange it to the pure Na^+ form. Meier found the unit cell to be ortho rhombic with

$$a = 18.13\ A^{\circ} \quad b = 20.49\ A^{\circ} \quad c = 7.52\ A^{\circ}$$

The unit cell formula of his sample was:-

$$Na_8\ Al_8\ Si_{40}\ O_{96}\ 24H_2O$$

The alumino-silicate network consists of characteristic chains enclosing elliptical channels of free diameter $5.81A^{\circ}$ (Fig. 1) which give mordenite its molecular sieve properties. These channels parallel to the (001) axis are formed by a ring of twelve tetrahedra comparable to those existing in faujasite. These channels are interconnected by narrower passages parallel to (010) axis (Fig. 2) having a minimum diameter of $2.8A^{\circ}$. Thus the zeolite can act as a molecular sieve with respect to small molecules.

Each (Si, Al) O_4 tetrahedron is part of one or more 5-membered rings in the framework and the numbers of 4-, 5-, 6-, and 8- membered rings of tetrahedra per unit cell are 4, 48, 16, and 16, respectively. The prevailing number of 5-membered ring is an outstanding feature of the mordenite framework. It has been shown that the most stable rings in silicates (i.e. lowest energy) are of 5 or 6 tetrahedra (4). The predominance of 5-membered ring and the high silica alumina ratio account for the extraordinary stability of mordenite.

Stacking Fault:-

Mordenite sorbes Ar, N_2, and O_2 rapidly, while CH_4 and C_2H_6 are only slowly occluded (Barrer 1944). Although the free diameter of the main elliptical channel is $5.81A^{\circ}$, the mordenite does not adsorb molecules whose critical

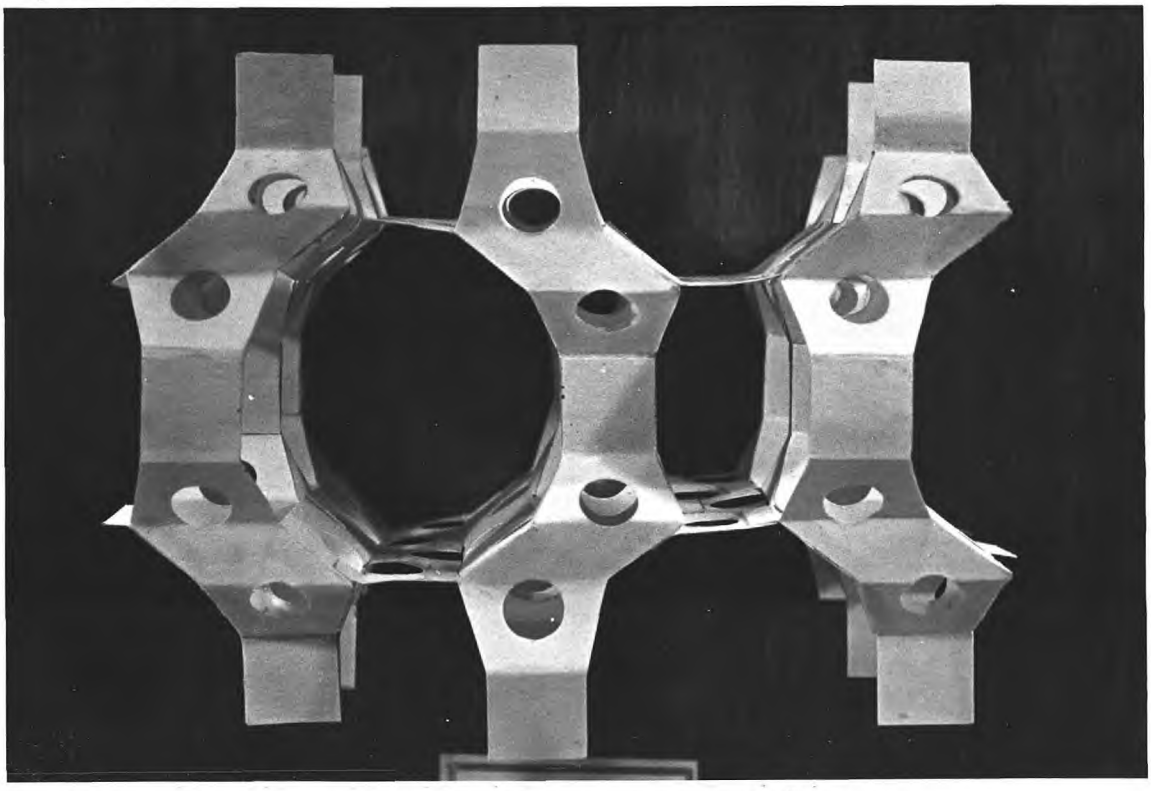

MODEL OF SYNTHETIC MORDENITE = ZEOLON (Na^+ FORM)
(showing large channels, diameter 5.8Å)

Fig.2

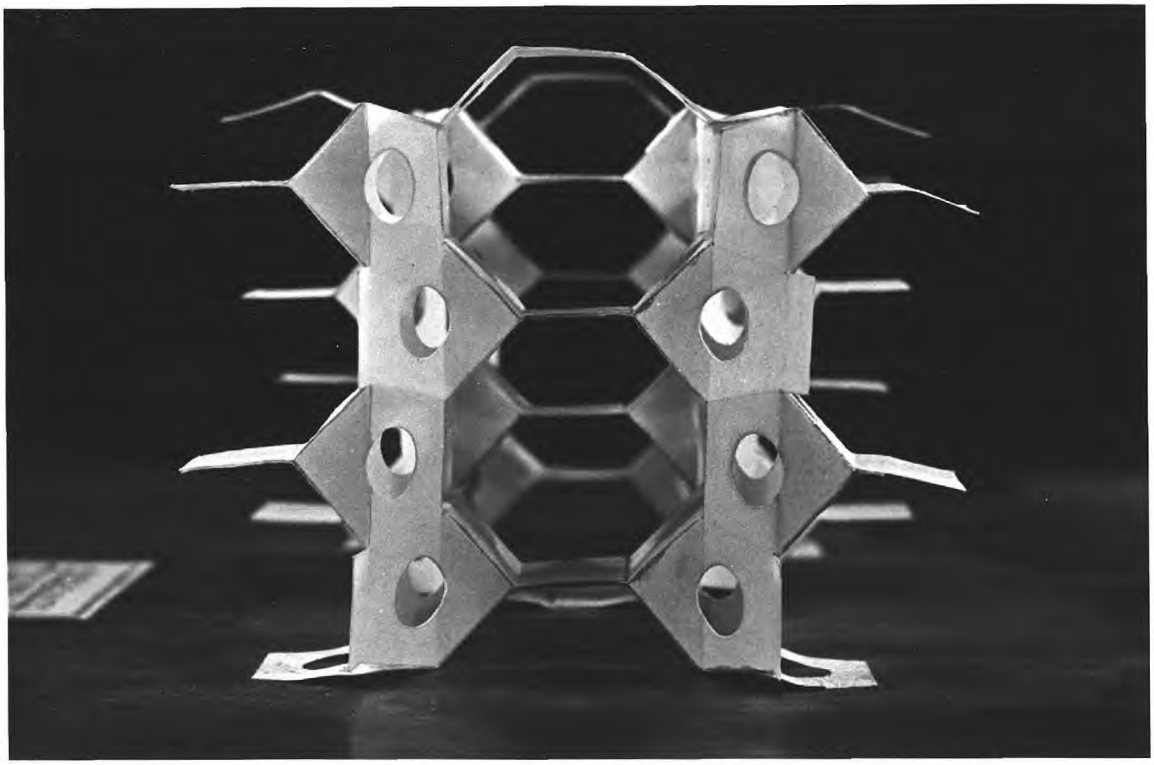

Same model, viewed through channels of diameter 4.0Å

dimensions exceed $4A^{\circ}$. This seems to suggest the existence of the crystal imperfections i.e. stacking fault, of which only comparatively few would be necessary to inhibit diffusion. This effect is discussed by Meier (1961).

Positions of Cations:-

Only 4 of the 8 Na^{+} ions per unit cell have been definitely located, they lie in the windows ($2.8A^{\circ}$ diameter) of the interconnecting channels. The remaining four Na^{+} ions have not been assigned positions and are, therefore, assumed to be randomly distributed within the large channel.

Analysis:-

Mordenite has a silica to alumina ratio of 10:1 and Meier's analysis agreed well with the formula

$$Na_8 \; Al_8 \; Si_{40} \; O_{96} \; 24H_2O$$

In present work the method of analysis used for synthetic sample is described by Vogel (5) and Meier (3) for alumino silicates. At all times, chemicals of the highest purity available were used, i.e. Analar reagents. The following composition of Na - mordenite was obtained:-

$$(3.50)\ Na_2O,\ (4.0)\ Al_2O_3,\ (39.5)\ SiO_2,\ (26.5)\ H_2O$$

The Na was determined radiochemically.

1.3 Gas Adsorptions:-

Gas sorption could either be absorption or adsorption and physical or chemical. Absorption means that the gas actually enters the electrical field between constituent atoms of the sorbent structure, so forming a solid solution or possibly a chemical compound, where as adsorption is

taken to mean the gas is sorbed only on the outer surface of the sorbent and the molecules sorbed on the outside of the sorbent only may experience a weak Van der Waal's attraction or a much stronger activated or chemical adsorption (chemisorption). In order to decide the type of adsorption, the following points may be considered:-

(a) Physical adsorption involves molecular interaction process, the formation of a physically adsorbed layer may be likened to the condensation of a vapour to form a liquid. The heat of physical adsorption is of the same order as the heat of liquification and is rarely more than twice or three times as large. Physically adsorbed layers, in particular those many molecular diameters thick, behave in many respects as thin layers of liquids. Chemisorption involves the transfer of electrons between the adsorbent and the adsorbate. The heat of adsorption can be comparable to that for the corresponding bulk chemical reation.

(b) The rate of physical adsorption is usually rapid especially at low temperature, equilibrium may be achieved in matters of seconds or minutes. In many cases chemisorption involves an activation energy, i.e. the rate is faster at higher temperature.

(c) A physically adsorbed layer can usually be removed by lowering the pressure, at the temperature at which the adsorption took place. Sometimes this could be a slow process owing to diffusion effects. The removal of a chemisorbed layer on the other hand is more difficult, usually high temperatures are needed.

(d) Under suitable conditions physically adsorbed layers several molecular diameter thick are found, chemisorption is complete when a monolayer has been built up.

(c) Physical adsorption can occur with any gas-solid system if the conditions of temperature are suitable, chemisorption can take place only if the gas is capable of forming a chemical bond with the surface atoms.

The usual method of expressing adsorption equilibria is in the form of adsorption isotherms

$$V = f(P)\ T$$

Isotherms are essentially related to plots of the free energy change as a function of amount adsorbed. Their shape can yeild qualitative knowledge of the adsorption process and a semi-quantitative measure of the fraction of the surface covered by adsorbate. At small adsorptions, Henry's law is valid, $V = KP$, i.e. the isotherms are straight lines.

In general isotherms may be classified according to the Brunauer (9) classification, the distinction between different types of isotherms generally arises from differences in pore structure and sorbate-sorbent interaction energy. All the isotherms in this work were either straight lines or of type 1 which represents unimolecular layer adsorption and is rectangular in shape.

In recent years thermodynamic methods for the investigation of the physical state of adsorbed molecules have been used quite frequently, e.g. Barrer and Wasilcivski (10) Barrer and Gibbons (11). Completely satisfactory analyses of results can only be obtained if the sorbent is energetically homogeneous and if experimental data are available over a wide, if not complete range of θ (where θ is the degree of saturation of the intercrystalline pore

space). This work describes the sorption of the rare gas krypton, on Na-mordenite. The isotherm data is analysed in terms of various ideal isotherm models, in order to decide whether the sorption is localized or mobile, and whether or not the interactions between adsorbate molecules are significant.

1.4 Neutron Irradiations:-

As early as 1943, Wigner predicted the existence of radiation damage in those parts of the reactor which absorb most of the energy of fission reaction, such as the fuel elements and the moderators. It was then confirmed experimentally that defects and imperfections are created when solid materials are exposed to radiations, to an extent depending on parameters such as type of radiation, flux, temperature and characteristic of the particular solid. Most of the research work, therefore, was directed towards the effects of radiations:-

i) On reactor fuel element to find out if damage resulted in loss of efficiency of power production.

ii) On reactor materials such as graphite and metals.

iii) And the most important concerning this work on processing materials required to separate, decontaminate and purify still fertile material and particularly fission products.

Present interpretation of the changes in the properties of solids brought about by high energy radiations centres around the production of several types of defects in the solid by the radiation. These defects are (a) vacancies, (b) interstitial atoms and (c) impurity atoms. Each of these defects is described briefly below:-

(a) Vacancies:- Vacant lattice sites may be created by collisions of energetic particles with the atoms in solid lattice. The energy transferred in these collisions is usually sufficient for the recoiling atom to create further vacant lattice sites by subsequent collisions. Thus for each primary collision, a cascade of collisions resulting in vacancies is initiated.

(b) Interstitial atoms:- The atoms that are displaced from their equilibrium positions in the lattice will stop in an interstitial, or non equilibrium position, provided they do not recombine immediately with a nearby vacancy.

(c) Impurity atoms:- Impurity atoms are formed under neutron bombardment by transmutation. A special case of this is the introduction of fission products by fission process. The effect of fission fragments is usually more pronounced than that of neutron induced transmutations, although both mechanisms are often insignificant, compared to other radiation effects.

Neutrons:- In the case of neutron irradiations, the type of interaction taking place depends to a large extent upon the energy of the neutron, and for this reason they are divided into groups according to their energy.

i) Fast Neutrons:- Their energies vary from 10 Kev to 10 Mev.

ii) Thermal Neutrons:- They usually have the energy of the order of 0.025 ev. at room temperature, being in thermal equilibrium with their surroundings.

The neutrons originating from the fission process are of primary interest. These neutrons possess an average energy of about 1 Mev, though the energy varies through a wide spectrum. These neutrons, as they pass through the

moderators, lose their energy until they are thermalised and they cause radiation damage by the formation of impurity atoms, resulting from neutron absorption, i.e. nuclear transmutation.

Elastic scattering is the most probable interaction of fast neutrons with lattice atoms, resulting in displacement, insterstitial etc. The energy of incident neutron is shared between the recoiling neutron and nucleus according to the law of conservation of energy and momentum and apart from gaining kinetic energy, the nucleus is unchanged. On the other hand inelastic scattering occurs if the neutron is absorbed by the nucleus and then a neutron with a lower energy re-emitted, leaving the original nucleus in an excited state which eventually returns to the ground state by emitting one or more x-rays. At thermal energies, another and most probable interaction process is capture of the neutron by the nucleus to give an isotope of the target element. In most reactor irradiations there are several times more thermal neutrons than fast neutrons and the most desirable place as a source of fast neutron is the immediate vicinity of a fuel element in a reactor.

Neutron, being uncharged, has a longer mean free path (of the order of 1 cm) than that possessed by heavy charged particles or electrons. This is of great advantage as neutrons can penetrate much greater thickness of material and can therefore be thought of as producing homogeneous damage effects. Actually, on a microscopic scale, the damage will tend to be highly concentrated, due to thermal spike for example.

Accompanying the libration of the neutrons during fissioning are energetic "gamma rays", generally assumed to be two or three times more numerous than the fast neutrons. These energetic gamma rays can be a source of radiation damage and cannot be filtered out without seriously decreasing the neutron flux, consequently the radiation damage resulting from γ - irradiation must always accompany the effects due to neutrons.

Thermal and Displacement Spikes:- A fast particle moving through a lattice, or an atom that has been hit just hard enough to vibrate with large amplitude without being displaced, will rapidly transfer energy to its neighbour which becomes abnormally excited. Thus heating to a high temperature a region of material around the track of fission fragment or knocked on atom, which starts expanding and at the same time there is a drastic increase in temperature. The result is called "thermal spike", i.e. rapid heating and quenching of a small volume of the material, the term being proposed by Seitz. The temperature may attain the melting point of the solid for the order of 10^{-12} seconds, but only involves about 10^{2}-10^{3} atoms per spike.

On average, a displaced lattice atom will have an energy of the order of several hundreds of ev and will suffer 10-100 collisions before becoming a trapped interstitial atom. It is therefore a few interatomic distances away from the vacancy which was its original position. The path of the projectile atom, therefore, is an area of a comparatively high degree of damage comprising many interstitials and vacancies. This is the type of damage to be expected from fast neutron bombardment. Most of the energy transferred to a displaced atom reappears as lattice vibration confined to

an area close to the paths of the projectiles. Brinkman proposed the name "displacement spike" for the volume of the lattice, distorted and heated in the above manner. He also suggested that this volume may actually be raised in temperature to the melting point, for the order of 10^{-11} seconds, and then rapidly recrystallize to the original form, involving in all about 10^3-10^4 atoms per spike.

Various terms involved will now be explained.

Neutron Flux:- It is also known as "neutron flux density" or "instantaneous flux" and is abbreviated as (nv) or ϕ where n = the number of neutrons per unit volume in the sample being irradiated and v = the mean velocity of the bombarding neutrons, therefore units of flux density are n/cm^3. $cm/sec = n/cm^2/sec$. This refers to a time interval of only one second (hence the name "instantaneous flux").

Neutron irradiation exposure or dose of bombardment are best known as "integrated neutron flux density", refers to a time interval of more than one second and is expressed by the symbols (nvt). The units are therefore n/cm^3. (cm/sec) $sec = n/cm^2$. For reactor irradiations the neutron dose can be expressed in the following ways depending on which is appropriate, e.g. 10^{18}nvt (total) or 10^{18}nvt (fast) or 10^{18}nvt (thermal).

The neutron dose may be defined as the number of neutrons that traverse an imaginery sphere of cross sectional area, 1 cm^2, within the sample. It is not the number of neutrons crossing a flat surface of the same area.

Cross Sections:- The probability of either scattering,

absorption or nuclear reaction, when a material is bombarded with neutrons is known as cross section C, and it is measured in barns (where 1 barn = $10^{-24}cm^2$). The cross section of an atomic nucleus may be thought of as a circular disc, centred on the nucleus, on a plane normal to the incident beam. If the neutron passes through this "area" then interaction or absorption occurs, otherwise scattering occurs. The scattering cross sections of most nuclei, for high energy neutrons, is about 3 barns, i.e. 3×10^{-24} cm^2.

1.4.1. Radiation Effect in Diamond, Silica, Quartz, etc:-

This section describes the effects of radiation upon materials similar in structure to zeolites, e.g. diamond, vitreous silica, quartz, alumina and Linde molecular sieve 13-X.

Diamond:- It has been observed (15) firstly to suffer from the formation of vacancies and interstitials and then to lose its crystallinity after prolonged fast neutron bombardment ($10^{21}n/cm^2$). Since this has important implications in the use of covalent refractory materials further studies were carried out, notably those of Crawford and Wittels (16).

Vitreous Silica:- This when exposed in a nuclear reactor was found to show an increase in density, resulting in amorphous state as a final product (17). The total dose required to change it into amorphous state is 2×10^{20} fast neutron $/cm^2$. These changes are attributed to ionization and to atomic displacements. Primak et al (18) suggests that in vitreous silica displaced atoms of O and Si lodge in the cavities within the structure, and permit the SiO_4 tetrahedra to relax into a more compact arrangement, thus

increasing the density. These atoms, however, seem to be loosely held or even uncombined, since on annealing by heating, the original density is restored (19). Simon (20) studied the Debye-Scherrer x-ray diffraction patterns of silica, before and after neutron irradiation and suggested that the decreased Si-Si bond distance in the irradiated material was due to a smaller Si-O-Si bond angle (138° as opposed to 142°). The Si-O bond length appears to be un-affected by the irradiation.

Quartz:- Fast neutron dose of approximately 2×10^{20} neutrons $/cm^2$, causes some changes in quartz which are similar to silica glass, with the exception that it is accompanied by a large decrease in density of quartz, 15% (17). It is somewhat unusual that these crystals of quartz reveal no macroscopic defects, however, Crawford and Wittels (16) observed the formation of macroscopic holes in quartz, after irradiation to a dose of only 8×10^{19} n/cm^2, with subsequent annealing at $950C^{\circ}$. The lattice expansion may be due to atoms lodging in parts of the structure not large enough to accommodate them (18). The damage is known to arise in two stages (21), up to $3 \times 10^{19} n/cm^2$, the lattice damage is predominately point defects and small disorder regions. Since more energy would be required to displace Si atoms, therefore, vacancies and interstitial atoms are assumed to be almost entirely due to oxygen atoms. At higher exposures, the shear strains set up by the disordered regions spread throughout the crystal, rendering it completely amorphous.

1.4.2. Neutron Irradiation of Alumina:- Young (22) was the first to study the effects of neutron irradiation on crystalline solids, employing physical gas adsorption methods. He studied the thermodynamical properties resulting from iso-

therms of krypton adsorbed on dehydrated alumina, before and after reactor irradiations.

It was not considered possible to study the radiation damage by electron microscope or field ion microscope, since the effects are usually too small to be observed by these methods. A more indirect method was thus adopted, that of physical adsorption of an inert gas at low temperatures, with subsequent analysis in terms of shape of adsorption isotherm and the differential molar entropy of the sorbed phases.

A significant increase in isosteric heat was observed resulting from a dose of 2×10^{18} fast neutrons. Young analysed the adsorption results using the isotherm methods of Garden and Kington (23) i.e. localized or mobile adsorption, with or without adsorbate molecule interactions. The most suitable model appeared to be one of localized sorption without marked lateral interactions, on surface of varying heterogeneity.

1.4.3. Neutron Irradiatiation of Linde Molecular Sieve 13-X:-

Rees and Williams (24) have recently studied the effects of neutron irradiation on Linde molecular sieve 13 - x, a synthetic zeolite, commonly known as NaX. It was noticed that neutron irradiation resulted in no observable change in the sorbent properties of NaX, provided the dose was less than 5×10^{17} n/cm^2. Beyond this dose, a progressive loss in sorption capacity was observed. However, it was established that the zeolite still retained its excellent sorbent properties even after a dose of 2×10^{19} n/cm^2. They did not find any change in the cation exchange properties of the zeolite up to a dose of 1.9×10^{19} n/cm^2.

The zeolite was found to be completely amorphous by x-rays, when irradiated to a dose of 7×10^{19} n/cm^2 and its sorption capacity was negligible.

The model based on localized sorption with molecule - molecule interaction was found to be the best.

CHAPTER 2

THEORETICAL

2.1. Gas Adsorption

2.2. Neutron Irradiation

2.1. Gas Adsorption:-

2.1.1. Summary of Symbols:-

$-\Delta H$ = Isosteric heat of adsorption = qst.
$-\Delta H = (\widetilde{H}g - \bar{H}s)$

$\widetilde{H}g$ = Molar heat content, or enthalpy, of gas molecules in the gas phase, at equilibrium pressure P (cm. Hg) and temperature T (^{o}k)

$\bar{H}s$ = Differential or partial molar enthalpy of sorbed Phase:-
$\bar{H}g = (\partial H/\partial n_a)_{P, T, n_s}$

n_s, n_a = Moles of sorbent and adsorbate

R = Gas constant

θ = Degree of saturation
$= \dfrac{\text{volume gas adsorbed at equilibrium}}{\text{volume sorbed at saturation (same temp.)}}$

K1, K2, K3, K4, K5
= Limiting isotherm model constants

$2W/Z$ = Interaction energy between two sorbent molecules sorbed on adjacent sites in the crystal lattice

Z = Co-ordination number of sorption site, i.e. no. of nearest neighbours occupied by adsorbate molecules

ΔS = Change in entropy system
$\Delta S = (\bar{S}s - \widetilde{S}g)$

$\bar{S}s$ = Differential or partial molar entropy of sorbed phase, i.e. gas in host lattice
$\bar{S}s = (\partial S/\partial n_a)_{P, T, n_s}$

$\widetilde{S}g$ = Molar entropy of gas in gas phase at P, T

$\tilde{S}og$	=	Molar entropy of gas at standard pressure (usually one atmosphere) and temperate T.
$\bar{S}th$	=	Differential thermal entropy
$\bar{S}c$	=	Differential configurational entropy
Sth	=	Residual thermal entropy, related to $1S_T$ by:- $\bar{S}s = I\bar{S}_T + \bar{S}th'$
$\bar{S}th'$	=	(ditto, where $\bar{S}s = 2\,\bar{S}_T + \bar{S}th''$)
$1\bar{S}_T$	=	Partial molar entropy resulting from one degree of translational freedom of the guest molecules within the intercrystalline environment
$2\bar{S}_T$	=	(ditto, for two degree of translational freedom)
t	=	Translational degree of freedom
v	=	Vibrational " " "
k	=	Boltzman's constant
h	=	Plank's constant
m	=	Molecular mass of adsorbate, i.e. molecular weight x 1.66 x 10^{-24} gm.
v	=	Volume gas adsorbed (cc.S.T.P./g sorbate)

2.1.2. Thermodynamics of Adsorption:-

Our present understanding of the thermodynamics of physical adsorption system is due largely to the work of Hill (25, 26) Everett (27). Reviews of recent developments in this field have been given by Hill (28), Everett (27) and Drain (29). Two different approaches to the thermodynamics of adsorption may be considered.

(a) Adsorption Thermodynamics:- The sorbed molecules are regarded as a single component phase in the potential field of the sorbent which is assumed to be unperturbed by adsorption. This approach leads to molar thermodynamic quantities and involves the evaluation of an independent variable characteristic of the sorbate, the spreading pressure (Hill, 25, 26). This is tedious and can be inaccurate especially at low pressures, leading to considerable error in the final thermodynamic quantities.

(b) Solution Thermodynamics:- The adsorbent-adsorbate system is considered as a single condensed phase of two components in equilibrium with unadsorbed gas. This approach leads to partial molar thermodynamic quantities. For small differences in the energy of the adsorbed molecules, the differential functions are found to be more sensitive than the molar functions (Garden, Kington and Laing).

(c) Tykodi's Method:- Tykodi (31) developed Gibb's approach (Hill, 26) by removing the restriction of thin layers, thus making it generally applicable to sorption. It is assumed that the total volume of the system, the gas and the sorbate are known and that the properties of the gas and the solids are separately well

defined. This method has been little used and is open to the same criticism as adsorption thermodynamics. In this work solution thermodynamical approach has been adopted.

2.1.3. Isosteric Heat of Adsorption:-

By employing standard solution thermodynamics the following expressions may be obtained, the rate of change of pressure with temperature is given by the Clausius - Clapeyron equation:-

$$\left(\partial \ln P / \partial T\right)_{na} = -\Delta H / RT^2 = \frac{\tilde{H}g - \bar{H}s}{RT^2} \qquad (A)$$

$$= -\Delta S / RT = \frac{\tilde{S}g - \bar{S}s}{RT} \qquad (B)$$

where $-\Delta H$ = qst is the isosteric heat of adsorption. This equation assumes that the gas behaves as an ideal gas, and that the volume of the gas in the gas phase greatly exceeds its volume in the sorbed phase, which is usually the case. The isosteric heat may be determined in the following ways:-

(a) From changes in equilibrium pressure with temperature i.e. by plotting $\log_{10} P$ Vs $^1/T$ for a fixed amount sorbed; the slope, or tangent if a curve results, multiplied by 2.303 R gives qst, in accordance with the expression:-

$$\text{Log}_{10} P = {}^{qst}/_{2.303\ RT} + C \qquad (C)$$

Performing this operation for a series of amounts sorbed leads to a plot of qst Vs. V (volume sorbed at equilibrium).

(b) By direct calorimetry, by measuring the heat evolved for every addition of gas.

(c) Plot log P vs V for each of a series of isotherms and obtain log P_1/P_2 corresponding to T_1 and T_2, then

$$qst = R \left(\frac{T_1 . T_2}{T_1 - T_2} \right) \ln P_1/P_2 \qquad (D)$$

It is important to obtain an average value of qst for each value of θ, from more than just one pair of isotherms, because qst may vary with temperature, and also misleading results may easily be obtained in reading the values of $\log_{10}P$ from the graphs.

In this work, four isotherms ($10C^{\circ}$ increments) were used to obtain six permutations, i.e. six values of qst.

The nature of the solid does not enter into the derivation of the above expression, as we have employed the amount of sorbent, not its surface area. It is a perfectly general treatment which applies regardless of whether the sorbent swells on sorption or number of sites change with temperature or pressure.

2.1.4. Interpretation of the Thermodynamical Properties of Sorption in Terms of Limiting Isotherm Models:-

The principal aims of investigating the sorption of one substance on another must be the evaluation of the thermodynamic properties of the sorbate and also the elucidation of the state of the adsorbed molecule. In recent years the thermodynamic properties of sorption have been used for interpreting the state of the adsorbed phase,

e.g. Garden, Kington and Laing (36). Barrer and Sunderland (37) Barrer and Wasilewski (10) Barrer and Gibbons (11).

The State of Adsorbed Molecule:- When a molecule is adsorbed on a surface it enters the potential field associated with the surface. This field will vary in a regular or periodic manner depending on the structure of the sorbent and the nature of the surface. Thus the adsorbate molecules may encounter potential barriers in the motion along the surface.

Two extreme cases may be considered but the actual state of the sorbed molecule may lie anywhere between these extremes:-

(a) If the thermal energy of the sorbed molecule is insufficient to overcome the potential barriers, it is assumed to vibrate about a mean position on the surface. A single molecule may not be permanently confined to a particular sorption site on the surface, however, it may, by a process of diffusion or desorption-resorption, occupy neighbouring sites. Thus although the molecule may occasionally move from one site to another the sorption is still said to be "Localised".

(b) If the average thermal energy of the molecules is larger than the height of the potential barrier then the molecules will be able to move freely over the surface and are said to be "mobile".

Localised and mobile models are the extreme cases and it is possible for a transition to occur from either one of the extreme cases to the other. Hill (38) and Morrison (39) have discussed the transition from a localised

adsorbed phase to a mobile phase as the temperature is increased. Kington et al (36) have shown that argon adsorbed on chabazite probably changes from a mobile to an immobile state as the degree of filling the cavities in the crystal approaches saturation, presumably due to the mutual caging effect of sorbed argon atoms.

Gas molecules adsorbed within the lattice of an alumino silicate structure can hardly possess three degrees of translational freedom, since they are confined in cavities and channels of molecular dimensions. The actual behaviour could be compared with one of three extremes:-

(i) No translational freedom or

(ii) One or two degrees of translational freedom

(iii) Rotational freedom may also be modified in the sorbed state. The possible extremes in the degrees of freedom of sorbed gas are given in the table for ideal models. The limiting state in which two rotational degrees of freedom are changed into rocking vibrations are also included in the table.

Ideal Models	Degree of freedom relative to environment
Localized	(i) 3V, 2R (ii) 4V, 1R (iii) 5V
Mobile with 1t	(i) 1t, 2V, 2R (ii) 1t, 3V, 1R (iii) 1t, 4V
Mobile with 2t	(i) 2t, 1V, 2R (ii) 2t, 2V, 1R (iii) 2t, 3V

Krypton gas molecules, used in the present work, are perfectly symmetrical and monoatomic, therefore do not possess degree of rotational freedom R. The "2t + 1V" system is frequently found in zeolites, in which the cavities are large compared with the dimensions of the sorbate molecules. If however these channels and cavities are only slightly larger than the gas molecules, the latter will possess "1t + 2V". Finally if the cavities are so small as to encage only one gas molecule then the "3V" system will exist, such a system also exists when localized adsorption occurs.

Models give descriptions of idealised systems and may not be applicable to real systems. Deviations may arise from surface heterogeneities, multilayer formation and mutual interactions between sorbed molecules. As we have already discussed that the complete sorption process need not be necessarilypurely localized or purely mobile. It is therefore necessary to consider all possible isotherm models when the state of adsorbed phase is being investigated. Throughout the following discussion it is assumed that the rigid lattice frameworks are unlikely to be affected by the presence of a potential field due to the sorbed gas. This assumption is usually considered an excellent approximation in physical adsorption but it is most unreal for chemisorption (28).

Isotherm Models for a Localized Sorbed Phase:-

The simplest case occurs when molecules are sorbed on a two dimensional array of energetically homogeneous sites. Langmuir (40) using a kinetic treatment obtained the following isotherm equation:-

$$K_1 = \frac{P(1-\theta)}{\theta} \qquad \text{(Model 1)}$$

where P = equilibrium pressure (cm. Hg)
and θ = degree of saturation

He considered the adsorbed layer to lie in dynamic equilibrium with the gas phase. Fowler (41, 42) related the equilibrium constant K_1 to the partition functions of the sorbed and gaseous molecules. As with all the isotherm models a necessary, but not sufficient condition for the above model to be applicable is that K_1 be a constant independent of θ, already defined.

The assumptions made for an ideal Langmuir models are:-

(a) The gas molecules are sorbed on sites which are independent of each other and are energetically equivalent.

(b) The sorbed molecules are localized, i.e. each one is confined to a site on the surface.

(c) There are no mutual interactions between adjacent molecules; this might be expected at low sorbate concentration, but seems less likely at high concentration, when sorbed molecules must be packed close together.

(d) The sorption is restricted to a monolayer.

Localized Model with Interactions:- If the sorption is localized and a mutual interaction between the sorbed molecules exists, then the isotherm equation must take account of the extra energy terms. The following equation was derived:-

$$K_2 = \frac{P(1-\theta)}{\theta} \exp. \frac{(-2\theta W)}{RT} \qquad \text{(Model 2)}$$

When W = 0 this expression reduced to the Langmuir model. Molecule-molecule interactions can lead to changes in configurational entropy, hence further modification can be made to the Langmuir model;

$$K_3 = P \frac{(1-\theta)}{\theta} \frac{(\beta + 1 - 2\theta)^Z}{(2-2\theta)} \qquad \text{(Model 3)}$$

where $\beta = \left\{ 1 - 4\theta(1-\theta) \left[1 - \exp\frac{(-2W)}{ZKT} \right] \right\}^{\frac{1}{2}}$

which involves the term $2W/_Z$, which is the interaction energy between two adjacent molecules and Z is the co-ordination number of a sorption site and may be determined from the geometry of the sorbent sites. This expression also reduces to the Langmuir model when W = 0. Fowler (43) derived this expression for K_3, taking into account the variation in energy of sites with coverage due to mutual interactions. The assumptions made in this derivation are as follows:-

(a) The interactions between sorbed molecules are constant and additive.

(b) Only nearest sorbed molecules interactions are allowed for.

Isotherm Models for a Mobile Phase:-

If the sorbed phase acts as a perfect two dimensional gas of point particles, the isotherm equation derived either from statistical thermodynamics (43) or from an equation of state (27) is:-

$$V = K.P. \qquad \text{(Model 4)}$$

This is, of course, Henry's Law (analogous isotherm for solution of gases in liquids) and only applicable to very dilute phases, and at temperatures above the critical temperature of the gas.

If the adsorbed phase is considered as having a finite co-area the following equation is obtained:-

$$K_5 = P \frac{(1-\theta)}{\theta} \exp. \frac{(-\theta)}{1-\theta} \qquad \text{(Model 5)}$$

This equation is often referred to as the volmer equation as it can also be derived from the Volmer equation of State (27, 38).

Mobile Model with Mutual Interactions:- Hill (38), assuming that the sorbed fluid obeys the Van der Waals equation of State, derived the following isotherm equation for mobile sorption with sorbate - sorbate interaction.

$$K_6 = P \frac{(1-\theta)}{\theta} \exp. \frac{(-\theta + \alpha\theta)}{1-\theta} \qquad \text{(Model 6)}$$

where $\alpha = 2a/bkT$ a and b being the two dimensional Van der Waal's constants.

All of these isotherm models are derived assuming that the adsorbent surface is energetically homogeneous. When this is not the case, these models cannot be rigorously applied. However useful and interesting information can still be obtained even if the theory can only explain the experimental results over a limited range of θ.

Intracrystalline sorption was originally considered

to be localized (44). Work by Rees (45) on two component interstitial solid solutions of hydrogen in metals extended this treatment; however the possibility of mobility must not be overlooked, since the free diameter of the cavities and channels in several zeolites greatly exceeds the size of the adsorbate molecule.

The isotherm constant K must be independent of θ for a particular mobile model to be valid. This, however, is not sufficient as experience has shown that a mere test of the shape of an isotherm is not conclusive. It would also be impossible to distinguish between one and two degrees of translational freedom. Therefore, as in the case of localized sorption, it is necessary to study the entropy functions of the sorbed phase.

2.1.5. Entropy of Adsorption:- For a monoatomic gas, the following expression for $\bar{S}g$ may be derived from statistical thermodynamics:-

$$\bar{S}g = R \ln KT/P + R \ln \frac{(2\Pi m\, KT)^{3/2}}{h^3} + 5R/2 \qquad (7)$$

$$\bar{S}s = \Delta H/T + R \ln \frac{(2\Pi m\, KT)^{3/2}}{h^3} \; KT/P + 5R/2 \qquad (8)$$

(For summary of symbols see page 30, 31)

If the sorbed molecules are localized, i.e. do not possess translational motion, then the partial molar entropy may be divided into differential thermal and configurational entropy terms (46)

$$\bar{S}s = \bar{S}th + \bar{S}c \qquad (9)$$

The thermal entropy for an inert gas sorbed by a zeolite originates from the electronic states of the molecules and the vibrations about the mean position on a sorption site. The configurational entropy term $\bar{S}c$, arises when we consider the number of distinguishable arrangements of N molecules sorbed on M sites in a localized system on a homogeneous surface (27) i.e. $\frac{M!}{N!\,(M-N)!}$

from this expression it may be deduced that

$$\bar{S}c = R\ln\frac{(1-\theta)}{\theta} \qquad (10)$$

and the entropy term applies to the isotherm models corresponding to K_1 and K_2, but K_3 (localized with mutual sorbate interactions) does allow for changes in configurational entropy, these in turn are allowed for in the expression (43).

$$\bar{S}c = R\ln\frac{(1-\theta)}{\theta}\frac{(2-2\theta)^{Z}}{\beta+1-2\theta} + W/T\,\frac{(\beta-1+2\theta)}{\beta} \qquad (11)$$

The difference between the value of $\bar{S}c$ obtained using this expression and that obtained from the ideal Langmuir model has been found to be negligible for the system, argon sorbed on chabazite (30). The residual thermal entropy is given by:-

$$\bar{S}th = \bar{S}s - \bar{S}c \qquad (12)$$

$$= \Delta S + \tilde{S}g - \bar{S}c \qquad (13)$$

$$= \Delta H/T + R\ln\frac{(2\pi m\,KT)^{3}/2\;KT/P + 5R/2 - R\ln\frac{(1-\theta)}{\theta}}{h^{3}}$$

For models 1 and 2 interactions are allowed for in model 2, but for model 3,

$$\bar{S}th = \Delta H/T + R \ln \frac{(2\Pi m KT)^{3/2}}{h^3} KT/P + 5R/2 -$$

$$R \ln \frac{(1-\theta)}{\theta} \frac{(2-2\theta)^Z}{\beta+1-2\theta} - W/T \frac{(\beta-1+2\theta)}{\beta} \qquad (14)$$

The thermal entropy must satisfy certain criteria (23).

(a) It must be independent of θ (over the range in which the sorption model is valid).

(b) It must be positive, having reasonable physical magnitude.

For non-localized systems, i.e. models 5 and 6 we have two expressions:-

$$\bar{Ss} = 1\bar{S}_T + \bar{Sth}^{-1} \qquad (15)$$

$$\bar{Ss} = 2\bar{S}_T + \bar{Sth}^{-11} \qquad (16)$$

Where $1\bar{S}_T$ and $2\bar{S}_T$ are the partial molal translational entropies resulting from one and two degrees of translational freedom of the guest molecules within their intercrystalline environment respectively. For the isotherm models K_5 and K_6 (mobile sorption without, and with sorbate molecule interactions), $1\bar{S}T$ and $2\bar{S}T$ may be formulated.

$$1\bar{S}_T = R \ln \left[\frac{(2\Pi m KT)^{\frac{1}{2}}}{h} L \frac{(1-\theta)}{\theta} \right] + R \frac{(\frac{1}{2}-\theta)}{1-\theta}$$

$$2\,\bar{S}_T = \left[R \ln \frac{2\pi m KT}{h^2} \; a \frac{(1-\theta)}{\theta} \right] + R \frac{(1-\theta)}{1-\theta} \qquad (17)$$

where L = co-length of a sorbed molecule (= co-volume $b^{1/3}$), and a = co-area (= $b^{2/3}$). Thus knowing Ss and $1\,\bar{S}_T$ (or $2\,\bar{S}_T$), the residual differential thermal entropy $\bar{S}th'$ (or $\bar{S}th''$) is obtainable.

Detailed analyses, using the methods described in this section are made on the experimental data obtained in this work.

2.2. Neutron Irradiation:-

In this chapter we shall discuss how the damage is produced in the lattice of Na - mordenite by neutron irradiations.

2.2.1. Summary of Symbols:-

Ed = Displacement energy of lattice atom (Ca. 25. ev.)

Emax = Maximum amount of energy that may be transferred to a lattice atom in a direct head-on collision by a bombarding neutron.

$\bar{E}$ = Average energy transferred in neutron lattice atom collisions (For glancing blows E approaches zero) $\bar{E} = Emax/_2$

E = Average energy of bombarding neutrons (1 Mev)

M = Atomic weight of lattice atom.

N = Atomic number of neutron = 1.

Np = No lattice atoms displaced by neutrons in primary collisions only.

Nd = Total no. of displaced atoms; $Nd = Np\ \bar{V}$ (24)

$\bar{V}$ = Average no. of atoms displaced by each knock-on atom; $\bar{V} = \bar{E}/2\ Ed$ (25)

ϕt = Total neutron flux (neutrons/cm^2)

Cd = Displacement cross-section of lattice atom.

n = No. of lattice atoms per unit volume of target.

f = Factor allowing for anisotropy and inelasticity in fast neutron scattering (taken as $2/_3$).

2.2.2. Energy Transfer:- Since the neutron carries no charge it produces radiation damage only by direct interaction with nuclei and it loses energy through elastic collisions with the lattice atoms. If the displacement energy of the lattice atom is Ed (usually taken as 25 ev) and if it receives an energy E, greater than Ed, as a result of a collision, then it will be displaced from its normal lattice site taking its electron cloud with it. This displaced atom is called "a knock on" atom and the process forming it is known as primary process. This atom may then come to rest in a non-equilibrium position, hence an interstitical atom as well as a vacant lattice site result from a collision. When the excess energy E, transferred to the atom, is greater than 2 Ed, it will become a new projectile. Initially, knock-on atoms cause damage by ionization and electronic excitation, but when their energy has fallen below the limiting energy for ionization, they suffer elastic collision with lattice atoms, causing further displacements. These secondary collisions, then form new projectiles leading to tertiary collisions and so on, until the energy possessed by the projectile atom is insufficient to actually displace another lattice atom. Thus there will be a net increase in the number of displaced atoms only if both have kinetic energy greater than Ed after the collision. More lattice atoms are displaced as a result of cascades, then from the primary processes in which each neutron is involved. This only accounts for 10-20% of total damage arising from neutron irradiation, the remaining 80-90% damage is the result of the ionization effects due to the passage of atoms and ions throughout the lattice (49).

If it is assumed that only head on collisions between lattice atom and neutron takes place, then a projectile atom in a monatomic solid, possessing energy E (greater than 2 Ed,) results in two projectile atoms with energy E/2, which will in turn lead (if E/2 is greater than 2Ed) to a total of four projectile atoms of energy E/4, and so on. This process will continue until E/n is less than Ed, when the projectile atom does not have sufficient energy to displace another, then it will promptly fall into the resulting vacancy. When solids contain more than one type of atoms, and when the bombarding particle is a neutron or heavy charged particle, the above process differs only in respect that when any two colliding particles possess different masses, their resulting energies will be different, according to the law of conservation of momentum.

The neutrons emitted on fissioning of U^{235} atom are distributed in energy from 0.5 Mev to 10 Mev. For calculations, the average energy of the fast neutrons will be taken as 1 Mev. The errors involved from the use of an average neutron energy are less than those arising from other stages in the calculations.

The maximum energy that can be transferred in a nuclear collision, when a bombarding neutron of mass N and energy E, makes a direct head-on collision with a lattice atom of mass M is given by

$$E_{max} = \frac{4\,EMN}{(M+N)^2} \qquad (18)$$

which may be approximated on the atomic weight scale, since N = 1, to

$$Emax = \frac{4\ EM}{(M+1)^2} = 4E/M \qquad (19)$$

The average amount of energy transferred in such a collision is:-

$$\bar{E} = Emax/2 = \frac{2\ EM}{(M+1)^2} = 2E/M \qquad (20)$$

The fraction of the total neutron energy that is transferred on average to a lattice atom, is therefore,

$$\frac{\bar{E}}{E} = \frac{2M}{(M+1)^2} = 2/M \qquad (21)$$

Therefore the smaller the lattice atom, the greater the energy transferred to it in a collision. For a silicon atom this fraction is Ca $1/15th$, and for the oxygen atom, it is Ca $1/10th$ of the neutron energy.

In general then, it is found that for atoms such as aluminium, oxygen and silicon, approximately 10-20% of the neutron energy appears as lattice energy (spikes, vacancies, interstitials) and approximately 80-90% in the form of excitation and ionization.

2.2.3. Number of Displaced Atoms:- In the preceeding section it has been shown that atoms can be knocked from their lattice sites by irradiation. These primary knock-on atoms will in turn produce new projectile atoms, only, if the bombarding particle transfers energy in excess of Ed. Therefore the number of displacement should be:-

$$Nd = Emax/4Ed = \bar{E}/2Ed \qquad (22)$$

where $\bar{E}$ is the average energy transferred to a knock-on Seitz (14) suggests instead:-

$$Nd = (E^{1}/Ed)^{\frac{1}{2}} \qquad (23)$$

where E^{1} is the average energy of all the primary knock-ons. No accurate experimental determination of the number of atoms displaced by incident radiations are available, but rough estimates have been made in a few instances, e.g. by changes in electrical resistivity of metals (50) changes in the intersities of x-rays and changes in density (21) and paramagnetic absorption lines. The effects of fast neutrons on alpha-alumina, by means of changes in optical properties, i.e. the growth of several absorption bands as function of radiation dose, has been studied by Dienes and Levy (51). In order to employ such measurements, however, it is necessary to separate the effects due to ionization from the effects due to displacements. This was found to be possible as colouration due to ionization attained saturation at a very low exposure. Calculations of the number of displaced atoms gave an overestimate of the actual number found by experiment, but the figure was of the same order of magnitude, as in the case for similiar calculations for metals (51). With graphite, the theoretical estimates exceed experimental figures by only a factor of 2, which is better than for most other materials; for quartz there is a factor of 5. This is to be expected

that the experimental results should be less than theoretical, because the theory makes no allowance for replacements, e.g. combination of vacant lattice sites and interstitial atoms (21). Several experiments have been conducted by Primak (19) with calibrated fluxes in an attempt to relate the number of displacements, i.e. damage to the flux. It is obviously necessary to possess a fairly precise knowledge of the behaviour of atoms within a bombarded material in order to determine quantitatively the extent of damage arising from irradiation.

The number of primary knock-ons produced per unit volume in a bombardment is given by Dienes and Vineyard as:-

$$Np = \phi . t . n_0 . Cd \qquad (24)$$

where ϕ = instantaneous neutron flux, t = duration of bombardment, no = no of atoms per unit volume of target material, and Cd = cross-section per atom for collision which produces displacements. Since each primary knock-on produces many more displacements, Np corresponds to only a fraction of the total no. of displacements:-

$$Nd = Np \ \bar{V} \qquad (25)$$

where $\bar{V}$ = the average no. of displacements per knock-on, is given by:-

$$\bar{V} = \bar{E}/2Ed = 2EMN/(M+N)^2 . f/2Ed = \frac{EMf}{(M+1)^2} \cdot \frac{1}{Ed} \qquad (25)$$

(Summary of symbols given at the beginning of this chapter)

$$Nd = \phi . t . \text{no. Cd.} \frac{EM\ f}{(M+1)^2 Ed} \qquad (26)$$

This expression thus allows calculation of an approximate no. of lattice atoms displaced by a given integrated neutron flux, although no allowance is made for the numerous replacements which must occur.

2.2.4. Thermal Neutrons:- They do not effect the zeolite by displacing the lattice atoms, or by ionization, but they alter the atomic nuclei by neutron capture and the reactions involved in that process will be discussed.

The chief isotope of aluminium is Al^{27}_{13}, this may undergo an (n,y) transmutation to form unstable isotope Al^{28}_{13}, which decays by beta emission to form the stable silicon atom Si^{28}_{14} ;

$$Al^{27}_{13} \ (n,y) \quad Al^{28}_{13} \xrightarrow{\beta-} Si^{28}_{14}$$

Since the half life of Al^{28}_{13} is only 2.3 minutes, any activity so produced will have completely decayed within one hour. This activity is to be expected from all irradiation of samples contained in aluminium irradition cans, upon removal of the sample from the reactor.

Silicon has Si^{28}_{14} as its principle isotope, neutron capture produces the stable Si^{29}_{14} which likewise may be transmuted to Si^{30}_{14}. This isotope is also present to the extent of 3% in the natural element and is the only silicon isotope which will undergo an (n,y) transmutation to form an unstable radionuclide. The reaction can be represented

by:-

$$Si_{14}^{30} \ (n,y) \ Si_{14}^{31} \xrightarrow{\beta-} P_{15}^{31}$$

The unstable Si_{14}^{31} promptly decays by beta emission to form a stable phosphorus isotope. The half life of Si isotope is only 2.65 hours, so decay is complete within a day. Since the activity of silicon so produced is very low, the advantages of silica ampoules for containing samples is obvious. The stable and most abundant isotope of Si can also undergo an (n, 2n) reaction forming the unstable Si_{14}^{27} which decays by positron emission to form stable aluminium.

$$Si_{14}^{28} \ (n, 2n) \ Si_{14}^{27} \xrightarrow{\beta+} Al_{13}^{27}$$

It can also undergo (n, P) reaction to form aluminium

$$Si_{14}^{28} \ (n, P) \longrightarrow Al_{13}^{28}$$

However, these two reactions are of little importance as compared with (n,y) reaction of Si_{14}^{30}.

The sodium cations present in Na-mordonite are of the stable isotope Na_{11}^{23}; they may suffer an (n,v) reaction to form unstable Na_{11}^{24} which decays by beta emission to form stable magnesium:-

$$Na_{11}^{23} \ (n, y) \ Na_{11}^{24} \xrightarrow{\beta-} Mg_{12}^{24}$$

Since half life is 15 hours, the activity is negligible within one week. Magnesium may also be produced by:-

$$Al_{13}^{27} \ (n,\alpha) \ Na_{11}^{24} \xrightarrow{\beta-} Mg_{12}^{24}$$

Oxygen - 16 undergoes neutron capture to form O_8^{17} which in turn may form O_8^{18}, both of which are stable. However, O_8^{18} may suffer an (n,y) reaction to form the unstable O_8^{19} which will decay within one day to stable flourine:-

$$O_8^{18} \ (n,y) \ O_8^{19} \xrightarrow{\beta-} F_9^{19}$$

Summerising, any activity resulting from a nuclear transmutation with aluminium should be "dead" within one hour, from silicon and oxygen within one day, and from sodium, within one week. If zeolite is still appreciably active after one week, the activity must arise from the decay of an impurity atom.

2.2.5. Calculation of Specific Activity:-

Specific activity S, may be defined as the amount of activity produced per unit weight of the irradiated element, expressed as curies per g. of target element. S is given by the expression (52) :

$$S = \frac{0.6 \ \phi \ C \ (1 - \text{exp.} - 0.693t/_T)}{3.7 \times 10^{10} A} \qquad (27)$$

where

ϕ = effective thermal neutron flux ($n/cm^2/sec$)

C = excitation cross section of target (barns)

t = irradiation time (same units as T)

T = half life of unstable radio nuclide produced

A = atomic weight of target element

3.7×10^{10} = no. of disintegration per second from one g. of pure radium = 1 curie

This equation is only approximate; it takes no account of burn up of the target element or of possible further neutron capture reactions and transmutations. However, an approximate estimate of the specific activity can be calculated.

By use of the following expression (53), it is possible to calculate the weight of radio-isotope produced as a result of thermal neutron capture:

$$M = 7.7 \times 10^{-9} \; A.T.S. \qquad (30)$$

where A = at wt. of target element

T = half life of decaying nuclide in days

S = specific activity c/gm.

CHAPTER 3

EXPERIMENTAL

3.1. Gas Adsorption

3.2. Neutron Irradiation

3.1. Gas Adsorption:-

3.1.1. Volumetric Sorption Apparatus:-

A volumetric sorption apparatus consisting of a gas burette, McLeod gauge, manometer and sorption cell was constructed. (fig. 3). The McLeod gauge and manometer were connected to the high and low vacuum lines and the burette was connected to a gas line. The separate items will now be described in some detail.

(1) Pumping System:- This is shown schematically in Fig. (4). The mercury diffusion pump operates in conjunction with a rotary oil backing pump. A pressure of 10^{-3} - 10^{-4} mm. Hg. can be achieved only by rotary oil pump, but together the moisture free system may be pumped down to 10^{-6} mm. Hg. pressure in approximately half an hour. The oil trap prevents oil from being sucked into the system in the event of a power failure and the buffer volume serves to back the diffusion pump when the oil pump is temporarily switched off. A trap cooled in liquid nitrogen prevents any condensible material from contaminating the mercury and oil pump. All traps were of large bore (6 - 8 mm) to ensure a good pumping rate, and greased with Apiezon grease type L, the most suitable for high vacuum systems operated at room temperature.

(2) Manometer:- A wide bore tubing (1 cm) was used for constructing manometer in order to reduce the meniscus depression effects. Menisci corrections (56) were applied on all occasions. The manometer read pressure in the range 0.2 to 55 cm of Hg. The fixed mark (m in Fig. 3) was

Fig.3

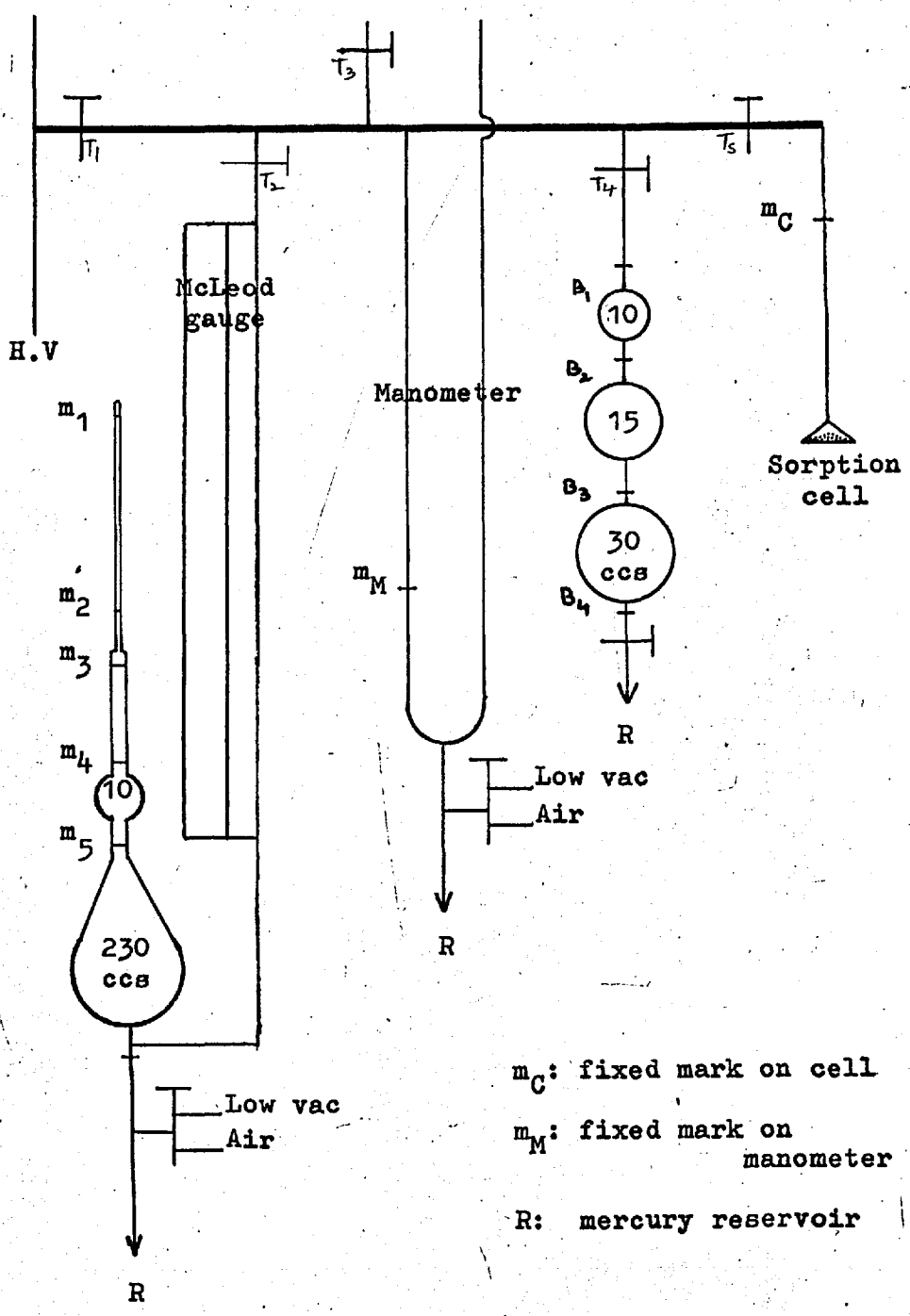

m_C: fixed mark on cell

m_M: fixed mark on manometer

R: mercury reservoir

Fig.4

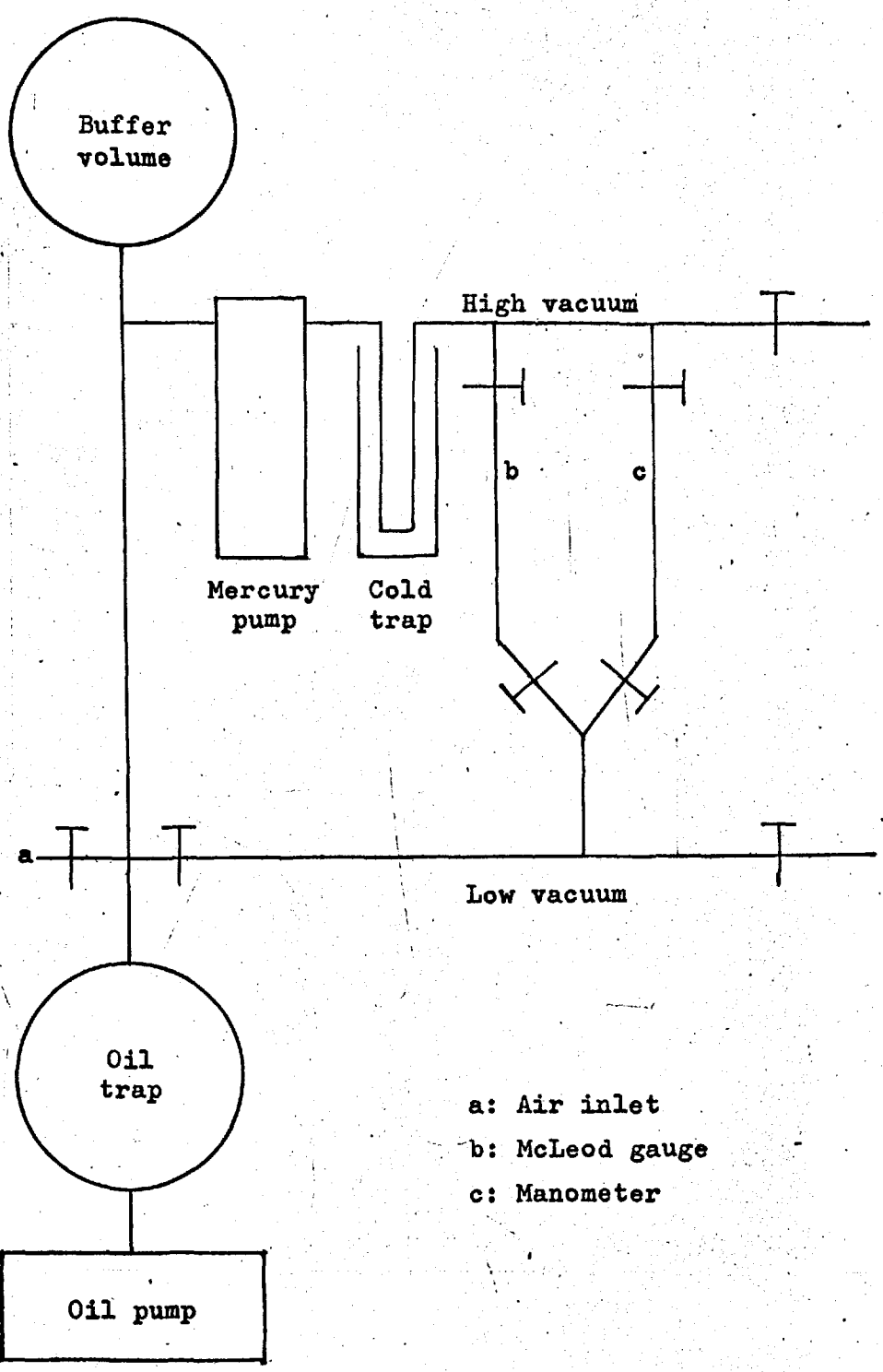
Buffer volume
High vacuum
b
c
Mercury pump
Cold trap
a
Low vacuum
Oil trap
Oil pump
a: Air inlet
b: McLeod gauge
c: Manometer

obtained by affixing a very thin strand of wire to the tube with "Sellotape". Mercury column heights were measured with a cathetometer reading to 0.001cm.

(3) McLeod gauge:- This was capable of measuring pressures better than 10^{-6} mm. Hg, and the total capacity was Ca. 245 cm^3. Five calibration marks were made on the gauge by laying two strips of "Sellotape" very close together and painting over the gap with black paint. A very fine line, easily visible with the cathetometer was left, on removing the "Sellotape". The gauge was calibrated before attachment to the system by filling to the mark with mercury and weighing. A very long thin capillary was used to transfer mercury to the capillary section of the McLeod gauge. It was weighed before and after each addition or subtraction of mercury, and the quantity of mercury itself was also weighed. Veridia tubing of uniform bore 1 mm. and 4 mm. was used for those tubes in which mercury columns were to be measured.

(4) Gas Burette:- This consisted of three bulbs of capacities Ca. 10, 15 and 30 mls. respectively. The volume of the bulbs between the calibration marks (B_1 - B_4) was found by weighing accurately the amount of mercury necessary to fill each bulb. Temperature fluctuations during sorption runs were minimised by surrounding each gas burette with an air-jacket.

(5) Doser Volume:- To find out the unknown capacity of the doser volume, pressure readings were taken with the manometer corresponding to the four different heights of mercury in the gas burette, and the doser volume was calculated using the expression:-

$$P_1 V_1/T_1 = P_2 V_2/T_2$$

and was found to be 31.70 cm^3. The unknown dosor volume, shown on Fig. (3), is the volume confined between taps T_1 to T_5 and mark mc. The sorption apparatus was glass blown on to and broken off at mark mc. The actual volume of the cell was determined from the weight of the mercury required to fill it. The dimensions of the cell are shown in Fig (5). The free volume of the cell was obtained by subtracting the volume of adsorbent, and plug of glass wool from total volume of cell.

3.1.2. Cryostat Bath:- The cryostat bath Fig (6) which was used in the temperature range -150 to $0C^{\circ}$, was constructed from a large strip-window Dewar vessel (D) (180 mm x 250 mm) and two beakers (N) and (P) of capacity 600c. c. and 2 litre respectively. The beaker (N) was covered on the outside with two sheets of aluminium foil and the free space between it and the beaker (P) was filled with asbestos wool (B). The beaker (P) was in intimate contact with a copper cylinder (C) and surrounded with liquid nitrogen which was used as refrigerant. The two beakers (N) and (P) were fixed to the perspex lid with a glue (F) prepared by dissolving perspex turnings in chloroform and adding red lead powder. This was very hard when dry, was insoluble in the bath liquid employed, and formed a seal to prevent the bath liquid from distilling over into the liquid nitrogen coolant. The perspex lid (E) was then sealed to the Dewar around its rim with plasticine. The perspex lid (E) was recessed

Fig.6

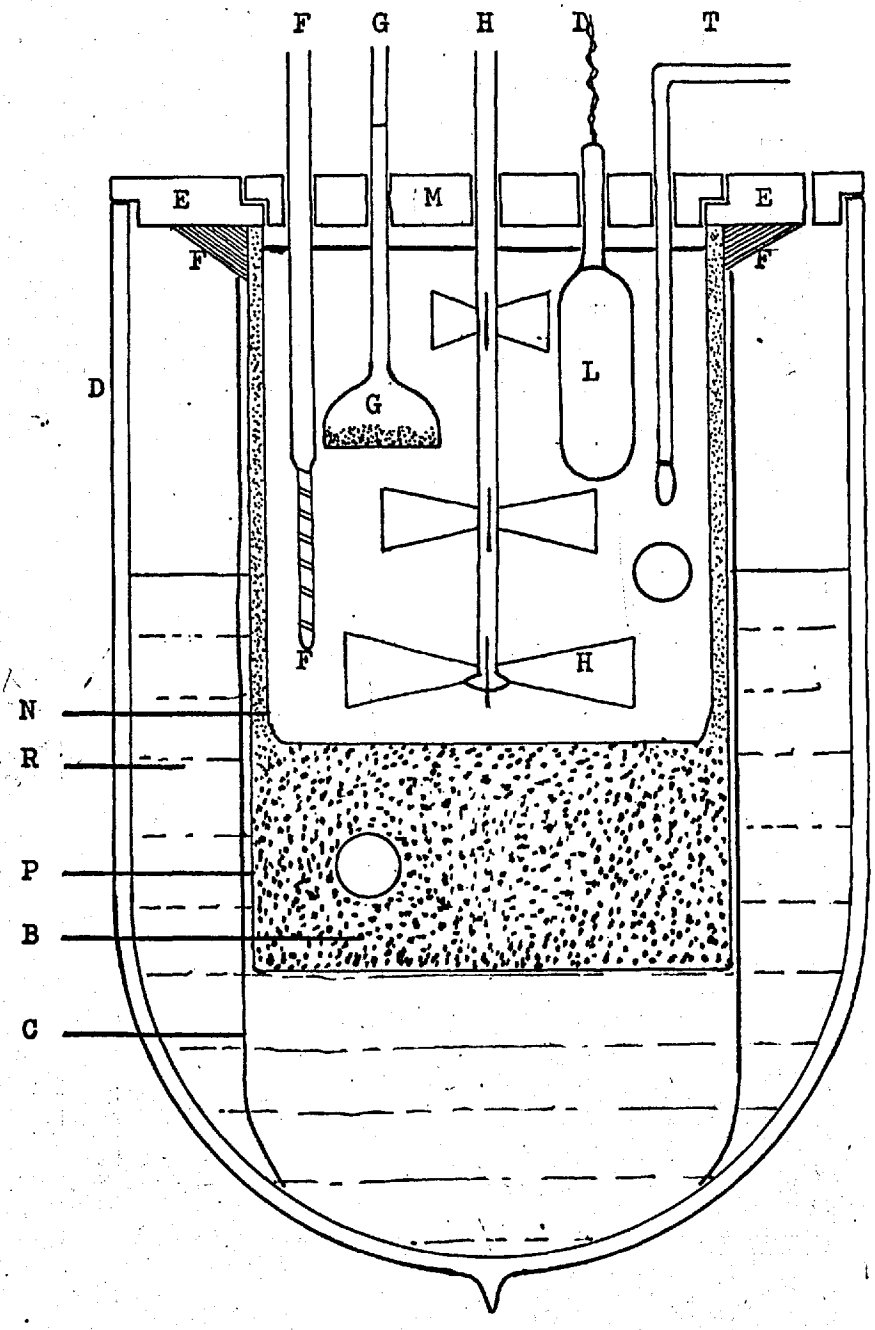

SORPTION CELL

Fig.5

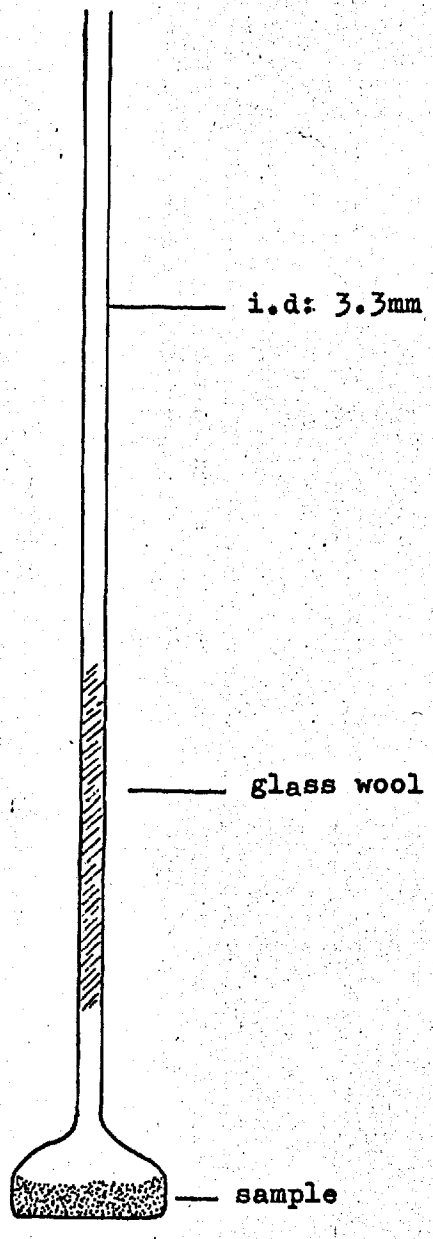

(Actual size)

in its centre and contained two semicircular removable lids (M) with several holes a piece. These allow entry of the various items required in the cryostat bath, i.e. metal stirrer (H), sorption cell (G), bimetallic spiral (F), vapour pressure thermometer (T), all of which were positioned relative to one another as shown in Fig. (6). Removal of heat from the bath by refrigerant (R) was compensated by a 15 - watt bulb (L), operating in conjunction with a "Sunvic T.S.7" bimetallic spiral. The heating bulb was wrapped in aluminium foil to prevent heating of the bimetallic spiral, or cell, or vapour pressure thermometer by radiation. Although good temperature control was obtainable using the system ($\pm$ 0.03C^{o}) with the bimetallic spiral control set at its most sensitive position, slow temperature drifts were occasionally observed which were corrected by manual adjustment of the control.

As the liquid nitrogen evaporated, at an approximate rate of $\frac{1}{2}$ pint, every half an hour, it was necessary for a constant temperature to frequently top up the system to a level depending on the temperature of the sorption run.

3.1.3. Bath Liquids:- Petroleum ether (B.P. 40C^{o}- 60C^{o}) was used as bath liquid and was found to be perfectly satisfactory in the range 0C^{o} to -100C^{o}. However, since it solidified in the region of -110C^{o}, temperatures below this required the use of isopentane as bath liquid (B.P. = +28C^{o}, F.Pt. =-158C^{o}). Since petroleum ether and isopentane are both highly inflamable liquids, suitable precautions were taken, e.g. absence of naked flame in the vicinity, the motor driving the stirrer was of the spark-free type, and liquid oxygen was never used as the

coolant, only liquid nitrogen.

For runs at 25C°, a 800 ml. beaker containing water was satisfactory, the room temperature acting as coolant, and a neon indicator lamp as heater. Liquid oxygen, contained in a Dewar vessel, was used as bath liquid, for argon sorption runs at 90. 19K°. Carbon dioxide and water vapours condensed out and frozen by the liquid oxygen were assumed to have no effect at this temperature.

3.1.4. Vapour Pressure Thermometer:- The temperature of isopentane and petroleum ether in the cryostat was measured with vapour pressure thermometers. An amonia thermometer was used in the range of - 40C° to - 70C°, a carbon dioxide thermometer in the range of -75C° to - 90C°, and an ethylene thermometer in the range - 100C° to - 150C°. For the sorption runs at 0C° and 25C°, a mercury in glass total immersion thermometer was used (0C° to 50C°). The construction of a vapour pressure thermometer will now be briefly outlined:-

The apparatus shown in Fig (7) was attached to the high vacuum line (H.V.) and pumped over night. The glass work was then flamed and pumping continued for a further 4 hours. Tap T_2 was then carefully opened and mercury from the reservoir (A) slowly admitted to the u - tube (O) until a height of approximately 55 cm. was attained on both sides. The mercury was carefully boiled in order to remove air bubbles and when finally a good vacuum was obtained the constriction (H) and (G) were completely sealed.

Carefully purified gas was frozen from (L) into (C) which was cooled in liquid nitrogen and the constriction (F) was sealed off. The condensate in (C) was

fig.7

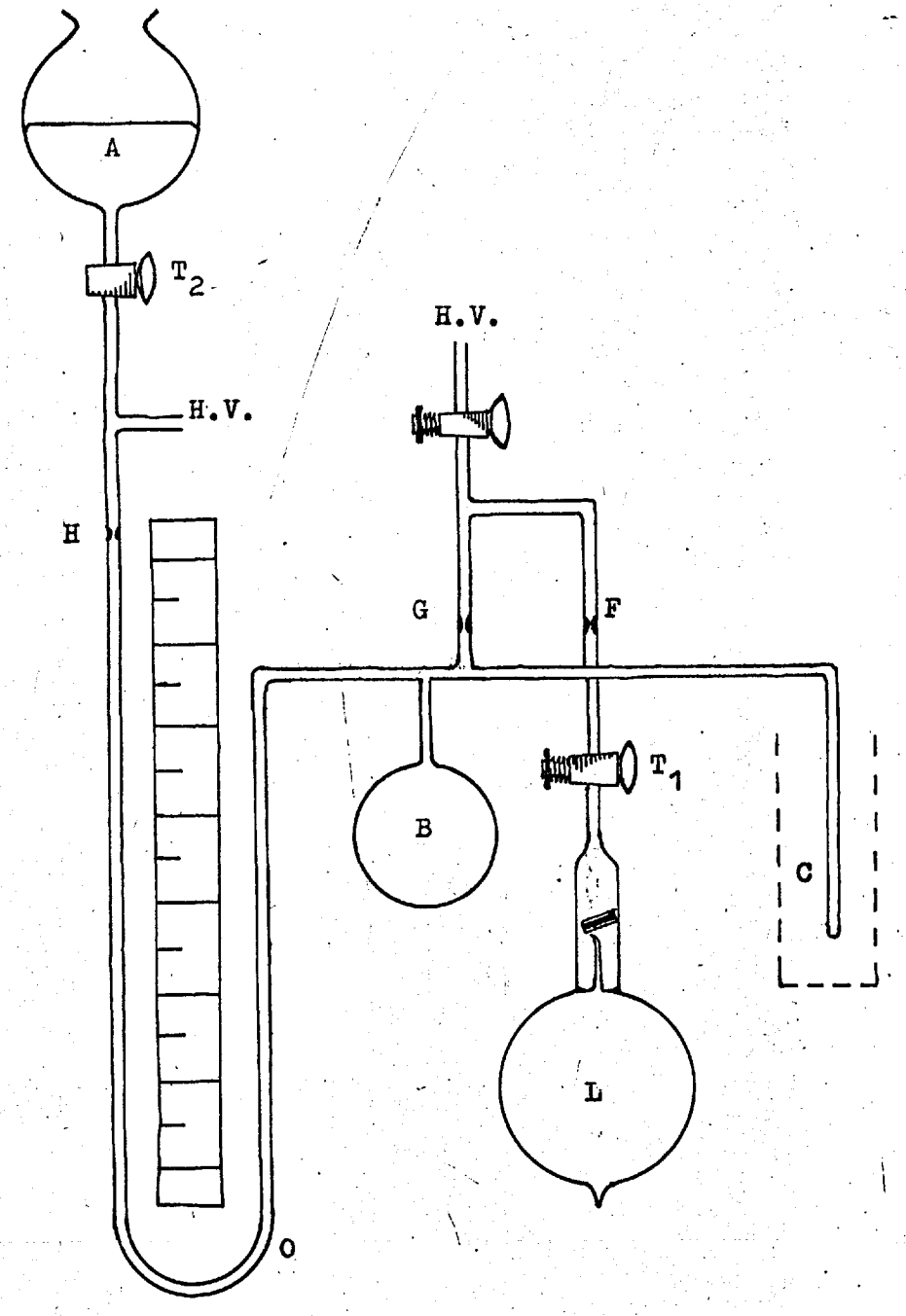

allowed to evaporate and enter the thermometer through the spring loaded tap T_1. Tap T_1 was closed when a pressure of approximately 100 cm. Hg. had built up in (O) and (C) was again cooled in liquid nitrogen. The construction of thermo-meter was completed by sealing off the constriction (F) while (C) was cooled in liquid nitrogen. The purpose of bulb (B) capacity 100 cm^3 is to increase the volume of gas in the thermo-meter so that on cooling, liquification occurs and not just thermal contraction of the gas.

3.1.5. Sample Preparation:- Approximately 1 gm. of sorbent was placed in a weighed sorption cell, the volume of which was known and its weight determined accurately. A small plug of glass wool was placed in the neck of the cell to prevent powder from being sucked into the sorption system during outgassing, and knowing its weight, an estimate of the volume of the gas that would then fill the remaining free space, could be made. The sorption cell was then glass blown on to the sorption apparatus.

Before each sorption run, the water content of the zeolite was obtained by heating 0.3 gm to destruction in a platinum crucible over a Meker burner at an approximate temperature of 1200C° for four hours and % of H_{20} was determined.

A standard outgassing procedure, i.e. to free the physically adsorbed water vapour, was used for each sorbent. The sorbent was first pumped for several hours at room temperature using the rotory oil pump only. The mercury diffusion pump is switched on and the pumping continued for several hours more. Then an electric

furnace was placed around the sorption cell and the temperature raised to 100C^{o} and maintained thus overnight. This whole operation involves a period of 24 hours. During the second day the temperature is slowly increased to 360C^{o} (Ca 20C^{o} per hour) under a vacuum of 10^{-5} to 10^{-6} mm. Hg. and maintained for another 24 hours, after which it is allowed to cool.

All the samples of Na-mordenite which were to be irradiated, were outgassed under the above conditions and sealed in silica ampoules. The sample has to be re-exposed after irradiation in order to fill the sorption cell. The irradiated material was sieved (200 mesh) so that traces of silica left while breaking open the silica ampoule, are removed. It was then stored over saturated ammonium chloride in a desiccator for a couple of days. It was consequently necessary to completely re-outgass irradiated samples. Samples 13 and 14 were irradiated at liquid nitrogen temperature and were the only exception to this rule. These were joined to the sorption apparatus, and seal was broken under high vacuum, using a specially designed break-seal apparatus for this purpose. (Described in detail in section 3.2).

Krypton, oxygen, hydrogen and argon were employed for the sorption work and helium for the initial calibration of doser volumes. All were supplied in litre bulbs, equipped with a break seal, from the British Oxygen Co. Ltd. The purity specifications were:-

Krypton	.....	99 - 100% (Balance xenon)
Oxygen	.....	Pure
Argon	.....	Spectrally pure
Helium	.....	Spectrally pure

3.1.6 Construction of Sorption Isotherms:- Isotherms are usually measured at 20° intervals always beginning at the highest temperature. All pressures on the manometer were read correct to 0.005 cm. using cathetometer. At lower temperature, however, it was found advantageous to employ the extra volume resulting from use of the McLeod gauge, in order to introduce a sufficiently large initial dose of gas to the sample. The tap of the McLeod gauge was usually closed, for subsequent points, the volume of the gas so removed from the system was subtracted from the total. The chief use of McLeod gauge was, of course, for the very low pressure measurements. Correction for the capillary depression of the mercury menisci were made using the data given by Kay and Laby (56). It was not necessary to bring the mercury in the manometer exactly to the fixed mark mM, the diameter of the manometer was known and it was therefore possible to calculate the change in the doser volume.

The doser volume was filled with the required gas and its pressure measured. The room temperature was noted. Using the perfect gas law the volume of the gas in the doser volume was converted to Cm^3 at S.T.P. Tap T_5 was then opened and the pressure and temperature again read when equilibrium was reached after thirty minutes.

After the first equilibrium point had been measured the mercury in the gas burette was raised to mark B_2. The new equilibrium point was measured and the mercury raised to mark B_3. Sometimes especially at low pressures raising the mercury level in the gas burette produces only very small changes in pressure and it is necessary

to close the Tap T_s and introduce a new dose of gas. By measuring the change in pressure and applying the ideal gas law, the extra volume of gas taken into the system can be calculated.

The above procedure was repeated until an equilibrium pressure of about 55 cm. Hg was reached and then a desorption isotherm was measured. This is merely the reverse of the sorption procedure, doses of gas are successively removed from the sorption system and frozen back into the gas line, using liquid nitrogen trap.

At - 150C°, as many as ten consecutive pressure readings were taken with McLeod gauge up to 0.5 cm. Hg. at which point the tap to the gauge was closed and succeeding pressures determined with manometer. After such a series of pressure measurements, it was considered that any cumulative errors so far incurred would be magnified in the isosteric heat curves which were to be calculated from these isotherms. Since the most important region of pressures was between 1 mm to 3 cm in this respect, this region was invariably repeated. At - 140C° only a few pressure measurements were made with the McLeod gauge, and at higher temperatures (-130C° and -120C°), pressure measurements could be made directly with the manometer, only using the McLeod gauge to supply a large enough initial dose to the sample.

The room temperature was maintained as near constant as possible throughout the pressure readings, especially when using the McLeod gauge, and a correction was made for the temperature of the gas between the room temperature section of the apparatus, and the gas in the sorption

cell itself (shown in Fig. 6 as length l)

3.1.7. Correction for Thermal Transpiration:- The difference between the temperature of the cryostat and the volumetric system, was as much as 175C°, during the sorption runs, also the diameter of the neck of the sample tube over which this difference existed was of the order of 2 mm, it was found to be essential to apply corrections for thermal transpiration. This must be applied because the pressure in the sorption cell is actually less than in the rest of the sorption system. Liang (59) gave the equation for the true equilibrium pressure (Pt mm. Hg.) as:-

$$Pt = Pm \left[1 - \frac{1 - (T_1/T_2)^{\frac{1}{2}}}{\alpha_{He}\, \phi^2_g\, Pm^2\, D^2 + \beta_{He}\, \phi_g\, Pm\, D + 1} \right]$$

where Pm = measured pressure (mm. Hg.)

T_1 = temperature of sample (K^o)

T_2 = " " volumetric system (K^o)

D = internal diameter of tube over which thermal gradient occurs (mm.)

α_{He} = constant for reference gas (He = 2.5_2)

$\beta_{He} = 7.68\ (1 - T_1/T_2)^{\frac{1}{2}}$

ϕ_g = pressure shifting factor of adsorbate ($\phi_A = 2.93$) ($\phi_{Kr} = 3.84$)

Although the correction is very small and of the order of 1 - 2%, it is significant enough to apply for low

pressure (McLeod) readings, in case of argon/90K° and krypton/$_{-150C^{o}}$ systems.

3.1.8. Sorption of Krypton:- Na-mordenite/Krypton system was studied at comparatively low temperatures (-100, -90, -70, -40, 0, +25C°) in order to establish the value of the isosteric heat of adsorption on the most energetic sorption sites.

Sorption runs in the temperature range -120 to -150C° were carried out very carefully, since these provided the data to which various limiting isotherm models could be applied. Isotherms were constructed with great care, so that accurate isosteric heat data could be calculated. For each isotherm (-120 to -150C°) the important range was between 1 - 10 cm. Hg, hence this was usually repeated. The sorption runs at 25C° were used to compare the effects of radiation where as Na-mordenite/Argon system at 90. 19K° was studied in order to compare the saturation capacities between the standard and irradiated samples.

3.2 Neutron Irradiation:-

3.2.1. Preparation of Samples for Irradiation:-

Silica ampoules used for irradiation purpose, were of the dimensions shown in Fig. (8a) and were contained in standard aluminium irradiation cans of the type shown Fig. (8b). All these silica ampoules were constructed with long necks and B_{10} ground silica cones, so that they could be fitted directly to the outgassing system. About 5g. of Na-mordenite were weighed into the silica ampoule, and dehydrated at 360C° under a vacuum of 10^{-6} mm. Hg. (see standard outgassing procedure page 66). After outgassing they were sealed off at the base of the neck. If they were not dehydrated, the irradiation decomposed the water (14% by weight) present in the sample, as upon unsealing the ampoules (24) a pressure of the order of one to two atmosphere was observed and considered to be due to the presence of hydrogen and oxygen.

3.2.2. Details of Irradiated Samples:- All the samples for the present work were irradiated in the core of "Herald" at Aldermaston. Each of the samples irradiated will be discussed, according to the details supplied by the U.K.A.E.A. reactor group.

After removal from the reactor, all the samples were allowed to decay over a period of one week, this being sufficient for all the expected activities to have decayed to an inappreciable level. Samples were, however, monitored upon return, with a Dynatron Monitor unit, type 1021C, and found within permissible limits.

IRRADIATION CAN AND AMPOULE

Fig.8

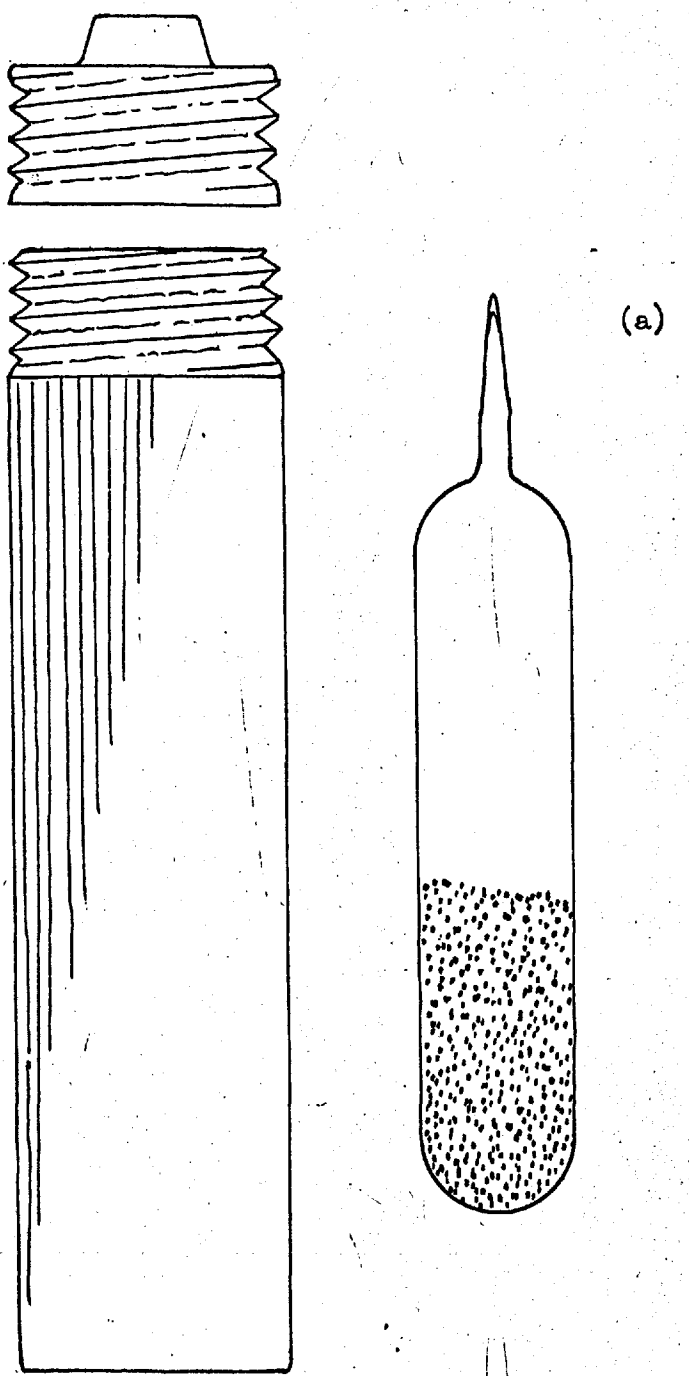

(Actual size)

Fig.9

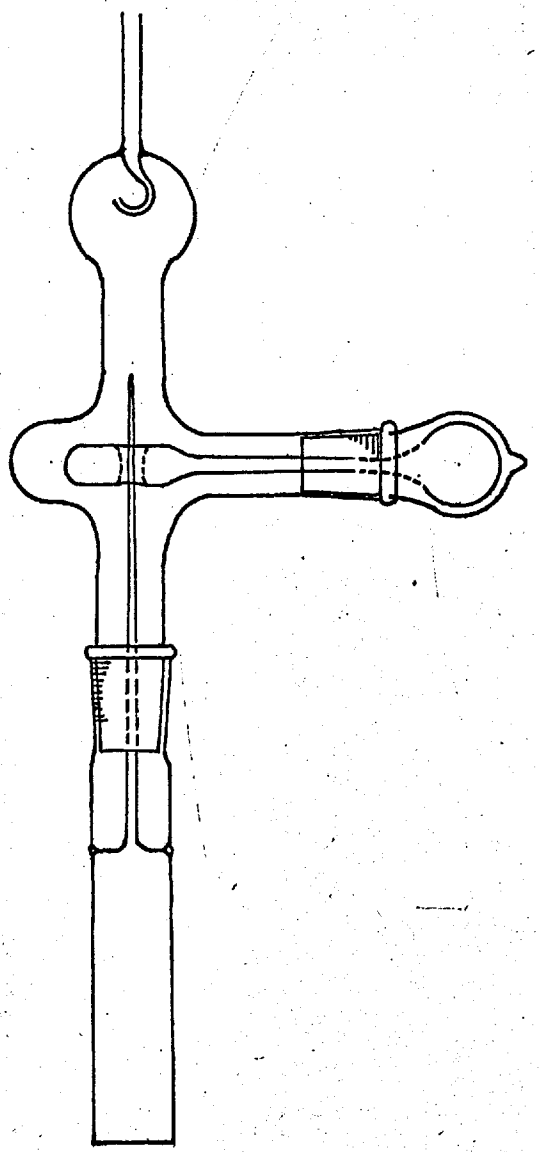

Superscript * has been used throughout this work and refers to irradiated and damage sample of Na-mordenite, i.e. those which were observed to suffer a loss in sorptive capacity. The standard samples are denoted by the superscript O.

Sample 1:- ($Na\text{-mordenite}^{*}_{1}$) This was irradiated in the fast flux of "Herald" at Aldermaston to an integrated neutron flux of 1.615×10^{19} n/cm^2, averaged over the fission neutron spectrum. The dose was measured employing Ni^{58}_{28} (n, p) Co^{58}_{27} transmutation; a nickel wire was included with the sample. The sample was found to be 14.7% damaged, using Na-mordenite/Argon system at 90.19K°.

Sample 2:- ($Na\text{-mordenite}^{*}_{2}$) This was irradiated to a total integrated neutron flux of 3.3×10^{19} n/cm^2 and the damage was 60.0%

Sample 3:- ($Na\text{-mordenite}^{*}_{3}$) This received an integrated neutron flux of 1.79×10^{19} n/cm^2 and was damaged slightly more than sample 1.

Sample 4:- ($Na\text{-mordenite}^{*}_{4}$) This was irradiated to a maximum integrated neutron flux of 1.36×10^{20} n/cm^2 and was found to be completely amorphous and to absorb only a minimum of Argon sorbate.

Sample 5:- ($Na\text{-mordenite}^{*}_{5}$) This was also found to be 100% damaged at an integrated neutron flux of 5.0×10^{19} n/cm^2.

Sample 6:- ($Na\text{-mordenite}^{*}_{6}$) This was irradiated to a total dose of 3.48×10^{18} n/cm^2 and the damage was 2.8%.

Sample 7:- ($Na\text{-}mordenite^{*}_{7}$) This received the same dose as sample 1.

Sample 8 and 10:- Both were irradiated to a total dose of 3.60×10^{19} n/cm^2 and the damage was 65.4%

Sample 11:- ($Na\text{-}mordenite^{*}_{11}$) This was irradiated to a total integrated neutron flux of 2.8×10^{19} n/cm^2 and was found to be 49.5% damaged.

Sample 12:- ($Na\text{-}mordenite^{*}_{12}$) This was another silica ampoule designed for gas analysis and irradiated to a total dose of 2.35×10^{19} n/cm^2. No gas could be found when the seal was broken under a vacuum of 10^{-6} mm. Hg.

Sample 13:- ($Na\text{-}mordenite^{*}_{13}$) This was irradiated at liquid nitrogen temperature, using the facilities provided at Aldermaston. A special silica ampoule and break seal apparatus of the dimensions shown in Fig. (9) were designed for this purpose. Great care was taken in maintaining liquid nitrogen temperature, throughout this experiment. This sample was irradiated to a total dose of 0.712×10^{18} n/cm^2 and the damage was 5.5%.

Sample 14:- ($Na\text{-}mordenite^{*}_{14}$) This was irradiated exactly under the same conditions as sample 13 and received a total dose of 0.80×10^{19} n/cm^2 The damage in this case was found to be 19.2%.

CHAPTER 4

Results and Discussion

4.1. Gas Adsorption

4.2. Neutron Irradiation

4.3. Some Experiments with Cation Exchange

4.1. Gas Adsorption

4.1.1. Detection of Damage in Irradiated Samples:-

The method employed to determine the damage sustained by the zeolite was to compare the amount of argon sorbed at 90°K. in the unirradiated material with the amount sorbed by the irradiated samples. Approximately 120 c.c. of argon (N.T.P.) are sorbed at a pressure of 54 cm. Hg by one gram of standard material.

All unirradiated and irradiated samples were outgassed according to the standard procedure (see section 3.2.1. page 66). Sorption runs with argon at 90K° were repeated in order to construct an accurate isotherm. The results of these runs for unirradiated and irradiated samples are shown in figure 10. Distinct decreases in sorptive capacity were observed with the samples given in the following table.

Table 1.

Sorption of Argon and Krypton

Sample	Neutron Dose (n/cm^2)	Saturated Capacity For Argon (90K°)	Saturated Capacity For Krypton (153K°-123K°)	% loss in Cap. For Argon	% loss in Cap. For Krypton
Na-mordenite * 0		120 c.c	104.7 c.c		
Na-mordenite * 1	1.615×10^{19}	102.9 c.c	89.3 "	14.2%	15.5%
Na-mordenite * 2	3.3×10^{19}	52.3	44.6 "	56.7%	59.4%
Na-mordenite * 3	1.79×10^{19}	101.2	87.3 "	15.9%	17.2%
Na-mordenite * 4	1.36×10^{20}	0	0 "	100%	100%
Na-mordenite * 5	5.0×10^{19}	0	0 "	100%	100%
Na-mordenite * 6	3.48×10^{18}	118.3	102.1 "	1.7%	2.9%
Na-mordenite * 8-10	3.60×10^{19}	48.1	36.4 "	60%	65.8%
Na-mordenite * 11	2.8×10^{19}	61.8	52.3 "	48.4%	50.5%
Na-mordenite * 13	0.712×10^{18}	-	-	5.5%	-
Na-mordenite 14	0.80×10^{19}	-	-	19.2%	-

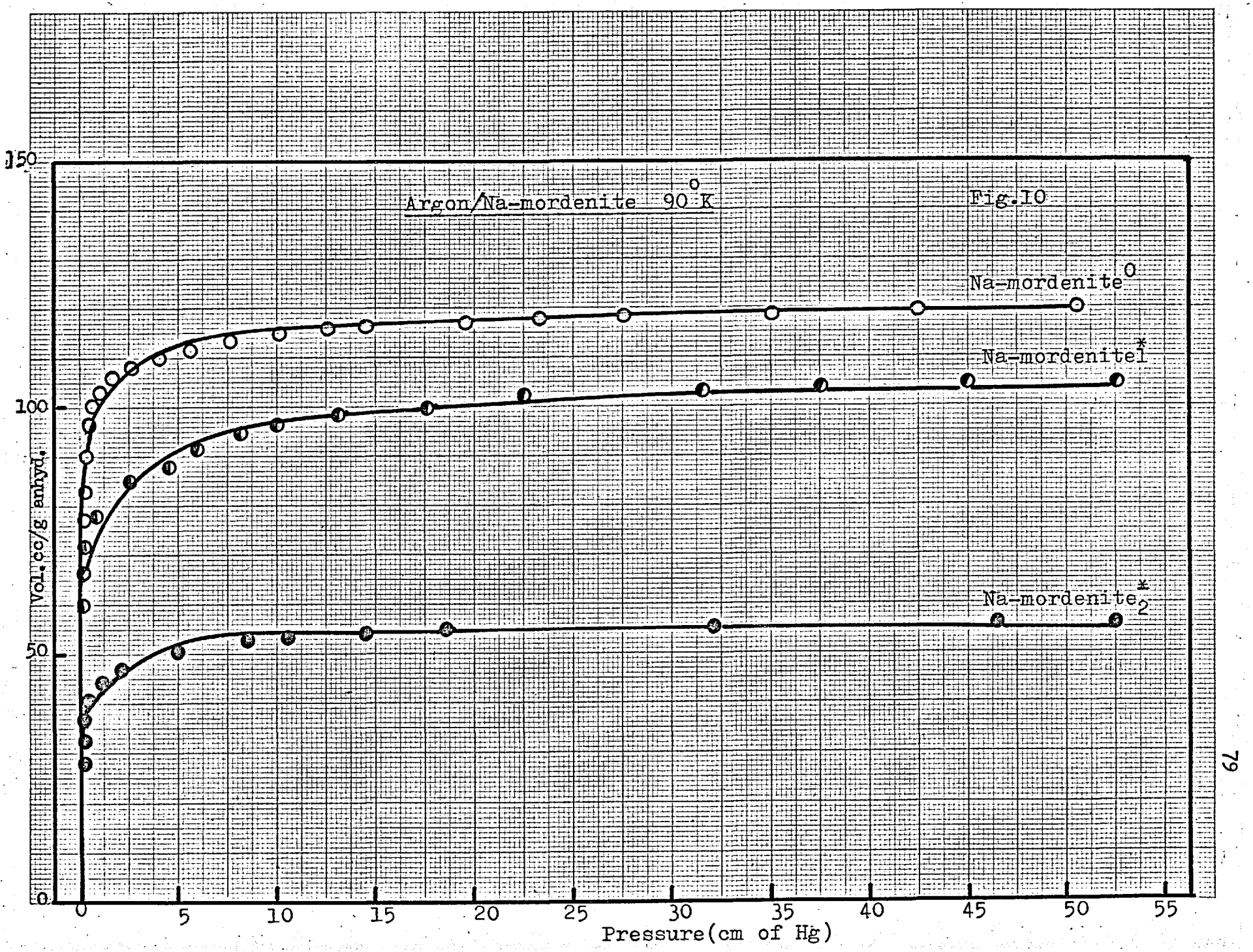
Argon/Na-mordenite 90°K
Fig.10
Na-mordenite°
Na-mordenite*1
Na-mordenite*2
Vol.cc/g anhyd.
Pressure(cm of Hg)
0
50
100
150
0
5
10
15
20
25
30
35
40
45
50
55

In order to ascertain if neutron irradiation affected the most energetic sites, sorption runs were also conducted on irradiated samples with krypton at 25C° where Henry's law is obeyed. In this case the volume of the gas sorbed at 52 cm. Hg. pressure was about 20 c.c. (N.T.P.) /g. There appeared to be no observable change in the case of Na-mordenite$^*_1$ (1.6×10^{19} n/cm^2). However, Na-mordenite$^*_2$ showed about 31% damage, whereas in the sorption run with argon at 90°K, the damage was 57%. This suggests that radiation induced damage does not have noticeable effect on the most energetic sorption sites when the fast neutron dose is 1.6×10^{19} n/cm^2, but as the dose is increased even the energetic sorption sites are affected to some extent. Results are shown in figure 11. The plot for Na-mordenite$^*_5$ at 25C° supports the fact that some of the energetic sites are still capable of sorption, whereas no sorption of argon at 90°K was observed.

Sorption of Na-mordenite$^*_1$ with krypton was studied from 25C° to -150C° in -10C° increments. Coincident isotherms with unirradiated material were obtained down to - 100C° (fig. 12). However, at - 110C° it showed 14.5% difference in sorption capacity, and this loss in sorption capacity increased slowly to 15.5% by -150C°. It seems that at temperature $<$ -100C° gas molecules do not have sufficient energy to diffuse into channels through windows which must be slightly smaller than the krypton atoms. This phenomenon was found with NaX (1). Irradiation with fast neutron causes the lattice to contract but no small areas of complete collapse can occur or the sorption in the irradiated material would be smaller than that for the standard sample at all temperatures.

The result of sorption runs with krypton for Na-mordenite$^*_1$

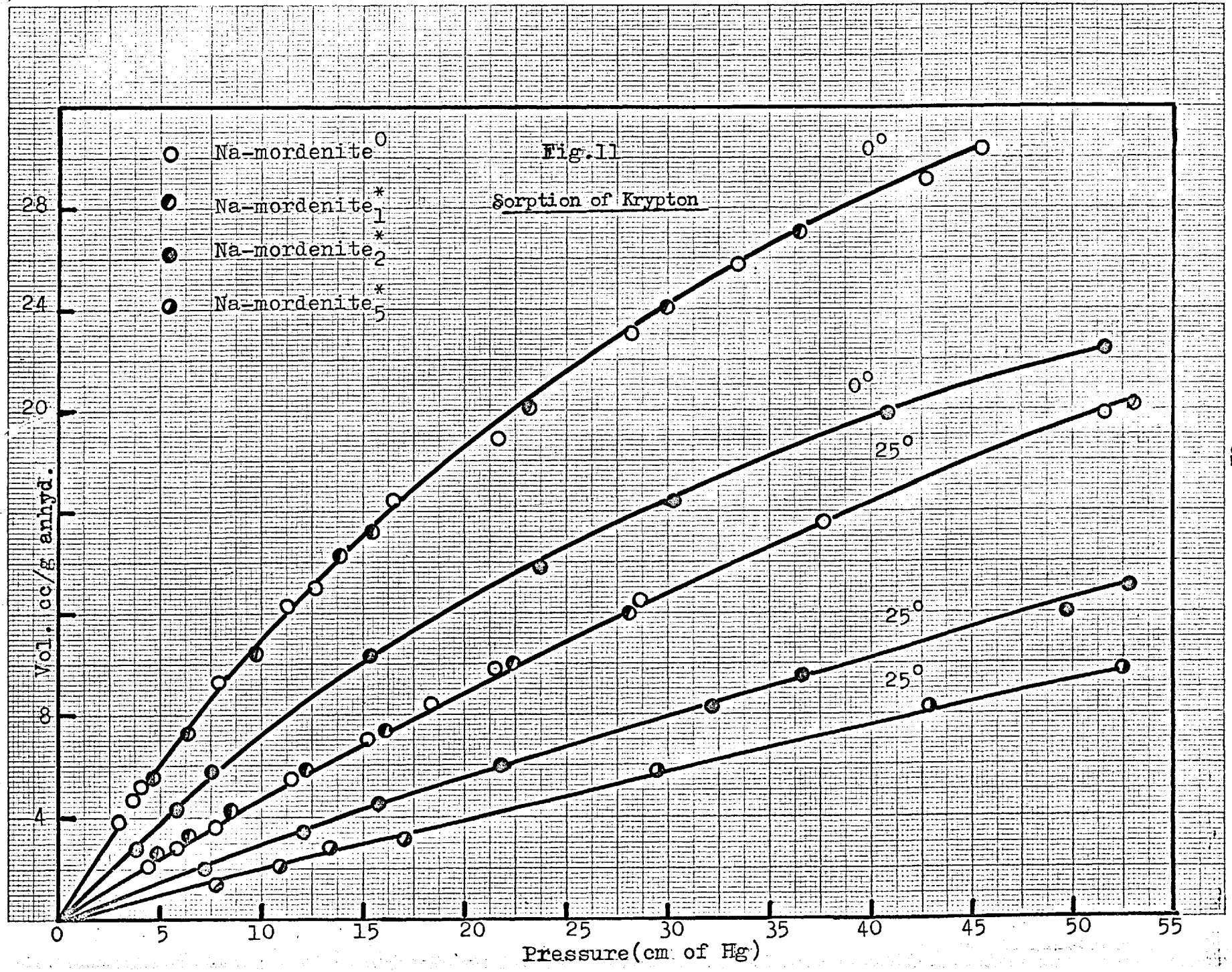
Fig.11
Sorption of Krypton
Na-mordenite 0
Na-mordenite* 1
Na-mordenite* 2
Na-mordenite* 5
0°
0°
25°
25°
25°
Vol. cc/g anhyd.
4
8
20
24
28
0
5
10
15
20
25
30
35
40
45
50
55
Pressure (cm of Hg)

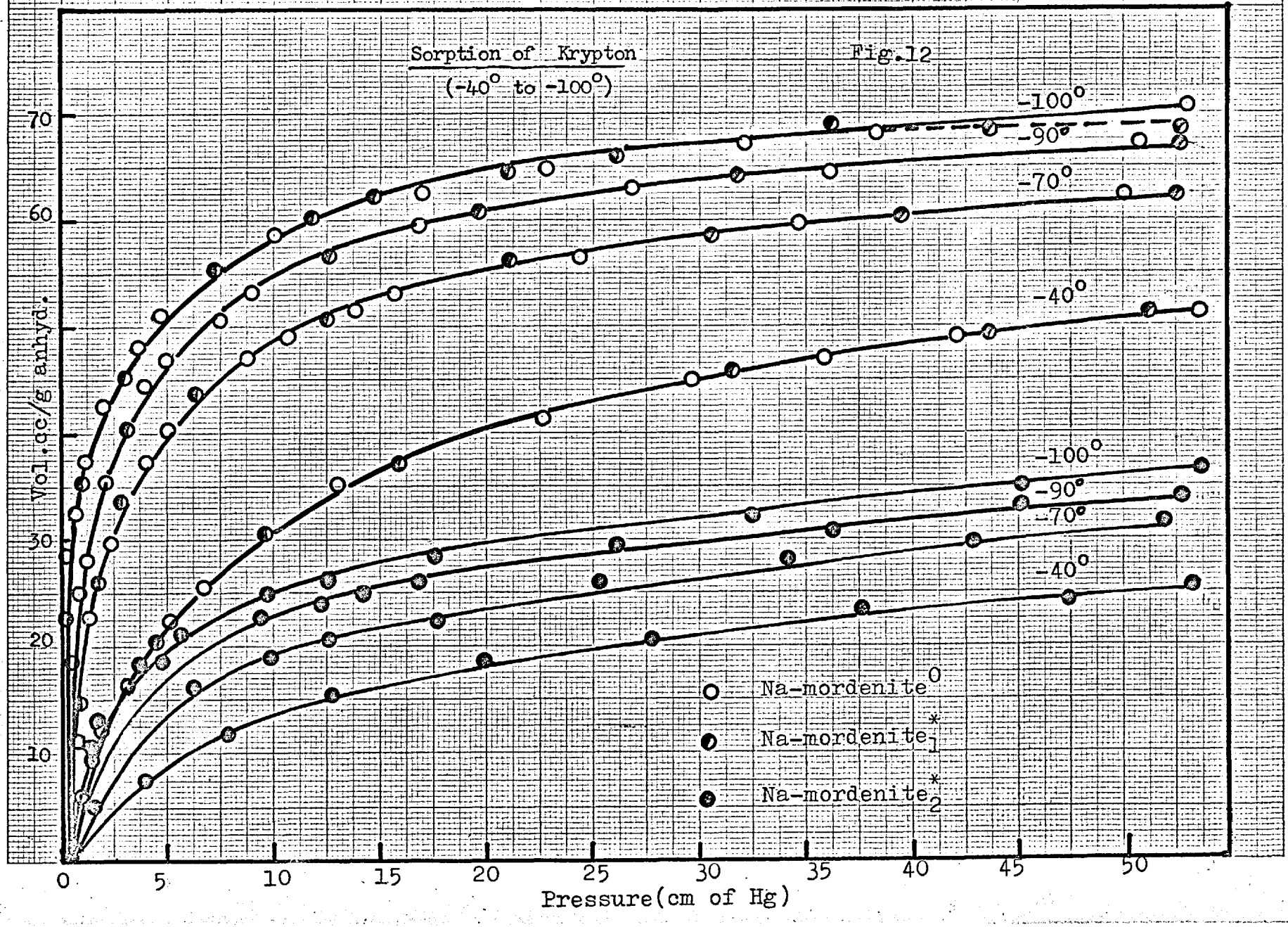
Sorption of Krypton
(-40° to -100°)
Fig.12
-100°
-90°
-70°
-40°
-100°
-90°
-70°
-40°
Na-mordenite0
Na-mordenite*1
Na-mordenite*2
Vol. cc/g anhyd.
Pressure (cm of Hg)
0
5
10
15
20
25
30
35
40
45
50
10
20
30
60
70

and Na-mordenite$_2^*$ in the temperature range - 120 to - 150C$^\circ$ are shown in figure 13. These results were employed to obtain isosteric heat data.

4.1.2. Adsorption of Krypton by Na-mordenite

Henry's law of adsorption is given by the following equation:-

$$V = K. P.$$

Below 0C$^\circ$, all the isotherms constructed for krypton/Na-mordenite system were found to be linear within the limits of detection up to between 20 and 40 c.c. adsorbed (N.T.P.) after which they gradually curve towards the abcissa. The low temperature isotherms were "rectangular" in shape corresponding to type 1 of Brunauer (9) classification which represents uni-molecular layer adsorption. The plots shown in figure 13 are typical of the isotherms constructed, all of which were found to be free of hystersis, i.e. adsorption points coincided with desorption points. Figure 13 also shows the isotherm at temperature -120 to -150C$^\circ$ for 60% damaged sample. They have been constructed along with the standard sample so that a comparison could be made.

4.1.3. Saturation Capacities of Na-mordenite for Krypton

Saturation capacities, i.e. the volume of gas required to completely saturate the intercrystalline volume, can be obtained by the various methods described below, together with their applicability or otherwise to the sorption of krypton by Na-mordenite.

(1) By extrapolating the linear position of a graph of $\log_{10}$ P against $\log_{10}$ V.

(2) Extrapolation of the rectangular isotherm as far as the

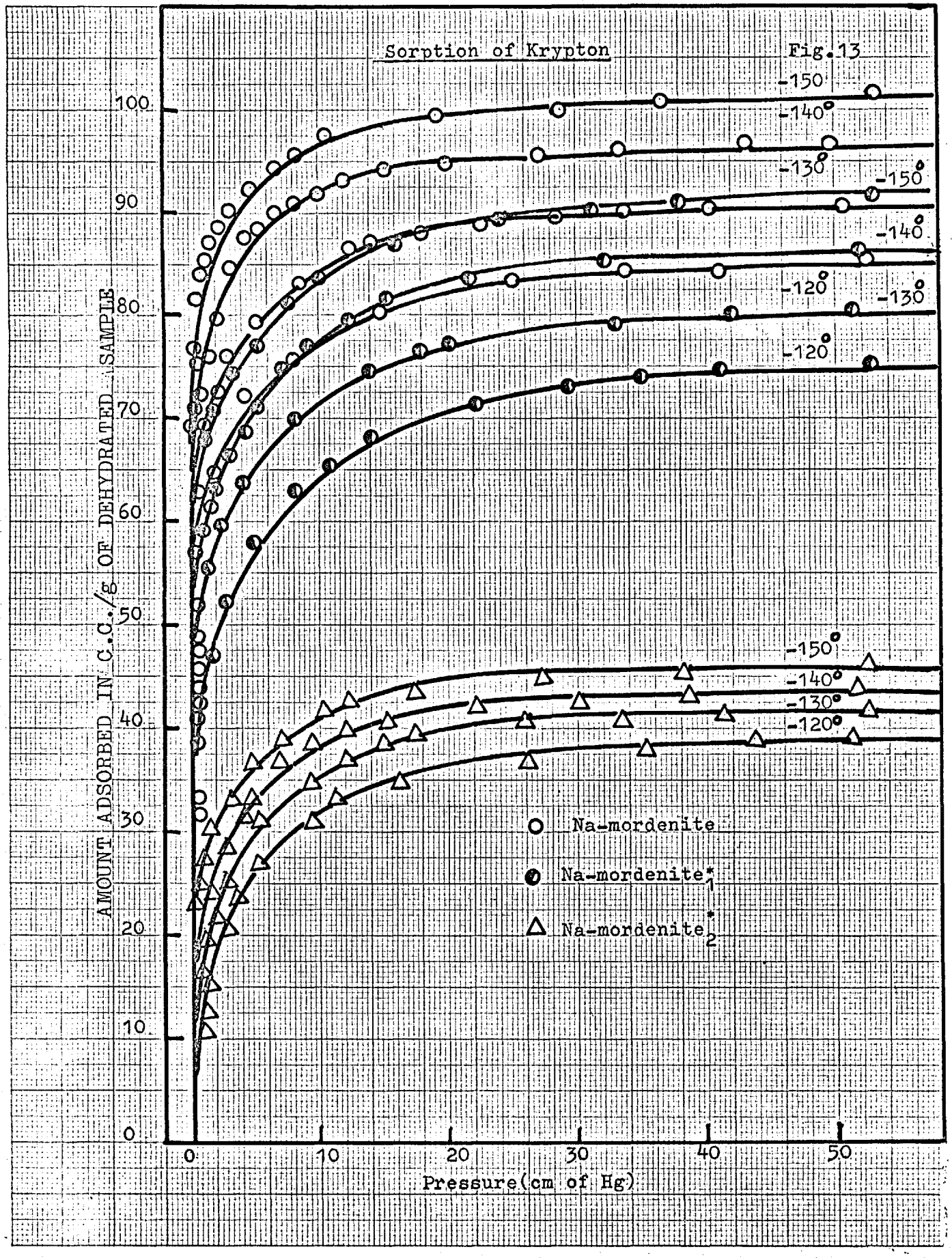
Sorption of Krypton
Fig. 13
-150°
-140°
-130°
-150°
-140°
-120°
-130°
-120°
-150°
-140°
-130°
-120°
Na-mordenite
Na-mordenite*1
Na-mordenite*2
AMOUNT ADSORBED IN C.C./g OF DEHYDRATED SAMPLE
0
10
20
30
40
50
60
70
80
90
100
0
10
20
30
40
50
Pressure (cm of Hg)

saturation vapour pressures for each temperature, when a direct reading of V sat. is possible on the ordinate axis. For krypton at -150C° this involves an extrapolation from approximately 54 cm. Hg. pressure up to 96 cm. Hg. and even larger at higher temperatures. Such extrapolation introduces too great an error, hence this method was not employed.

(3) Comparison with volume of water required to saturate the intercrystalline pore space. This method is open to criticism as it assumes that the water and krypton molecules both occupy the same cavities and channels.

(4) Plots of (P/V) against (P) were drawn for the isotherms constructed between the temperatures -120C° and -150C°. These plots give a straight line at low pressures (in accordance with Langmuir isotherm) which becomes very gentle curve at higher pressure. From the limiting slope of these graphs in the high pressure regions, values of saturation volumes may be obtained. Since the curvature of these plots is barely discernable, a reliable value of V. sat is easily calculated. The results thus obtained both for irradiated and unirradiated samples are tabulated as follows:-

Table 2

Saturated Capacities for Standard and Damaged Samples (c.c. Kr (N.T.P.)/g. dehydrated Na-mordenite

Temp. (C°)	Na-mordenite°	Na-mordenite*$_1$	Na-mordenite*$_2$	Na-mordenite*$_5$	Na-mordenite*$_{11}$
-120	87.0 c.c.	75.4 c.c.	39.4 c.c.	0 c.c.	42.7 c.c.
-130	93.0 c.c.	81.0 c.c.	41.0 c.c.	0 c.c.	46.4 c.c.
-140	100.0 c.c.	86.0 c.c.	43.5 c.c.	0 c.c.	50.3 c.c.
-150	104.7 c.c.	89.3 c.c.	45.7 c.c.	0 c.c.	53.1 c.c.

Na-mordenite$^{*}_{5}$ sorbed only 3.0 c.c. of argon at 90K^{o} and 54 cm. Hg. pressure, whereas the standard sample sorbed 120 c.c. argon under the same conditions. The "isotherm" was found to be non-reproducible, even if a few hours were allowed for "equilibrium" to be attained before each pressure reading was taken. Gas was found to trickle in continuously at 90K^{o}. Since krypton is a larger atom than argon, no attempt was made to measure the sorption of krypton in this sample, and the % loss in the saturation capacity is quoted as 100% for this sample. Na-mordenite$^{*}_{4}$ also gave similar results. The % loss in saturation capacities for the other samples are shown in the following table:-

Table 3

% loss resulting from radiation damage in saturation capacity for krypton:-

Temp. (C^{o})	Na-mordenite* 1	Na-mordenite* 2	Na-mordenite* 5	Na-mordenite* 8	Na-mordenite* 11
-120	14.9%	59.3%	100%	65.0%	49.6%
-130	15.2%	59.6%	100%	65.5%	50.1%
-140	15.4%	60.0%	100%	65.7%	50.5%
-150	15.6%	59.7%	100%	65.4%	50.7%

An x-ray photograph of Na-mordenite$^{*}_{5}$ showed a few single lines, thus indicating mostly amorphous material. Therefore, it can be concluded that Na-mordenite$^{*}_{5}$ suffered some form of lattice collapse as a result of an integrated neutron flux of 5.0×10^{19} n/cm^{2}. Since the high temperature krypton

sorption indicated a lattice contraction the sorption of hydrogen, which is smaller in size than argon or krypton was studied. However, as with argon little hydrogen was sorbed by this sample. However, the sorption of hydrogen in Na-mordenite* at 90°K was measured and compared with standard Na-mordenite[11]. A decrease in damage from 50% (with argon at 90°K) to 26% was observed as shown in figure 14c. This could be argued on the basis that more hydrogen molecules are capable of diffusing through the contracted channels of Na-mordenite than argon or krypton because of the smaller size of hydrogen molecule whereas in the case of Na-mordenite* there is complete collapse of the lattice[5] or complete collapse of the entrances of the channels such that no sorption can take place.

4.1.4. Intracrystalline volume of Na-mordenite:-

Saturation capacities of Na-mordenite for krypton decreased with increase in temperature. This is shown for the standard and irradiated samples in figure 14a.

The intracrystalline volume of Na-mordenite may be calculated as follows:-

At the saturation vapour pressure of krypton at -150C°, one g. Na-mordenite sorbs 104 c.c. (N.T.P.) gas. Since one mole (83.8 g) occupies 22.4 litres at N.T.P. 104 c.c. is equivalent to 0.389 g of krypton. The density of liquid krypton (adsorbed gas is assumed at saturation to possess the properties of bulk fluid, (see following section) at -150C° is 2.390 g/c.c. Therefore, 0.389 = 0.163 c.c. krypton at N.T.P. sorbed by one g of anhydrous Na-mordenite.

Figure 14b shows the plot of tabulated liquid krypton

Fig.14 (a)

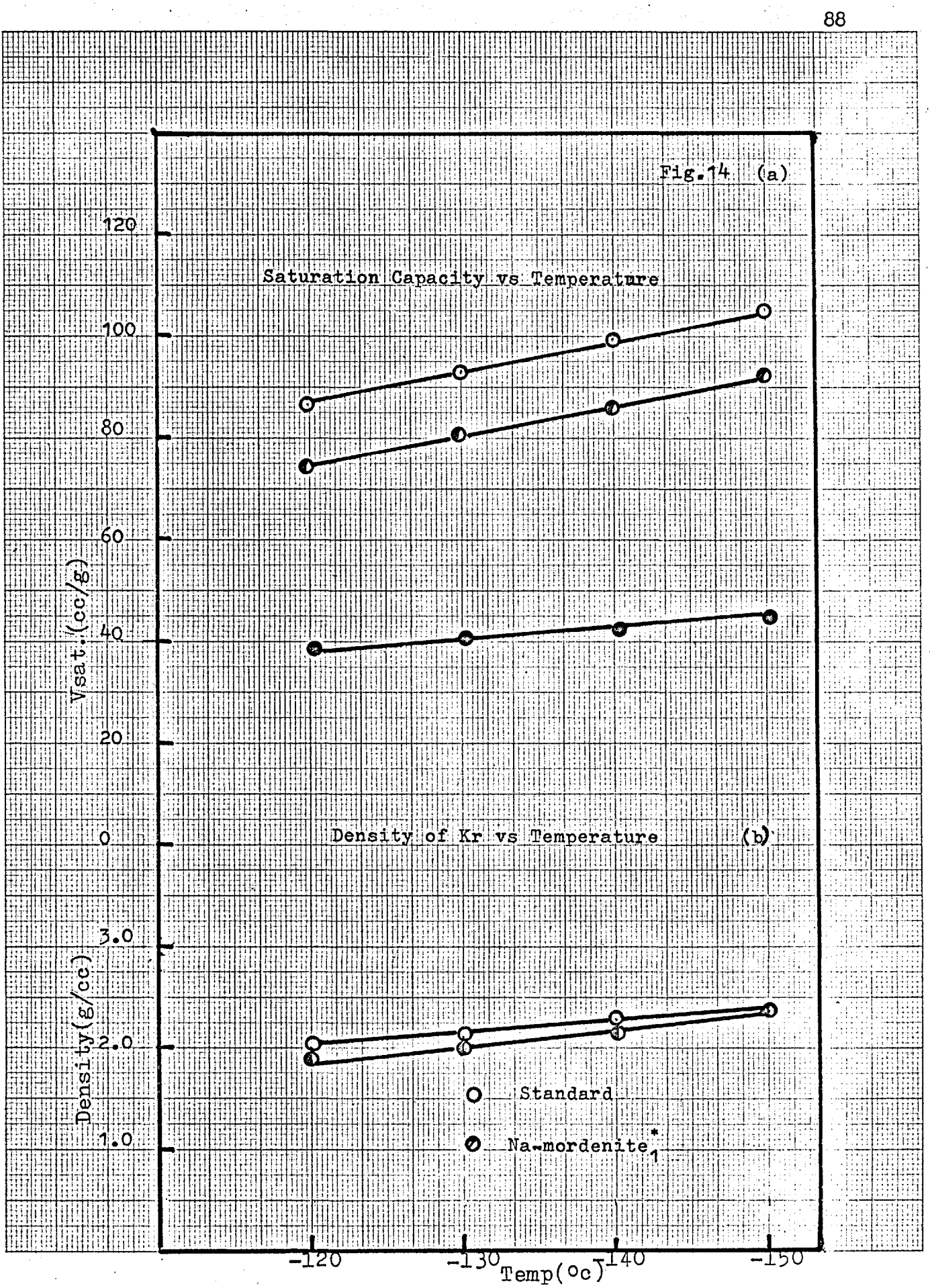
Saturation Capacity vs Temperature
120
100
80
60
40
20
0
Vsat.(cc/g)
Density of Kr vs Temperature (b)
3.0
2.0
1.0
Density(g/cc)
Standard
Na-mordenite*1
-120
-130
-140
-150
Temp(°c)

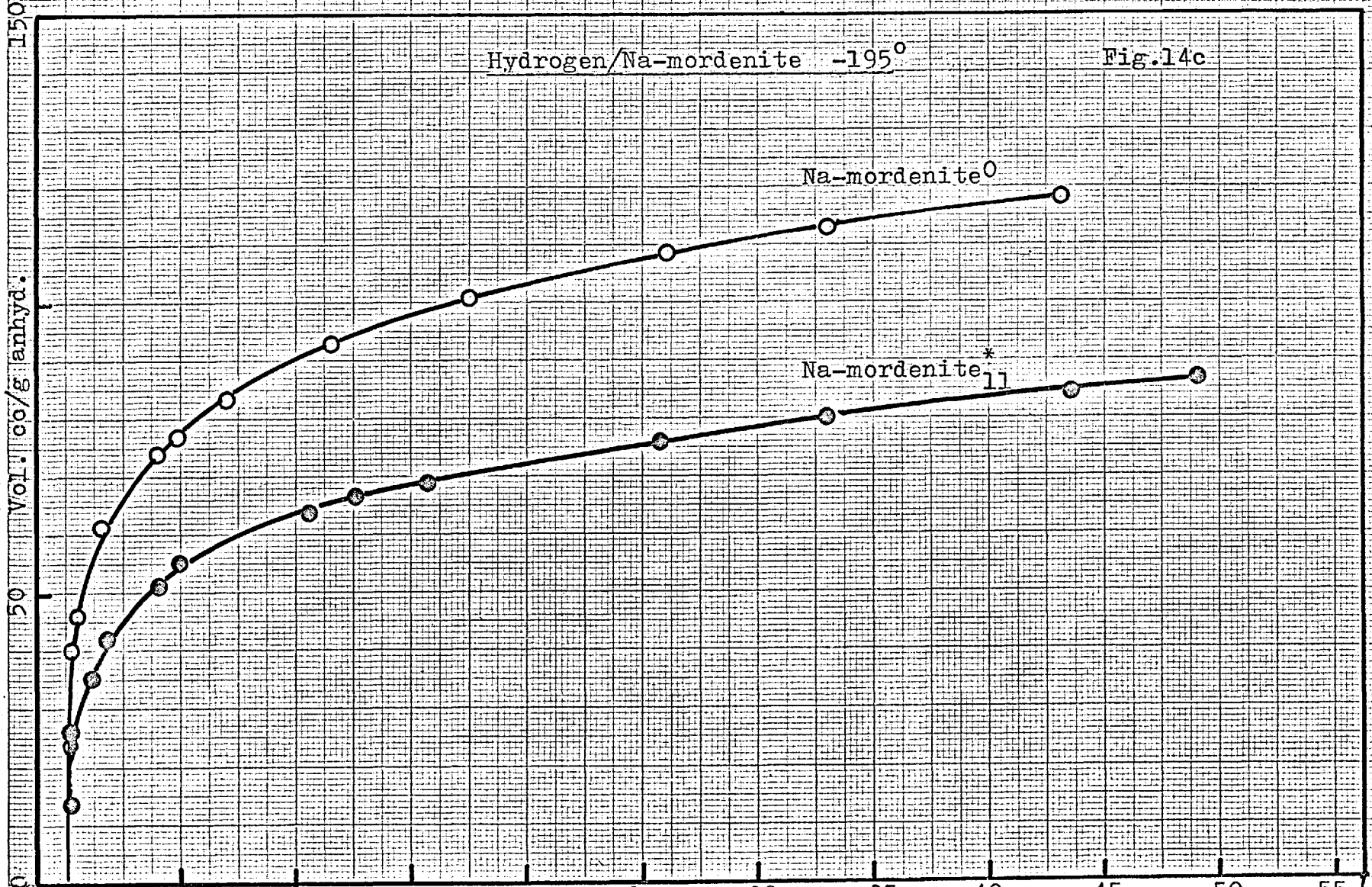
Hydrogen/Na-mordenite -195°
Fig.14c
Na-mordenite°
Na-mordenite*II
Vol. cc/g anhyd.
0
50
150
0
5
10
15
20
25
30
35
40
45
50
55
Pressure(cm of Hg)

densities at various temperatures. The calculated densities of sorbed krypton gas are also shown, using the value of 0.163 c.c./g Na-mordenite as intracrystalline volume. Since the saturation capacities of krypton in the damaged samples is less than for the standard samples, it is reasonable to assume that the intercrystalline volume will be proportionately less. Using values of 0.132 c.c./g and .065 c.c./g for Na-mordenite$^{*}_{1}$ and Na-mordenite$^{*}_{2}$ respectively, the plot of sorbed krypton density against temperature are then found to be coincident with the plot for Na-mordenite^{o}. Since the density plots are almost parallel to that for the liquid krypton densities, it may be concluded that at saturation, sorbed krypton approximates to the state of a bulk fluid, both in standard and damaged samples.

4.1.5. Isosteric Heats of Sorption of Krypton in Na-mordenite:-

Isosteric heats of sorption for the system Kr /Na-mordenite have been measured from zero coverage up to approx. $\theta = 0.95$. The Clausius-Clapeyron equation (A) was used to calculate the isosteric heat. Integrating this equation between the limits T_1 and T_2, corresponding to pressures P_1 and P_2, then:

$$2.303 \log_{10} P_1/P_2 = \Delta H/R \left[\frac{1}{T_1} - \frac{1}{T_2}\right] \qquad (A)$$

$$\text{or } \Delta H = 2.303\ R.\ \log_{10} P_1/P_2 \left[\frac{T_1 . T_2}{T_1 - T_2}\right] \qquad (B)$$

Plots of $\log_{10} P$ against V, (the amount sorbed) were used to obtain the values of ΔH which are plotted against θ (where θ in this case must be taken as the average of the saturation capacities at T_1 and T_2) in figure 15. Six plots of ΔH may be obtained from four isotherms, and an average plot should provide a fairly accurate illustration of the change in ΔH with θ. The curve for the damaged sample, Na-mordenite$^*_1$ was found to be coincident with the curve for the standard sample (fig. 15), but the curve obtained from the 60% damaged sample of Na-mordenite$^*_2$ is flatter, indicating a more homogeneous sorbent (fig. 15).

The initial heat of sorption is more than 1 k.cal/mole larger than in NaX (1) showing that sorption is occurring in a much more compact channel system. In section 1.2.1. it was shown that Na-mordenite consists of large channels of diameter 5.8 A° and small channels of diameter 4.0 A°. Since krypton molecule has a diameter of 3.9 A°, it appears that initial high heats are due to the sorption in the 4.0 A° channels. Decrease in heats of sorption to 4.9 k.cals/mole, represents sorption in the large channels of diameter 5.8 A°. At $\theta = 0.75$ when sorption is beginning to take place on sites such that the krypton atoms are not in immediate contact with the channel walls, a further decrease in the heat of sorption is observed.

The heat curve obtained for Na-mordenite$^*_1$ was identical with the heat curve for the standard sample within experimental errors. Na-mordenite$^*_2$ showed a decrease in the saturation capacity which could be attributed to either of the following:-

(a) General lattice contraction, same no. of cages but some or all smaller in volume or

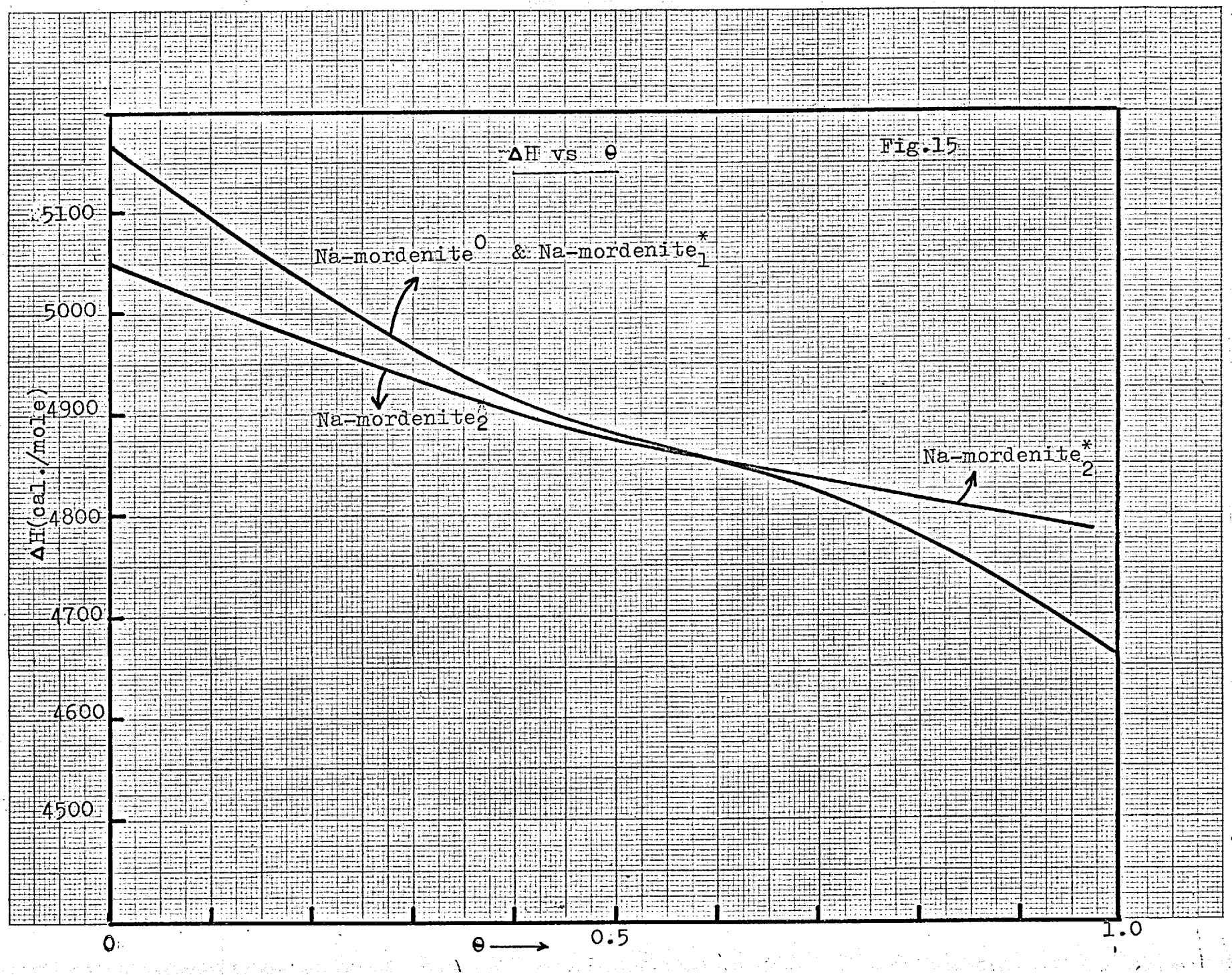
-ΔH vs θ
Fig.15
Na-mordenite^{0} & Na-mordenite$^{*}_{1}$
Na-mordenite$_{2}$
Na-mordenite$^{*}_{2}$
5100
5000
4900
4800
4700
4600
4500
ΔH(cal./mole)
0
0.5
1.0
θ

(b) Complete destruction of some cages, leaving others virtually intact or

(c) Combination of both (a) and (b).

If some amorphous regions were formed on neutron irradiation and no sorption took place on these regions, little change in heat curve would be expected. The 15.5% damaged Na-mordenite agrees with this. However, if (b) or even (c) occurred then Henry's Law sorption would be affected, i.e. at 25C° there should be loss in capacity. Na-mordenite$_1^*$ shows no decrease in sorption capacity at 25C° although it is 15.5% damaged at lower temperatures. If (a) operated then sorption characteristics would be little affected by contraction until this contraction was considerable. It would seem as was found with Na-X that contraction is the dominant factor on irradiation. When 60% damaged sample was studied, it gave a heat curve different from the standard sample (fig. 15). It showed 30% decrease in sorption at 25C°. Contraction is now considerable and possibly no sorption is occurring in the small channels of diameter 4.0 A°, although in all probability some complete collapse of the structure is also occurring.

The ΔH curve for the 60% damaged sample is much more uniform in nature, dropping only from 5.05 k cals/mole to 4.78 k cal/mole over the whole range of θ. The sorbent is therefore much more homogeneous in nature. This may be produced if sorption in the small channels does not take place. The following calculations were made in order to find out if small channels are blocked to krypton sorption at low temperatures.

Volume of unit cell of Na-mordenite = a x b x c $10^{-24} Cm^3$ (where a, b and c are dimensions of unit cell in A°, see

fig. 1). Taking density of anhydrous Na-mordenite as 1.8 c.c./g. No. of unit cell/g can be calculated as = $\frac{10^{24}}{a \times b \times c \times 1.8} = \frac{2.063 \times 10^{20}}{}$ pore volume was found to be 0.163 c.c/g (see page 87).

$\therefore$ Pore volume of unit cell = $\frac{0.163}{2.063 \times 10^{20}} = \underline{795\ A^{o3}}$

From Na-mordenite model it is found that one unit cell consists of two large channels, therefore, considering the channels elliptical in shape, the volume of large channels can be calculated as = 2 x π x a x b x c (where a and b are the radii of the channel and c is a dimension of unit cell).

= $\underline{480A^{o3}}$

$\therefore$ Volume of small channel = (795 - 480) = $\underline{315A^{o3}}$

Volume of small channels was also calculated from geometry of unit cell, considering four small channels in a unit cell.

$\therefore$ Volume of small channel/unit cell = $\pi \times 2^2 \times 6.6 \times 4$ = $\underline{332A^{o3}}$ (where 2 = radius of channel, 6.6 = length of channel and 4 = no. of channel/unit cell). Therefore volume of small channels calculated from geometry is in fair agreement with the volume calculated by subtracting the volume of large channel from the total volume, within reasonable error.

Taking ratio of capacity of Na-mordenite/g with only large channels to the capacity with all the channels, it is shown that 60% sorption takes place in large channels. This ratio for Na-mordenite$_2^*$ (60% damaged at low temperature

and 30% damaged at high temperature) was found to be 57%. This can lead to the suggestion that part of zeolite is contracted and part of it is completely damaged. As the diameter of small channels is 4.0 A^{o}, therefore on irradiation these channels become too small for krypton (3.94 dia) sorption and it can be assumed that practically no sorption is taking place in small channels. The large channels have diameter 5.8 A^{o}, even on contraction it would still be large enough for krypton sorption but at low temperatures, small numbers of krypton molecules have got sufficient energy to diffuse through therefore damage appears to be more. At higher temperatures krypton molecules have more kinetic energy and most of them can easily get into the channels, thus decreasing the damage at higher temperature. This has been supported by reduction in the initial Δ H in case of Na-mordenite$^{*}_{2}$. As the large channels are also contracting then there will be fewer molecules of krypton sorbed on sites removed from the channel walls so that the final ΔH should be greater and this explains the change in heats at higher θ value in case of 60% damaged sample. It can, therefore, be concluded that large channels in Na-mordenite are probably responsible for most of sorption. Na-mordenite$^{*}_{8}$ (65%) and Na-mordenite$^{*}_{11}$ (50%) gave similar heat curves within experimental errors.

All these samples were checked for crystallinity by x-ray analysis. Na-mordenite$^{*}_{5}$ ($5.0 \times 10^{19} n/cm^{2}$) had only a few single lines in the photograph, indicating that most of the sample was completely amorphous.

Na-mordenite$^{*}_{2}$ ($3.3 \times 10^{19} n/cm^{2}$) when compared with the standard sample, the following observations were made:-

i) Noticeable displacement in all the visible lines in a direction indicating a decrease in lattice dimension, i.e. a lattice contraction.

ii) Every line was not only displaced but also broadened, indicating some disorder in the lattice, e.g. distortions resulting from interstitials and vacancies. The x-ray data and heat curve for Na-mordenite$^{*}_{2}$, therefore, support the idea of contraction of the lattice.

4.1.6. Change of Heat of Sorption with Temperature:-

The isotherms for the system krypton/Na-mordenite, over a temperature range +25 to -100C^{o} were constructed and employed to determine if there was any effect of temperature on the isosteric heat, and if not, to establish the value of ΔH in the range $\theta = 0$ to 0.3 for very low temperature studies. There does appear to be a slight change in ΔH with temperature, the heat of sorption decreasing as the temperature decreases. The high temperature isotherm data (+25 to - 100C^{o}) could not, therefore, be employed to establish the value of ΔH over the range $\theta = 0$ to 0.3 for the low temperatures (-120 to -150C^{o}) data.

TABLE 4

Temps. of 2 isotherms (C^{o})		ΔH (k cal/mole)	Temps of 2 isotherms (OC)		ΔH (k cal/mole)
+25	0	5.1	-100	-120	4.8
0	-40	5.0	-120	-130	4.8
-40	-70	5.0	-120	-140	4.7
-70	-90	5.0	-120	-150	4.7
-70	-90	4.9	-130	-140	4.8
-70	-100	5.0	-130	-150	4.6
-90	-100	4.9	-140	-150	4.6

4.1.7. Comparison of Isotherm Data With Ideal Models of Sorbed State:-

Henry's Law $P = K\theta$ does not apply over very extensive range of θ, therefore, other isotherm models have to be considered. Localized and mobile the two main types of sorption possible were mentioned in section 2.1.4., each represents an extreme case and the experimental results may not agree with one or the other over the whole range of coverage. The various limiting isotherm models will now be discussed.

4.1.8. Localized sorption with no interaction between sorbed molecules:-

Langmuir (40) derived the following expression:-

$$K_1 = P\,\frac{(1-\theta)}{\theta} \qquad \text{(Model 1)}$$

where P = equilibrium pressure and θ = degree of saturation. If an isotherm model is applicable the isotherm constant K must be independent of θ over the range $\theta = 0$ to 1. Plots of K_1 against θ, for the isotherms conducted at temperatures -120 to -150C°, are shown in figure 16. It is noticeable that this simple isotherm model for localized sorption improves as the temperature is lowered and K_1 is fairly constant up to $\theta = 0.60$ at -150C°. Between $\theta = 0.7$ and $\theta = 0.95$, K_1 rises very rapidly to a maximum before decreasing again. No data could be obtained beyond $\theta = 0.95$, as the saturation vapour pressure of krypton at -150C° it too high. However, since the decrease in K_1 at this high coverage is attributed to capillary condensation and multi layer formation on the zeolite surfaces, it is not relevant to this discussion of intercrystalline

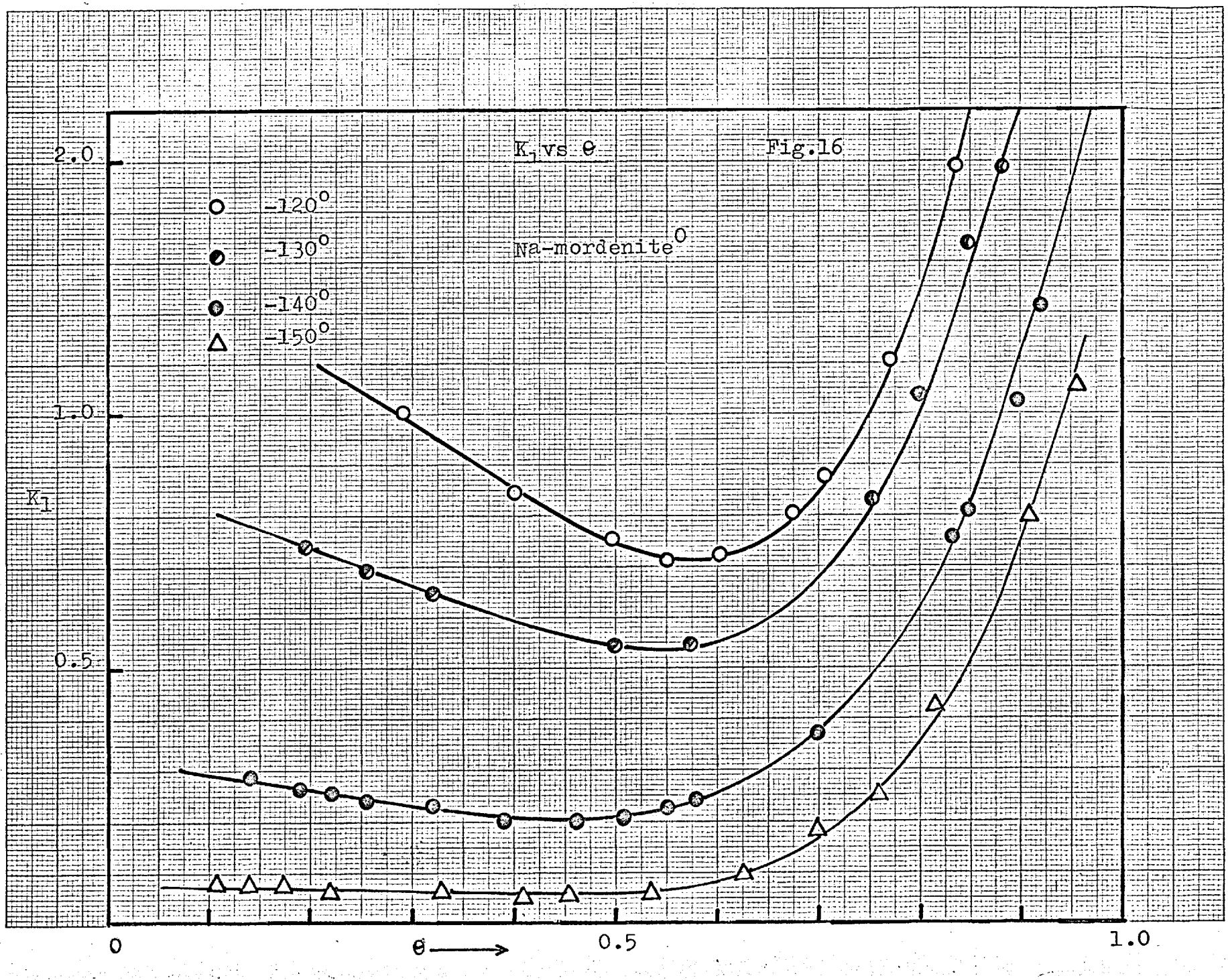
K_1 vs θ
Fig.16
Na-mordenite
-120°
-130°
-140°
-150°
2.0
1.0
0.5
K_1
0
θ ⟶
0.5
1.0

sorption, although the increase in K_1 up to the maximum is. A pronounced increase in K_1 has previously been observed by Barrer and Reuxroft (61) Barrer and Stuart (62) and Rees and Williams (1). Barrer and his associates explained the increase in K_1, in terms of a change thermal entropy. This assumes that the energy of sorption between sorbate and sorbent remains constant up to the whole range of θ, but in the present work it is already shown in fig. 16 that K_1 is constant up to $\theta = 0.50$ and that beyond this value of θ, krypton molecules are sorbed on sites away from channel walls which led to a decrease in ΔH, giving rise to corresponding increase in K_1.

Any isotherm model which allows for sorbate molecule interactions should be more realistic for the sorption studied, since in the confined interspaces of Na-mordenite, sorbed molecules are certain to exert their attractive forces towards each other.

4.1.9. Localized sorption with interactions:-

To allow for sorbate molecule interactions, the simple Langmuir expression for localized sorption may be adapted by the addition of an exponential term containing the energy $2W/_z$, which is the interaction energy between a pair of sorbed molecules; (N.B. $2W/_z$ is negative because it is an energy of attraction) and z is defined as the co-ordination number of a molecule when sorbed on a sorption site.

$$K_2 = P \frac{(1-\theta)}{\theta} \exp. \frac{-2W\theta}{RT} \qquad \text{(Model 2)}$$

We shall now discuss how the values of the total molecule-molecule interaction energy (2W) were obtained.

4.1.10. Determination of Experimental Values of the Total Molecule-molecule Interaction Energy (2W):-

It was shown by Barrer and Reucroft (61) that an experimental value of 2W could be obtained from the isotherm model K_2. Equation (M.1) may be written as:-

$$\log_{10} \frac{P(1-\theta)}{\theta} = \frac{\theta 2W \log_{10} e}{RT} + \log_{10} K_2 \qquad (10)$$

By plotting $\log_{10} \frac{P(1-\theta)}{\theta}$ against θ, we obtain in the range of validity of this isotherm expression, straight lines of negative slope equal to $\frac{2W \log_{10} e}{RT}$ from which value of 2W can be obtained. These plots are shown in figure 21 to be linear up to $\theta = 0.5$. Logarithm of the isotherm constant K_2 can be obtained by extrapolation to the ordinate axis. The slope of these plots changes from negative to positive around $\theta = 0.5$, which does not, however, mean that the attractive forces existing between two krypton molecules become a repulsive force, but rather that the isotherm model is unsatisfactory beyond this value of θ. The values of (2W) so obtained are shown in the table following:-

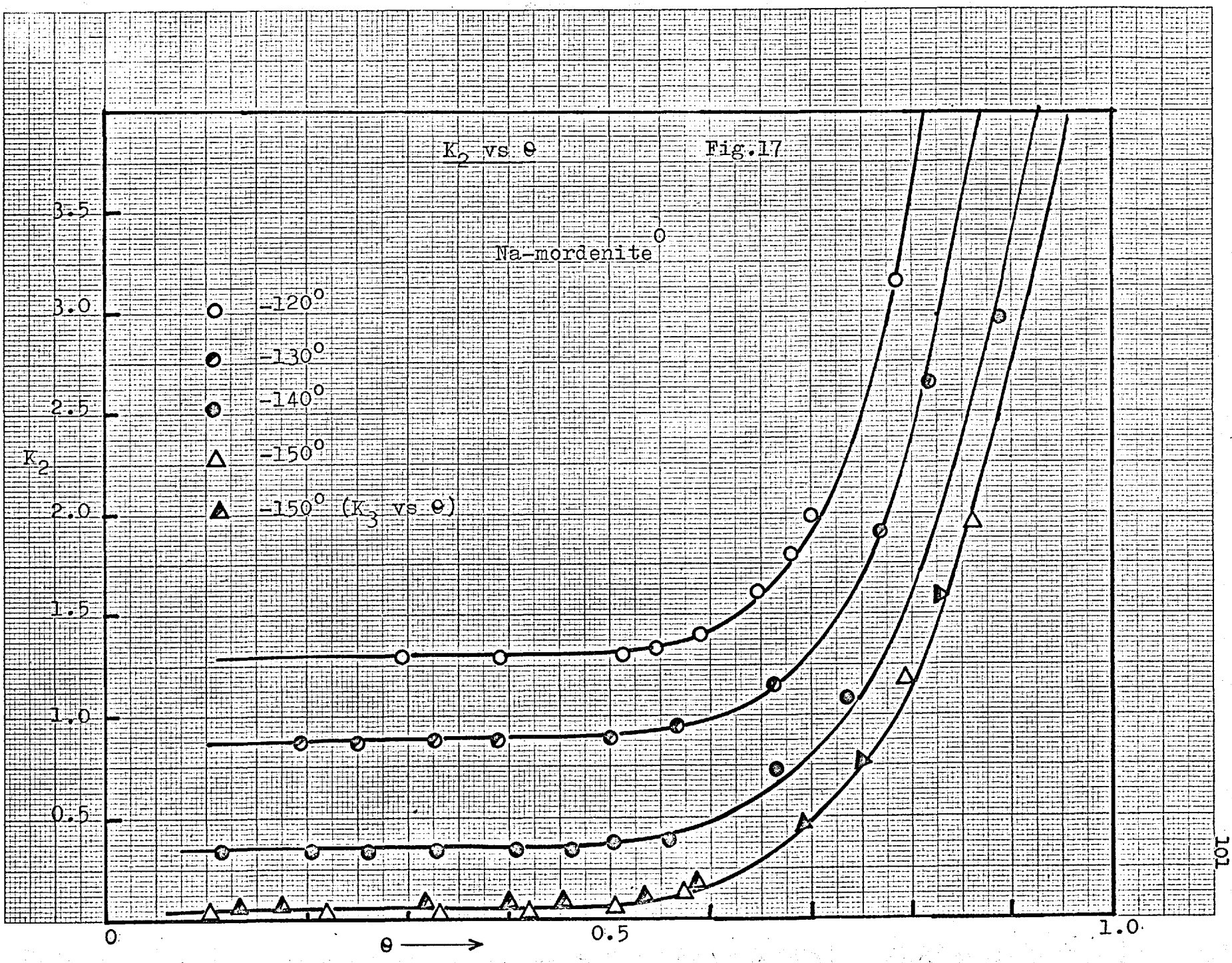
K_2 vs θ
Fig.17
Na-mordenite
-120°
-130°
-140°
-150°
-150° (K_3 vs θ)
K_2
3.5
3.0
2.5
2.0
1.5
1.0
0.5
0
0.5
1.0
θ

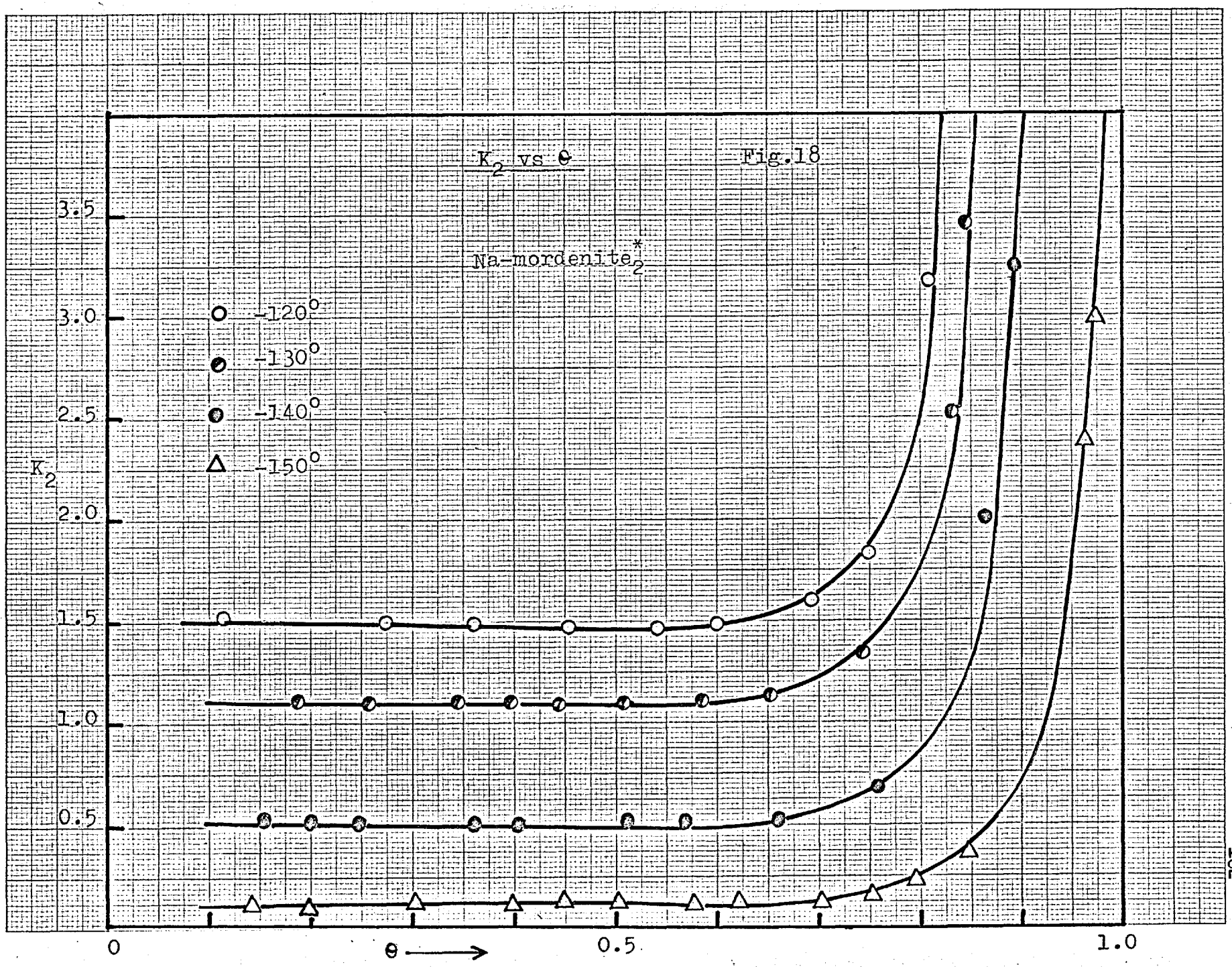
K_2 vs θ
Fig.18
Na-mordenite*2
-120°
-130°
-140°
-150°
K_2
3.5
3.0
2.5
2.0
1.5
1.0
0.5
0
0.5
1.0
θ ⟶

TABLE 5

Temp. (C°)	-150	-140	-130	-120	Average For θ	Average For θA
Na-mordenite°						
i) For θ	382	364	341	342	358	-
ii) For θA	532	435	494	455	-	479
Na-mordenite$_2^*$						
i) For θ	341	350	330	340	340	-
ii) For θA	492	403	423	425	-	436

The values shown in table 5 for θ and θA (adjusted θ as explained on page 105) are used for calculating throughout this work.

The difference between the experimental values, 358 and 340 cal/mole, for 2W, may be the result of experimental error, or more likely could be explained as follows. From the x-ray data discussed in section 4.1.5., it is believed that there has been a lattice contraction in Na-mordenite$_2^*$. The sorption results support this by showing that the number of krypton molecules that fill the channels at saturation, is less than for Na-mordenite° under identical conditions. Therefore, as 2W/z is constant for krypton the value of 2W will depend on z. When the lattice contracts, due to irradiation, z will decrease and 2w will also be smaller.

Plots of K_2 against θ for the temperature range -120 to -150C^{o} are shown in figure 17. In each case K_2 is constant up to $\theta = 0.5$, after which it starts increasing rapidly. By being constant up to $\theta = 0.5$, at various temperatures studied, K_2 provides a better explanation than K_1 for sorption of krypton by Na-mordenite, it is unsatisfactory above this value of θ. It should be noted however, that since this model is valid up to $\theta = 0.5$, it does explain the interactions between the sorbed molecules up to this point.

A second exponential term was introduced into the expression for K_2 by Barrer and Reucroft (61) i.e.

$$K_{2A} = P \frac{(1 - \theta)}{\theta} \quad \text{exp.} \quad \frac{(-2W\theta)}{RT} \quad \text{exp f } (\theta) \quad \text{(Model 2A)}$$

where the first exponential term has the usual significance and the second exponential term allows for the "freezing" of the sorbate molecules as they gradually lose thermal entropy by filling the intercrystalline pore space. For the system, carbon tetraflouride sorbed by NaX, an expression which satisfactorily explained the isotherm data up to $\theta = 1$, was obtained by them. However, the values used in the exp f (θ) term were purely arbitrary and is therefore of little significance.

On comparing figure 17 and 18 it is observed that in the case of the 60% damaged sample K_2 becomes constant almost up to $\theta = 0.75$ whereas in the standard sample it was constant only up to $\theta = 0.50$. Due to the contraction in the channels, the sorption capacity of Na-mordenite$^{*}_{2}$ has decreased considerably and a large fraction of the krypton atoms must

be sorbed on the channel walls. The rest of the krypton molecules are sorbed on sites removed from the channel walls. The decrease in ΔH found previously occurs at coverage where a rapid rise in K_2 occurs. Na-mordenite$_1^*$ (15.5%) gave K_2 values identical with standard sample.

Rees and Williams (1) have shown that this rapid increase in K_1 and K_2 at high coverage in NaX is not due to thermal entropy changes but must be due to the decreasing heats of sorption. The maximum in the ΔH Vs θ curve was assumed to indicate that sorption in the range $0<\theta<0.75$ takes place on a uniform field of surface potential while subsequent sorption occurred on sites of reduced potential. In order to test this theory they multiplied all θ values by the factor 1.33 i.e. $\theta = 0.75$ now becoming $\theta A = 1$. (All adjusted values represented by θA). Similar treatment was applied to Na-mordenite data. As the channels and cages in Na-mordenite are smaller than the supercages and windows in NaX, it was expected that the factor in this case would be smaller than 1.33, because of smaller number of krypton molecules which are not in contact with the channel walls. This factor was found to be 1.25, therefore, all the values of θ were multiplied by 1.25 and θA was obtained. Plots of K_2 against θA at various temperatures are shown in figure 19. K_2 is now constant over the range $0<\theta A<0.90$, which is a considerable improvement on the constancy of K_2 calculated from the original θ values. Little change is observed in K_1 at lower coverages but when $\theta A \rightarrow 1$, K_2 now decreases instead of the rapid increase found as $\theta \rightarrow 1$. The decreasing values for the equilibrium constant may be due to larger values of 2W caused by Z decreasing already discussed.

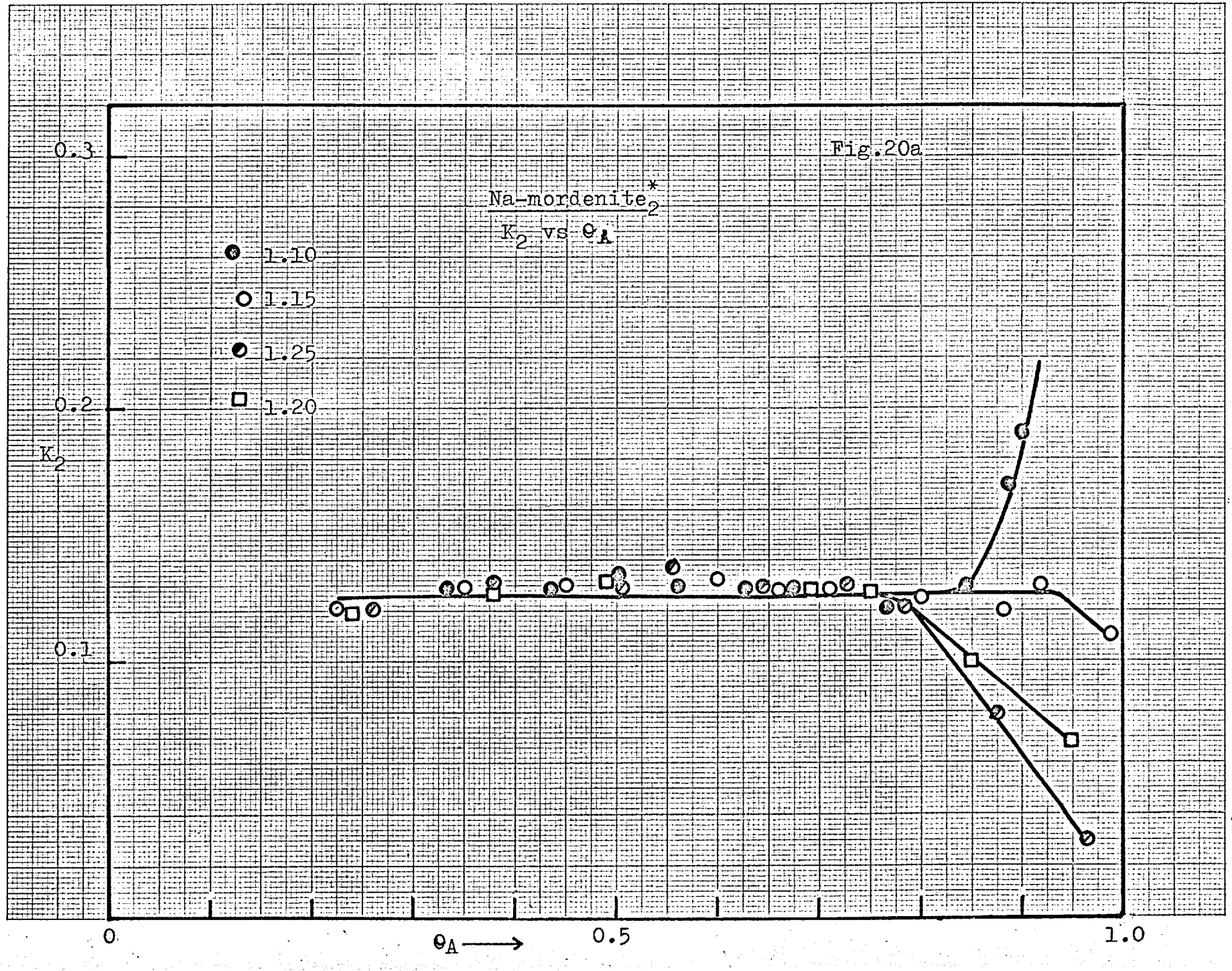
Fig.20a
Na-mordenite*2
K2 vs θA
1.10
1.15
1.25
1.20
0.3
0.2
0.1
K2
0
0.5
1.0
θA

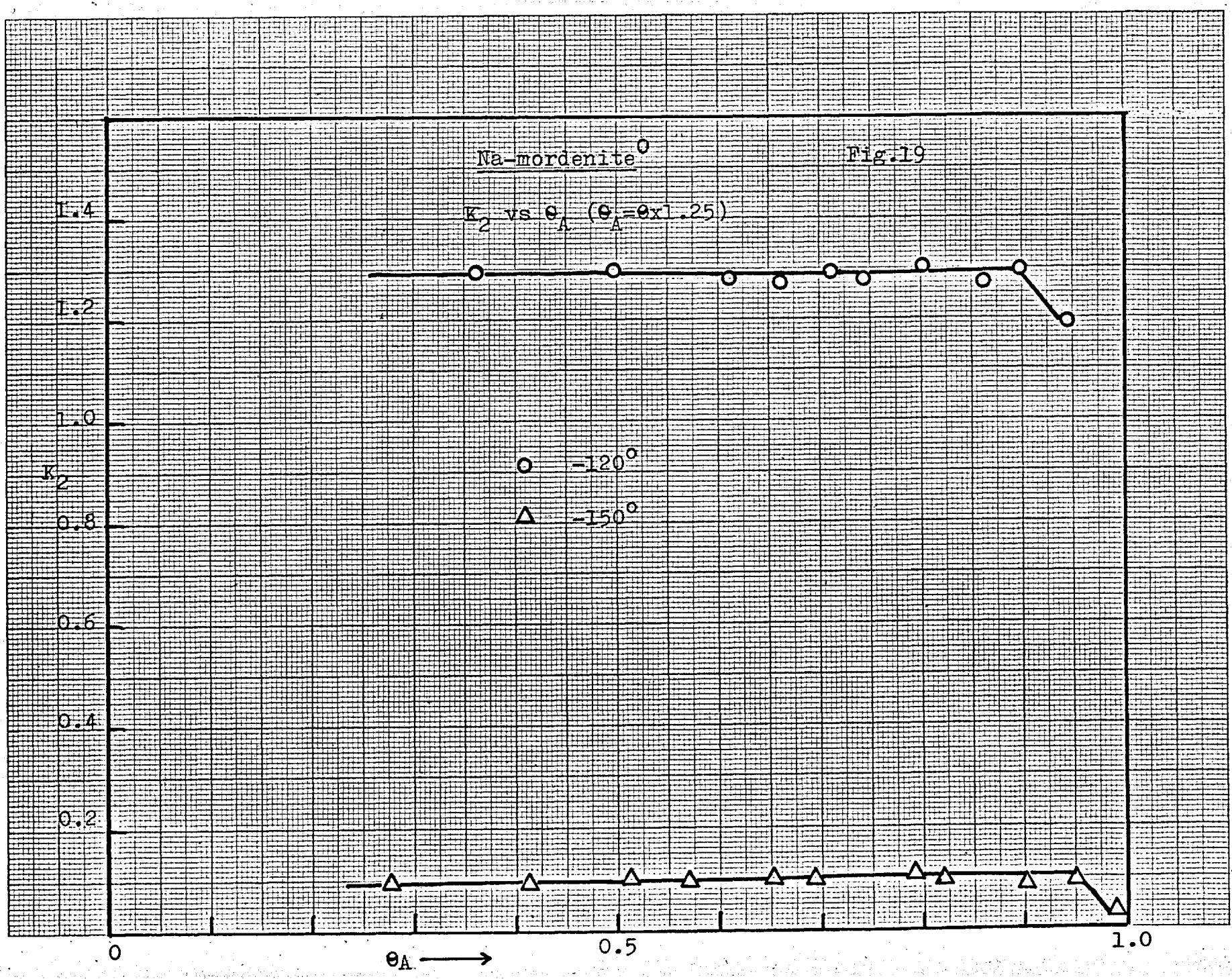
Na-mordenite
Fig.19
K_2 vs θ_A ($\theta_A = \theta \times 1.25$)
1.4
1.2
1.0
0.8
0.6
0.4
0.2
K_2
○ -120°
△ -150°
0
0.5
1.0
θ_A ⟶

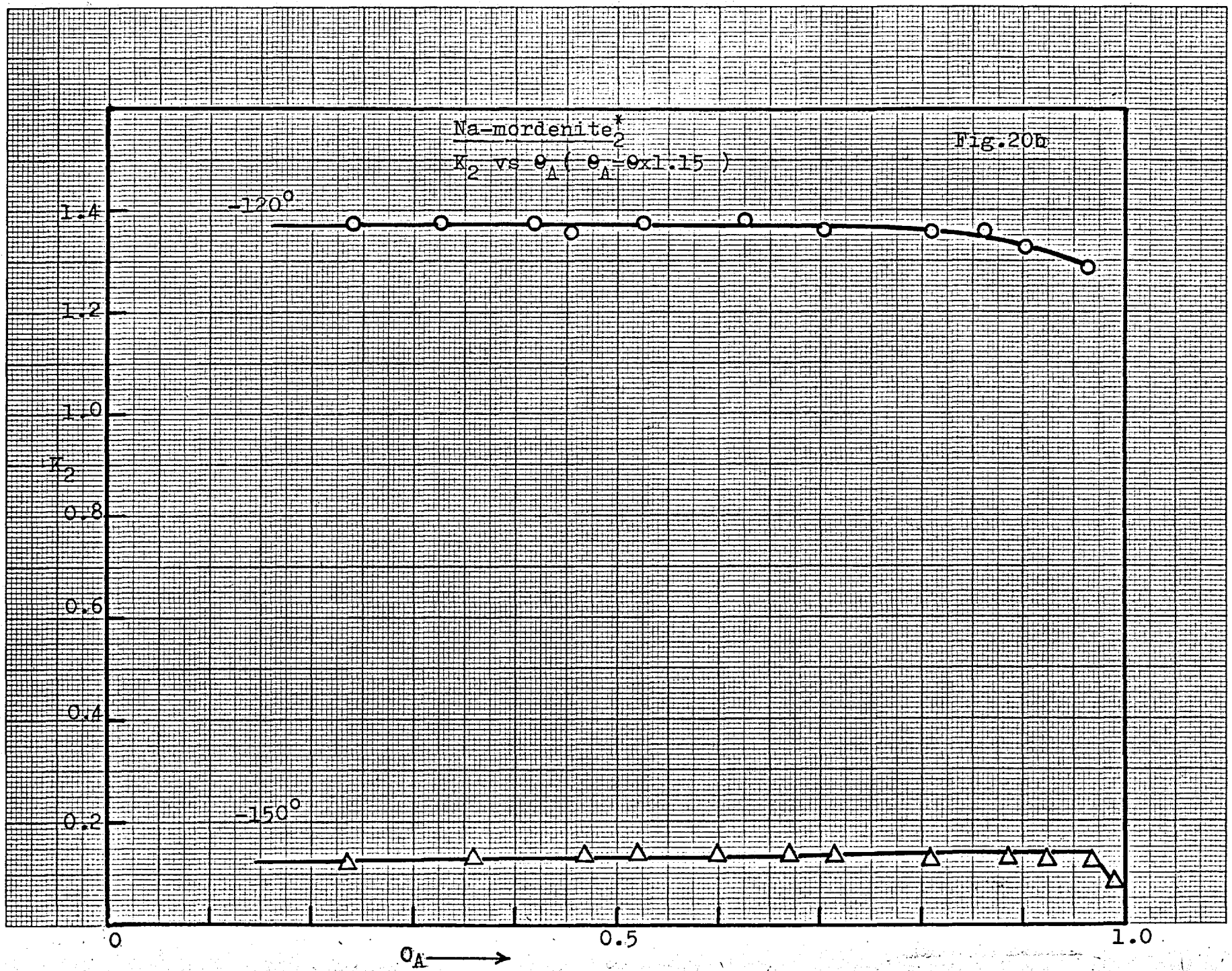
Na-mordenite*2
K2 vs θA (θA=θx1.15)
Fig.20b
-120°
-150°
1.4
1.2
1.0
0.8
0.6
0.4
0.2
K2
0
0.5
1.0
σA

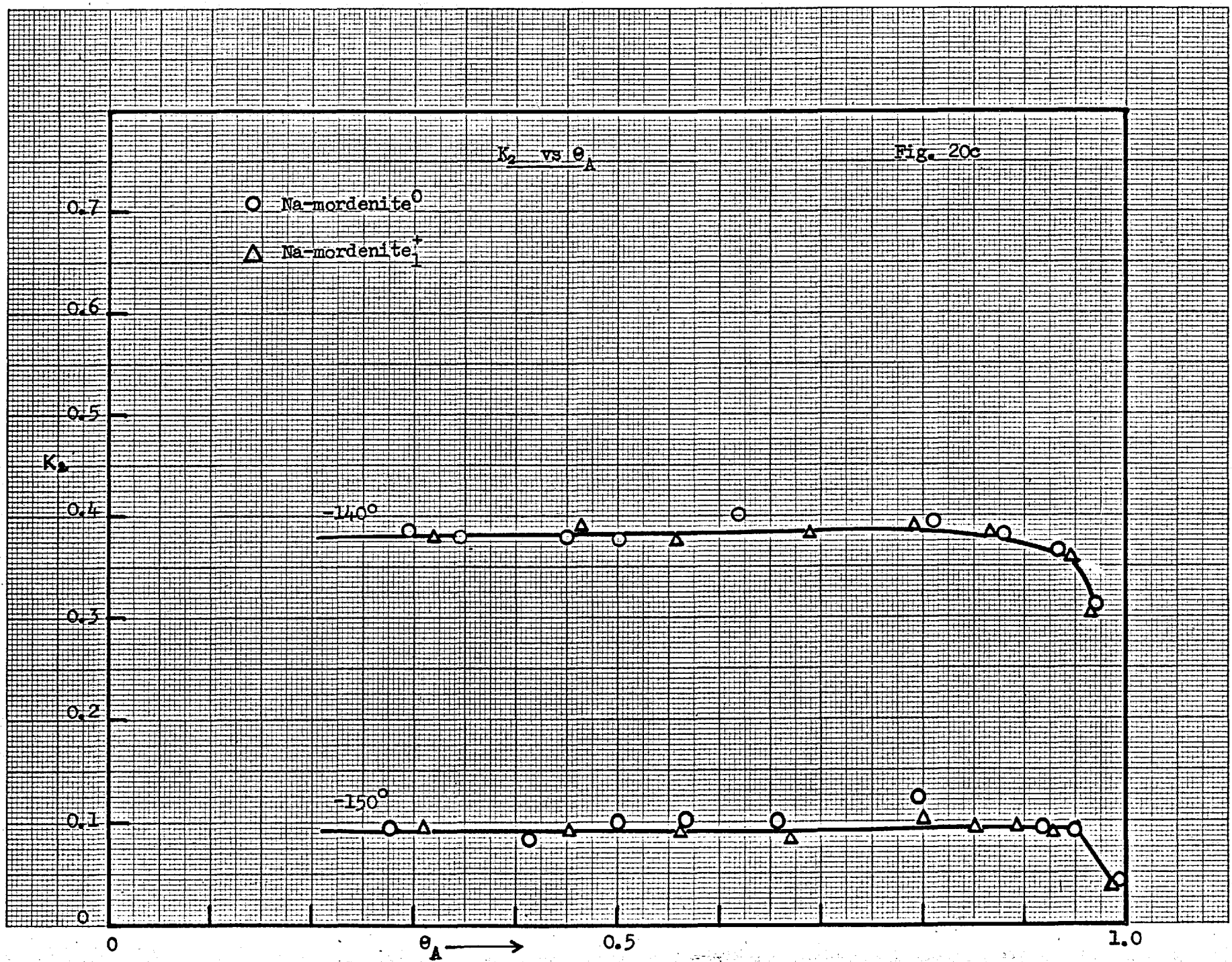
K_2 vs θ_A
Fig. 20c
Na-mordenite^0
Na-mordenite$^+_1$
0.7
0.6
0.5
K_2
0.4
0.3
0.2
0.1
0
-140°
-150°
0
θ_A ⟶
0.5
1.0

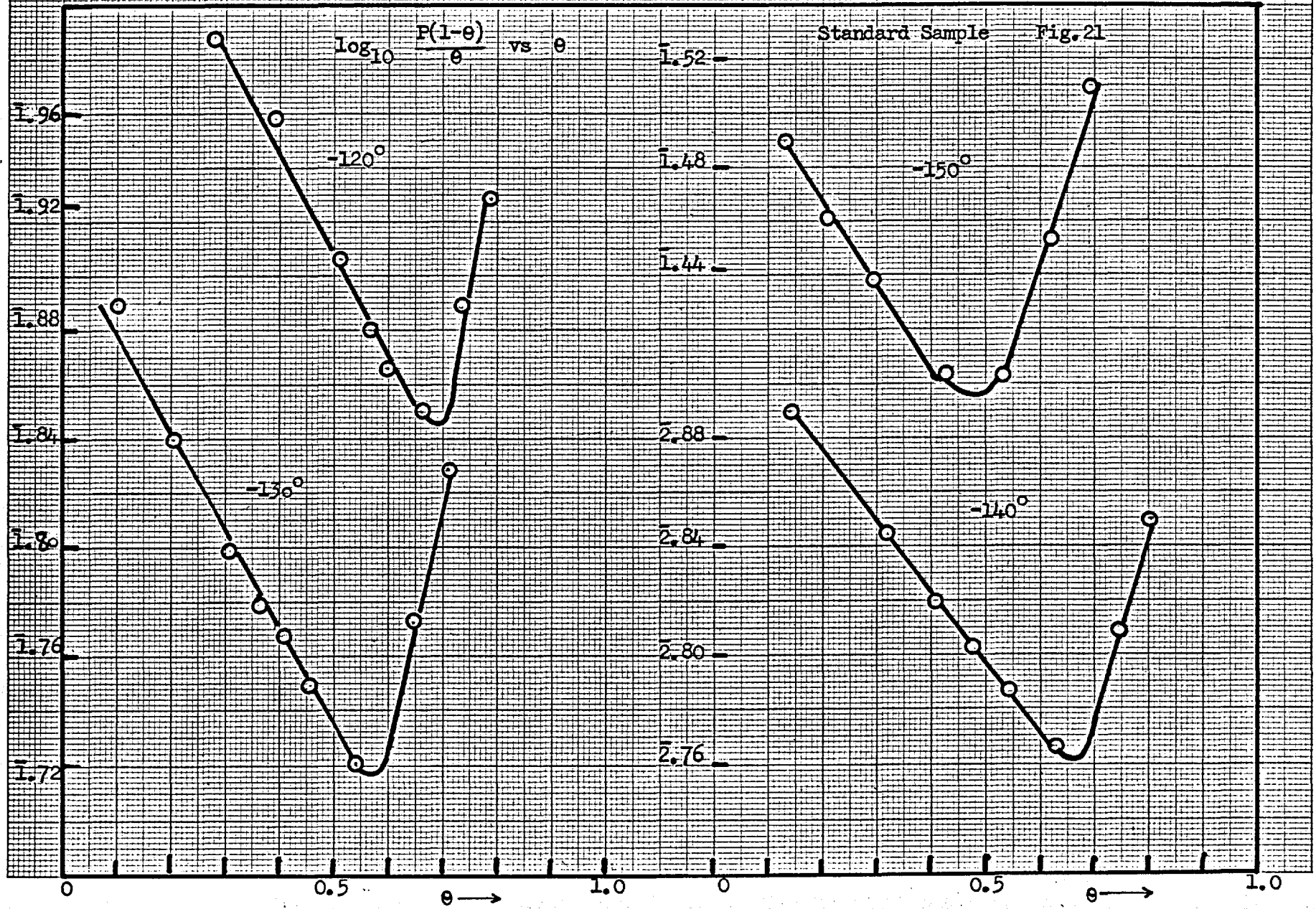
$\log_{10} \frac{P(1-\theta)}{\theta}$ vs θ
Standard Sample
Fig. 21
$\bar{1}.96$
$\bar{1}.92$
$\bar{1}.88$
$\bar{1}.84$
$\bar{1}.80$
$\bar{1}.76$
$\bar{1}.72$
-120°
-130°
$\bar{1}.52$
$\bar{1}.48$
$\bar{1}.44$
$\bar{2}.88$
$\bar{2}.84$
$\bar{2}.80$
$\bar{2}.76$
-150°
-140°
0
0.5
1.0
θ
0
0.5
1.0
θ

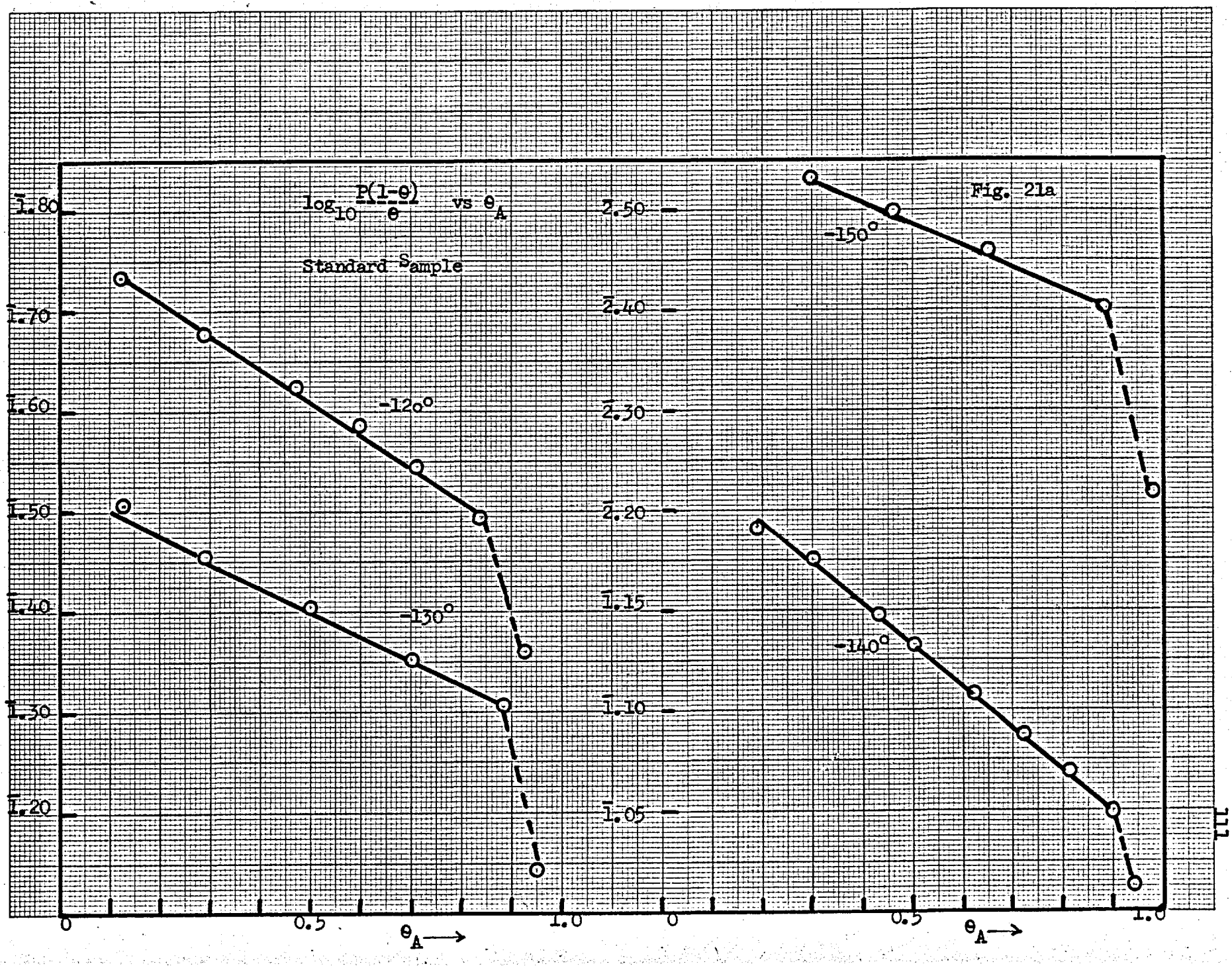
$\log_{10}\frac{P(1-\theta)}{\theta}$ vs θ_A
Standard Sample
Fig. 21a
$\bar{1}.80$
$\bar{1}.70$
$\bar{1}.60$
$\bar{1}.50$
$\bar{1}.40$
$\bar{1}.30$
$\bar{1}.20$
-120°
-130°
$\bar{2}.50$
$\bar{2}.40$
$\bar{2}.30$
$\bar{2}.20$
$\bar{1}.15$
$\bar{1}.10$
$\bar{1}.05$
-150°
-140°
0
0.5
1.0
θ_A
111

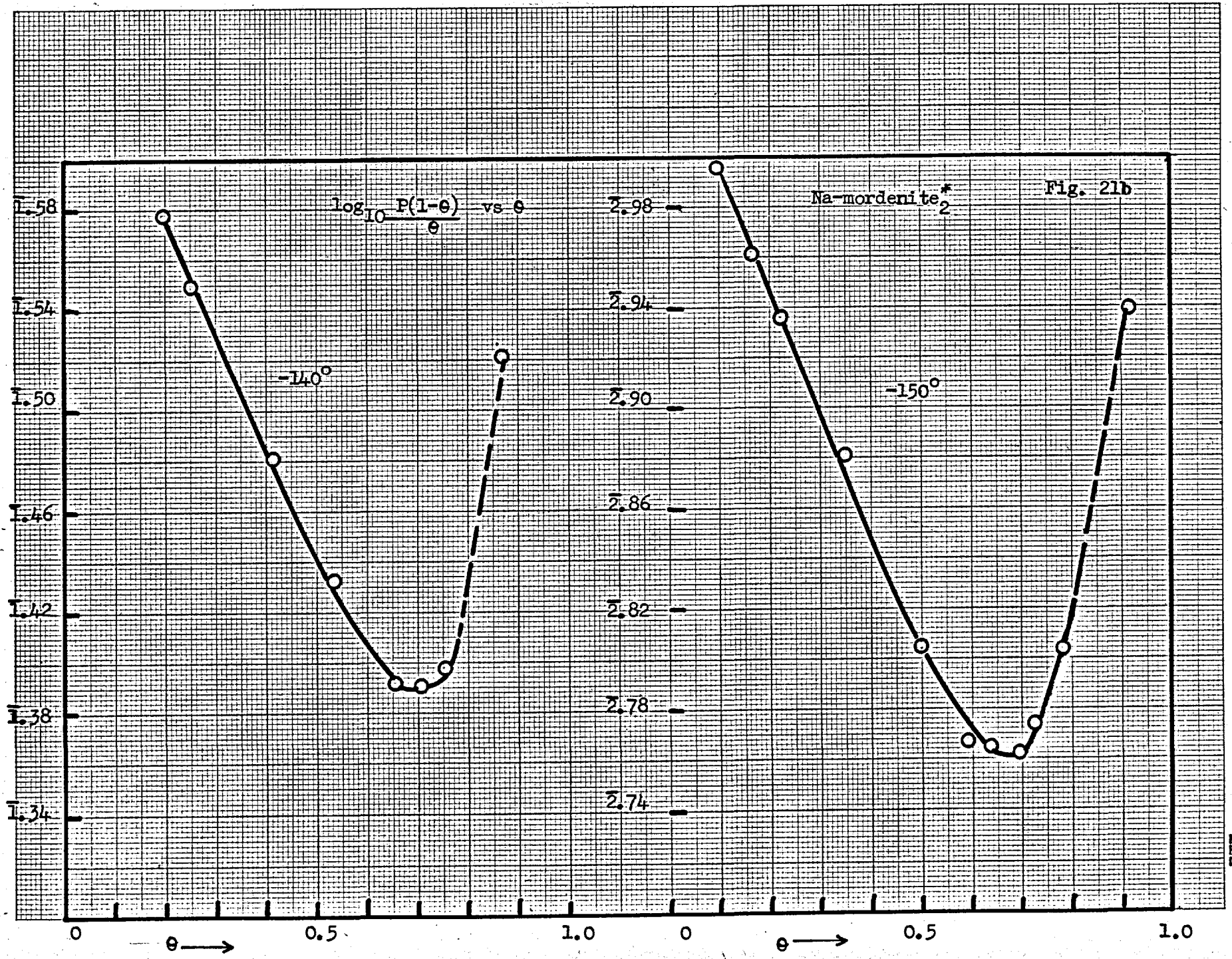
$\log_{10}\frac{P(1-\theta)}{\theta}$ vs θ
Na-mordenite*2
Fig. 21b
-140°
-150°
1.58
1.54
1.50
1.46
1.42
1.38
1.34
2.98
2.94
2.90
2.86
2.82
2.78
2.74
0
0.5
1.0
θ
0
0.5
1.0
θ

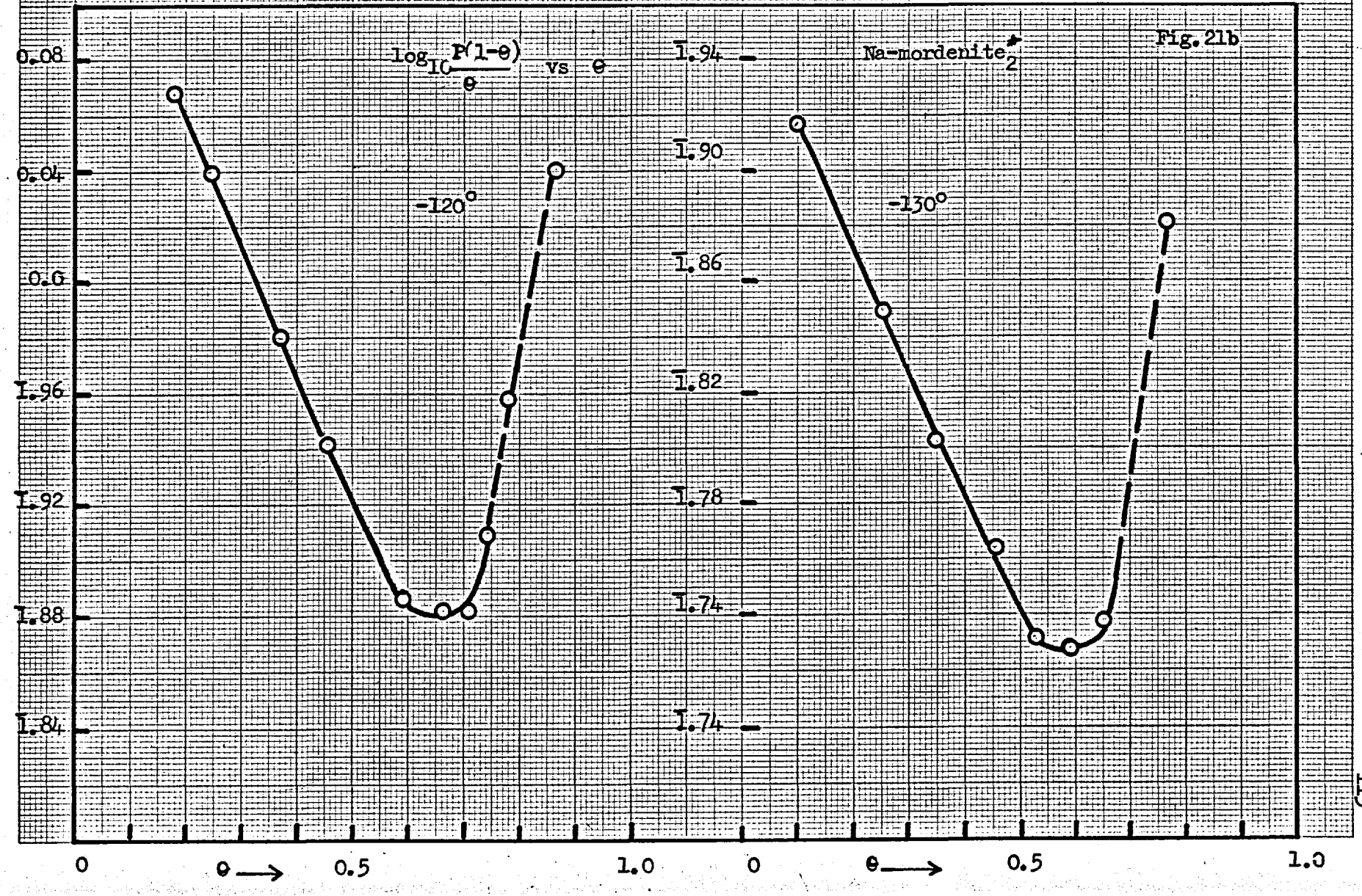
$\log_{10}\frac{P(1-\theta)}{\theta}$ vs θ
Na-mordenite #2
-120°
-130°
0.08
0.04
0.6
1.96
1.92
1.88
1.84
1.94
1.90
1.86
1.82
1.78
1.74
1.74
0
θ →
0.5
1.0
0
θ →
0.5
1.0

Fig. 21b

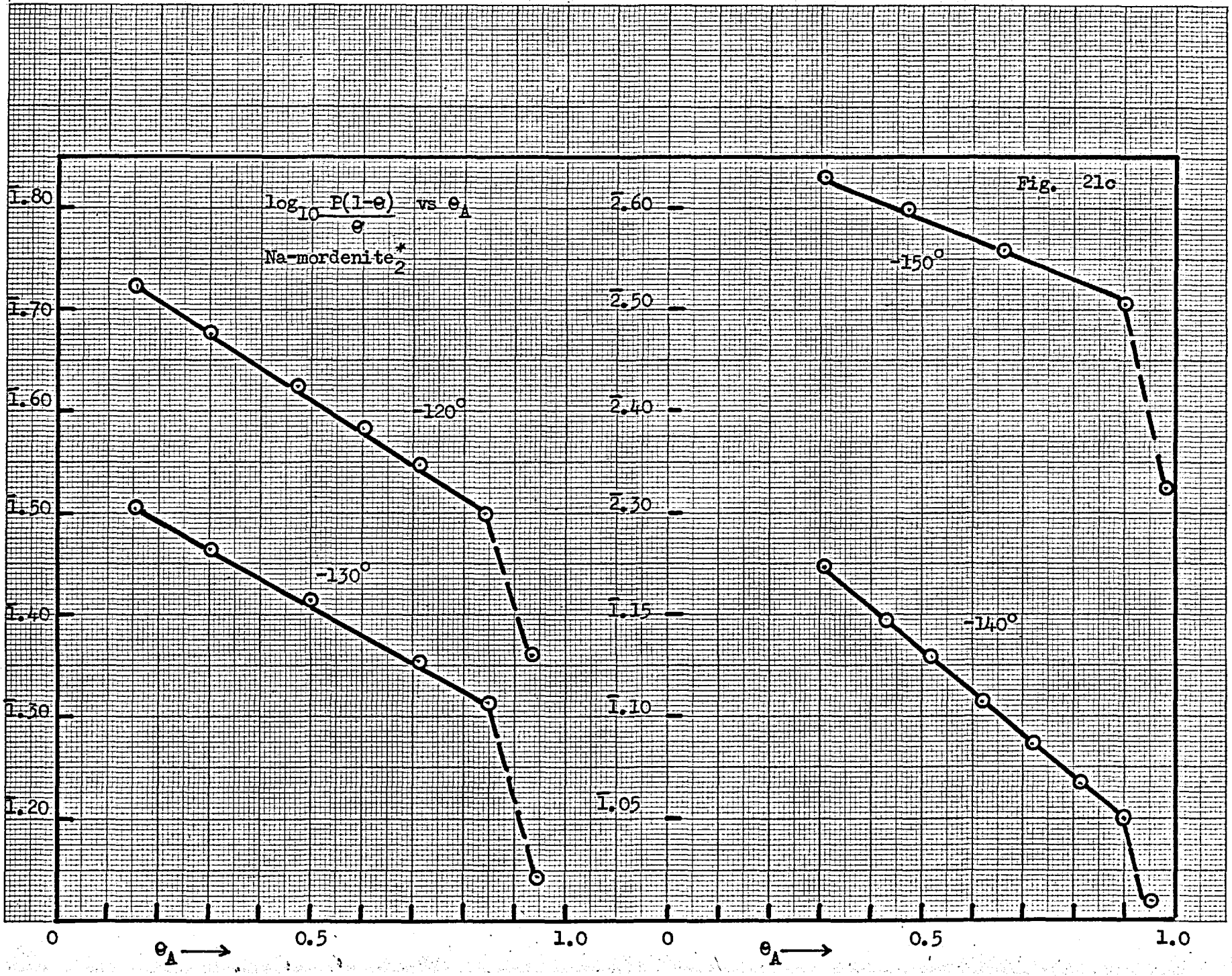
$\log_{10} \frac{P(1-\theta)}{\theta}$ vs θ_A
Na-mordenite*2
Fig. 21c
-120°
-130°
-150°
-140°
$\bar{1}.80$
$\bar{1}.70$
$\bar{1}.60$
$\bar{1}.50$
$\bar{1}.40$
$\bar{1}.30$
$\bar{1}.20$
$\bar{2}.60$
$\bar{2}.50$
$\bar{2}.40$
$\bar{2}.30$
$\bar{1}.15$
$\bar{1}.10$
$\bar{1}.05$
0
0.5
1.0
θ_A ⟶

When the same factor 1.25 was applied to 60% damaged sample, the rise in K_2 at higher coverage is replaced by a drop in K_2 in this range of coverage but the constancy of K_2 over the initial range of θ is not much improved. This was quite understandable, as we have already shown from x-ray analysis and changes in isosteric heat curve, that the channels of Na-mordenite$^*_2$ have contracted. Therefore, there will be fewer krypton molecules adsorbed in the channels reduced in size but the fraction sorbed in immediate contact with the channel walls is increased. This suggests that the adjustment factor for Na-mordenite$^*_2$ will also be smaller. The plots for various factors are shown in figure 20a, and it is clear that maximum constancy of K_2 is obtained when θ is multiplied by the adjustment factor of 1.15. It means that the adjustment factor should go on decreasing as the damage increases. In present work we did not study samples in the range 65-100% damage, because of the difficulty in subjecting the samples to the specific dose required but in the 65% damaged sample the adjustment factor was found to be the same as for the 60% damaged sample.

These results indicate that the hypothesis put forward by Rees and Williams is satisfactory for the sorbent studied in this work. The adjustment factor of 1.33 for the open NaX is reduced as expected to 1.25 for the more compact Na-mordenite and in a damaged Na-mordenite$^*_2$ which is known to have a contracted lattice, the factor is further reduced to 1.15.

4.1.11. Localized Sorption with Interactions making allowances for changes in Configurational Entropy:-

The isotherm model K_3 can be expressed as follows:-

$$K_3 = P\,\frac{(1-\theta)}{\theta}\,\frac{(\beta+1-2\theta)^Z}{(2-2\theta)} \qquad \text{(Model 3)}$$

where $\beta = \left[1 - 4\theta(1-\theta)\left(1 - \exp.\frac{(-2W)}{ZKT}\right)\right]^{\frac{1}{2}}$

The value of 2W has already been obtained, various values for Z (3,4,5) were taken. K_3 appears to be insensitive to changes in Z, and the plots are found to be practically coincident with K_2 plots as shown in figure 17, showing that K_3 is also constant up to $\theta = 0.5$ and then increasing rapidly. It, therefore, appears that changes of configurational entropy (allowed for in Model K_3) are also unable to explain satisfactorily the increase in the isotherm constant beyond $\theta = 0.5$. The adjusted factor 1.25 used for model 2 was also applicable in model 3 and the plots for the adjusted values are shown in figure 19.

4.1.12. Mobile sorption without interactions between mutually sorbed molecules:-

The following equation was derived from the volmer equation of state (38) :-

$$K_5 = P\,\frac{(1-\theta)}{\theta}\,\exp.\,\frac{(-\theta)}{1-\theta} \qquad \text{(Model 5)}$$

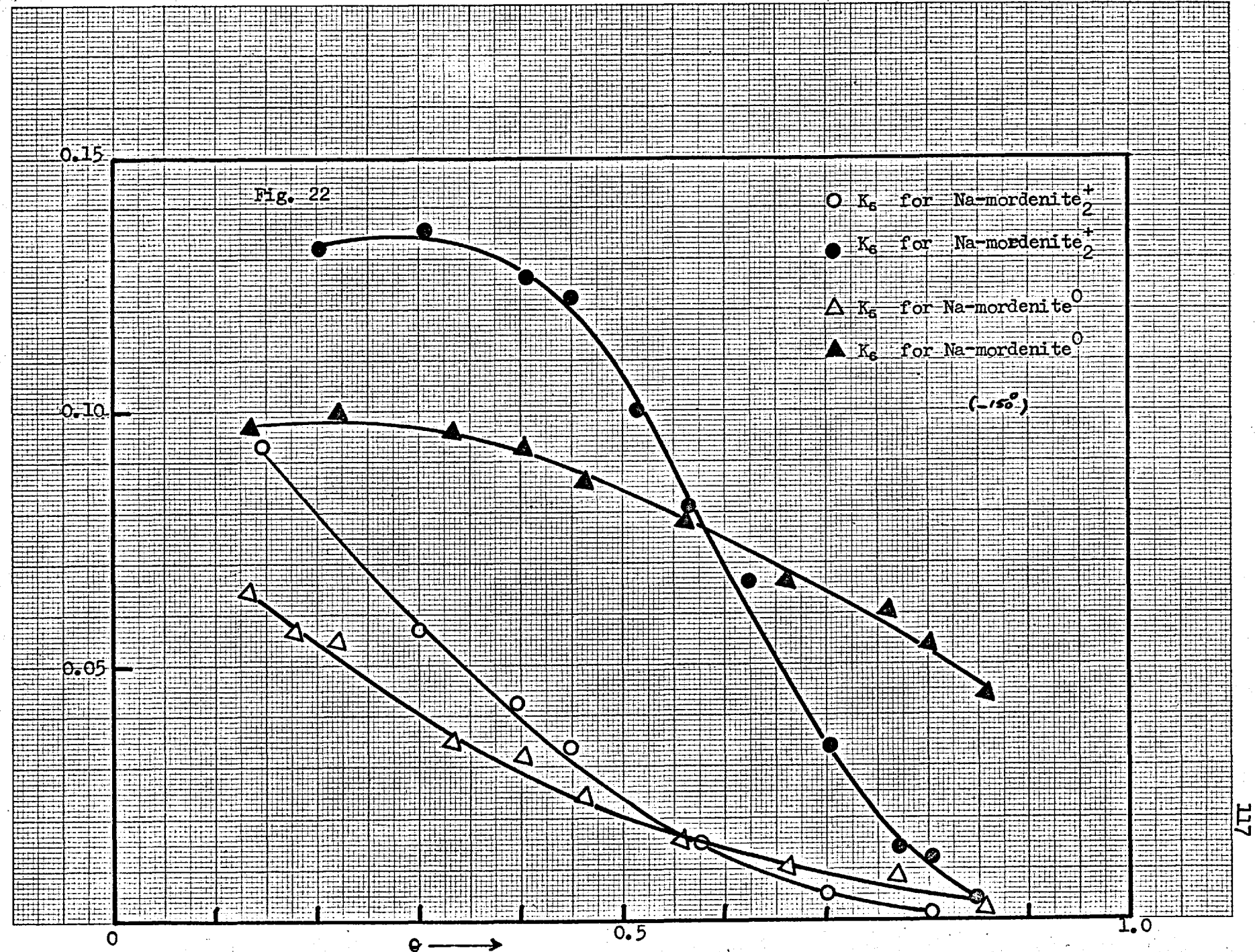
Fig. 22
0.15
0.10
0.05
0
0.5
1.0
θ ⟶
○ K_6 for Na-mordenite$^{+}_{2}$
● K_6 for Na-mordenite$^{+}_{2}$
△ K_6 for Na-mordenite^{0}
▲ K_6 for Na-mordenite^{0}
(-150°)

It is shown in figure 22 that K_5 decreases over the entire range of θ , and hence this model 5 inadequate.

4.1.13. Mobile sorption with Interactions:-

Hill (38) derived the following expression from the van der Waal's equation of state.

$$K_6 = P\frac{(1-\theta)}{\theta} \exp.\left(\frac{-\theta+\alpha\theta}{1-\theta}\right) \qquad \text{(Model 6)}$$

where $\alpha = {}^{2a}/_{bKT}$ a and b being two dimensional van der Waal's constant for the adsorbate.(Related to three dimensional constant by an expression given by Hill (46)). Plots of K_6 against θ are shown in figure 22. K_6 decreases steadily with θ and could be explained by one of the following:-

(i) the thermal entropy increases for the more tightly packed molecules, which is unlikely,
(ii) the van der Waal's equation of state used in the derivation could be inadequate for this system. (This is partially responsible).
(iii) the system is not one of the mobile sorption at all.

From the above discussion it can be concluded that sorption of krypton by Na-mordenite is localized at low temperatures (-150C°). The constancy of K_2 and K_3 is excellent over the range $0<\theta<0.5$. The addition of the molecule-molecule interaction term in model 2 makes a decided improvement but the added sophistication of allowing for changes in the configurational entropy due to the mutual sorbate attraction does not improve K_3 over K_2. K_2 is

further improved when adjusted θ values are used so that only sorption occurring on a uniform field are considered. K_2 is now constant over the range $0 < \theta A < .90$.

It should also be emphasised that it cannot be assumed that a particular model adequately explains the sorption process occurring, even if one of the ideal models does provide a constant value for K. Young (22) and Barrer et al (64) have already noted that a far more rigorous test of the state of the sorbed phase can be obtained by looking at thermal entropy. Thermal entropy must satisfy certain criteria, in order to explain the experimental data (36).

(i) It should be independent of θ, and

(ii) It must be positive, having a reasonable physical magnitude.

Therefore, the entropy functions associated with the isotherm models, shall now be discussed.

4.1.14. Entropy of occlusion of krypton by Na-mordenite. Localized sorption:-

The entropy of sorbate, as shown in the theoretical section (2.1.4), may be expressed as follows:-

$$\bar{S}s = \bar{S}th + \bar{S}c \qquad (9)$$

where $\bar{S}s$, $\bar{S}th$, $\bar{S}c$ represent the differential molar entropy of sorbed gas, thermal and configurational entropy terms respectively. This expression is confined to systems of localized sorption, where the sorbate possesses no degree of translational freedom. The configurational entropy is

related to by the expression:-

$$\bar{S}c = R \ln \frac{(1-\theta)}{\theta} \qquad (10)$$

and the molar entropy of the sorbed phase, at equilibrium pressure P and temperature T, is given by:-

$$\bar{S}s = \Delta H/T + R \ln \frac{(2\Pi m KT)^{3/2}}{h^3} KT/P + 5R/2 \qquad (8)$$

Both of these expressions contain known constants, e.g. R, K, h etc., and experimentally obtainable functions such as θ and ΔH. Therefore, if the isotherm data is available to provide P and ΔH, a value of $\bar{S}th$ for any value of θ, at any temperature may be calculated from equation (9). Figure 23 shows the plots of the differential entropy functions (-150C°) $\bar{S}s$ and $\bar{S}th$ for Na-mordenite° and Na-mordenite $^{*}_{2}$ (60% damaged). A steady decrease in $\bar{S}s$ was observed in the standard sample up to $\theta = 0.5$ and up to $\theta = 0.75$ in case of Na-mordenite$^{*}_{2}$. As $\bar{S}th$, the differential thermal entropy should be quite sensitive to changes in the characteristics of the sorption sites. Fig. 23 shows that this is the case as $\bar{S}th$ for Na-mordenite$^{*}_{2}$ is reasonably constant up to $\theta = 0.75$ as against standard sample where it is constant only up to $\theta = 0.5$, showing the effect of reduction in channel size in Na-mordenite$^{*}_{2}$ due to irradiation. These entropy factors are the same for Langmuir's model and for modified Langmuir model K_2 which allows for mutual sorbate molecule interactions.

[illegible] significant entropy changes

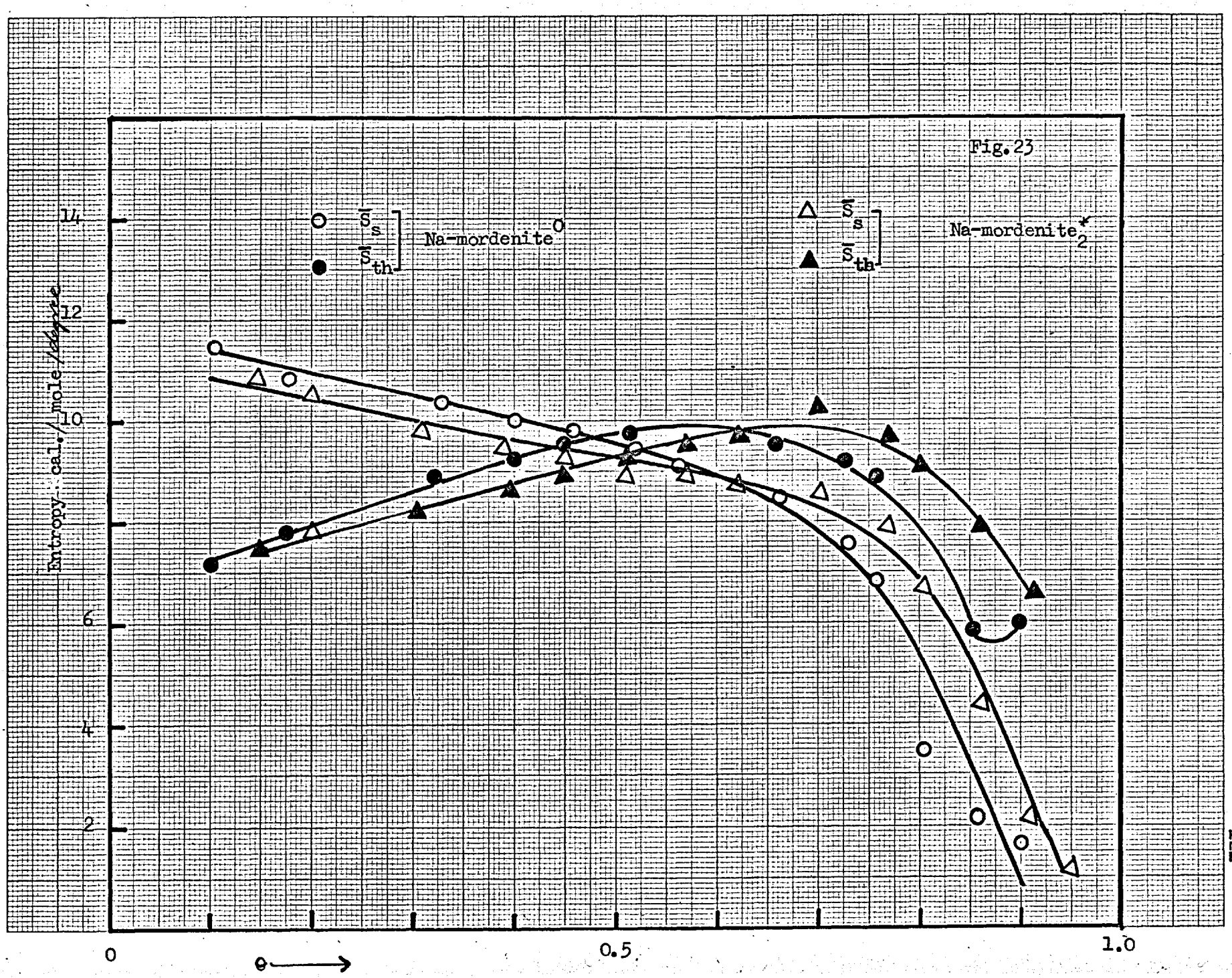
Fig. 23
$\bar{S}_s$
$\bar{S}_{th}$
Na-mordenite$_0$
$\bar{S}_s$
$\bar{S}_{th}$
Na-mordenite$_2^*$
Entropy - cal./mole/degree
14
12
10
6
4
2
0
0.5
1.0
θ

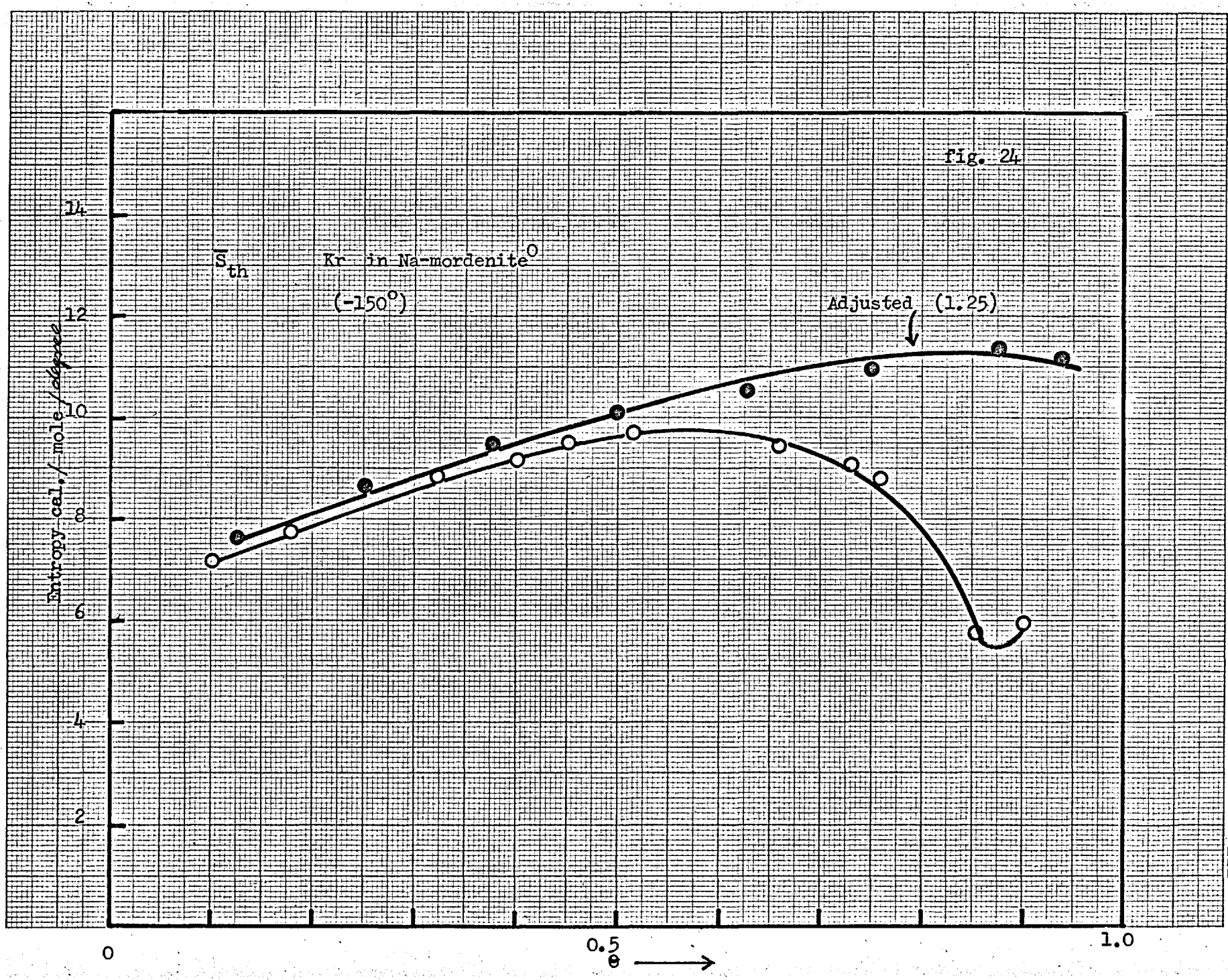
fig. 24
$\bar{S}_{th}$
Kr in Na-mordenite^{0}
(-150°)
Adjusted (1.25)
Entropy, cal./°K.-mole/space
14
12
10
8
6
4
2
0
0.5
1.0
θ

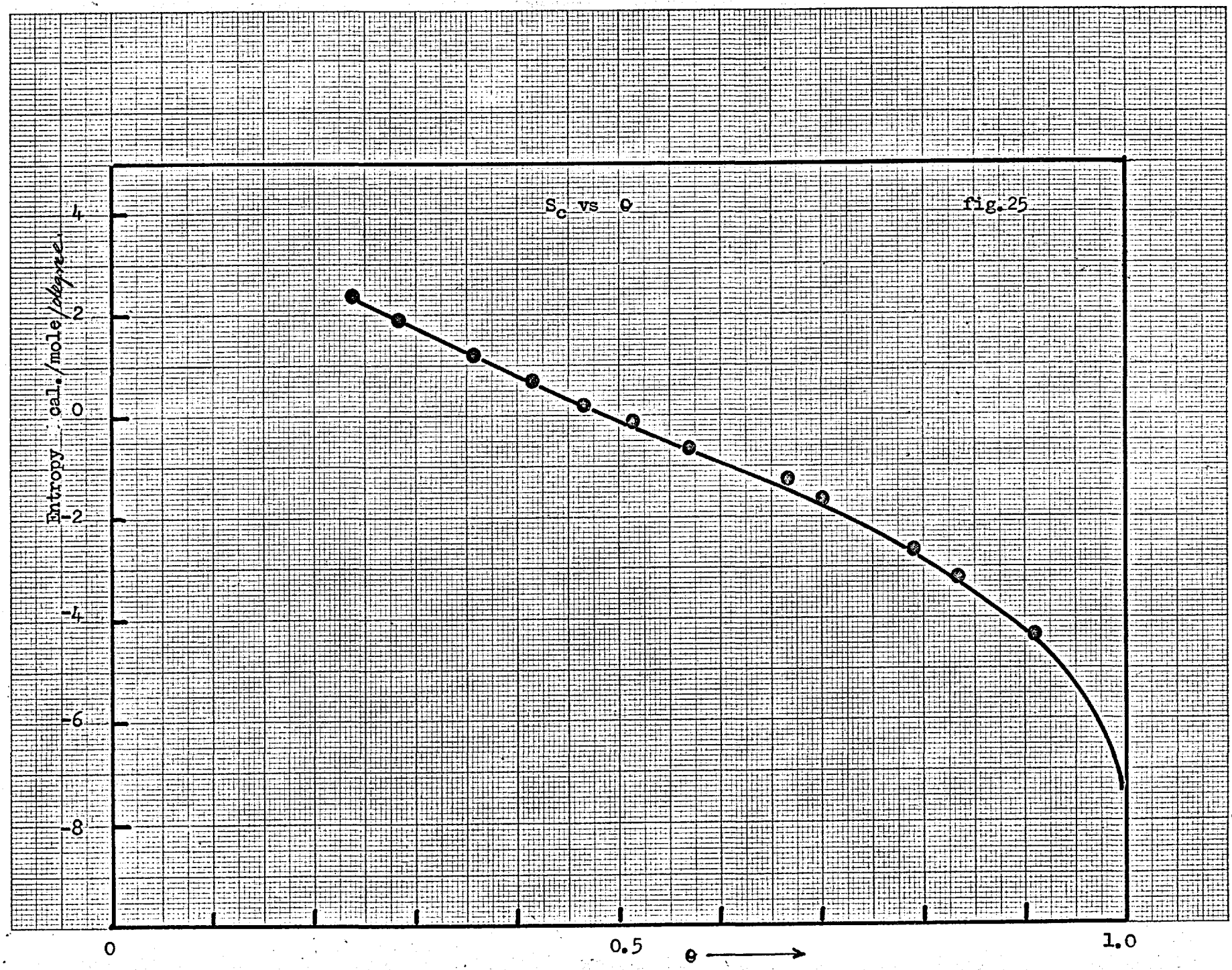
S_c vs θ
fig. 25
Entropy - cal./mole/degree
4
2
0
-2
-4
-6
-8
0
0.5
1.0
θ

$\bar{S}c$ can be calculated from equation (10) when the distribution of the sorbate molecules on the sorption sites is a random one. When mutual sorbate interactions affect the distribution of the sorbate molecules then $\bar{S}c$ is given by:-

$$\bar{S}c^{\circ} = R \ln \frac{(1-\theta)}{\theta} - Z R \ln \frac{(2-2\theta)}{\beta+1-2\theta} + W/_T \frac{(\beta-1+2\theta)}{\beta} \quad (26)$$

There is little difference between $\bar{S}c$ as given by equation (10) and $\bar{S}c^{\circ}$ given by equation (26). The second and third terms in equation (26) introduced because of the non-randomness of the distribution of the sorbed molecules almost cancel each other leaving $R \ln \frac{(1-\theta)}{\theta}$ as the dominant term in $\bar{S}c^{\circ}$ and changes of Z and 2W do not affect these conclusions. The plot of $\bar{S}c$ is shown in figure 25.

In conclusion, then of the localized models K_2 proves to be the most appropriate. Considering both the constancy of this isotherm model, and the fairly constant value of thermal entropy over a wide range of θ , this model is considered to best explain the sorption of krypton by Na-mordenite.

Na-mordenite$^{*}_{2}$ (60% damaged) was employed to find out if neutron irradiation resulted in any change in the conclusion drawn regarding the isotherm model and corresponding entropy functions, for sorption of krypton by the standard sample. Some significant changes in thermodynamics properties have already been observed, e.g. change in isosteric heat curve. The heat of sorption curve in case of standard sample

suggests that decrease in heat may be due to sorption on non-wall sites around $\theta = 0.8$, fig. (15). The ΔH Vs θ curve for 60% damaged sample, also shown in fig. (15) is much more uniform in nature, suggesting that sorbent is much more uniform in nature. This might have been produced as sorption in small channels does not take place as shown by the calculations on page 93 . Therefore, as suggested by Rees and Williams (1) that only sorption between $\theta = 0$ and 0.80 is taking place at a homogeneous surface potential, and the rapid increases in K_1, K_2 and K_3 are therefore due mainly to the rapid decrease in ΔH as shown in fig (16), (17) and (18). In order to test this theory all θ values were multiplied by the adjustment factor of 1.25, which makes a decided improvement on the constancy of K_2 with θ fig (19). This adjustment factor makes a decided improvement in plot of log 10 $\frac{P(1-\theta)}{\theta}$ against θ shown in fig. (21 a,b), the plot now being linear to θA approaching 1, fig (21c) and (21d). In figure (18) K_2 against θA is shown for a sample of the same sorbent which has been irradiated with fast neutrons. This treatment has been proved to contract the lattice, which is further supported by a smaller adjustment factor (1.15) in this case.

If localized sorption model is operative then $\bar{S}th$ should be constant independent of θ. $\bar{S}th$ is not very constant as shown in fig. (23), when θA is considered $\bar{S}th$ is now greatly improved, fig (24). These results indicate that the hypothesis put forward by Rees and Williams (1) is satisfactory for the sorbent studied. The adjustment factor of 1.33 for the open NaX is reduced as expected to 1.25 for the more compact synthetic mordenite

and in a damaged mordenite which is known to have a contracted lattice the factor is reduced to 1.15.

Na-mordenite$^*_{10}$ (65% damaged) and the Na-mordenite$^*_{11}$ (50% damaged) supported these observations by providing data similar to Na-mordenite$^*_2$, within experimental errors. The close similarity in the results for standard and Na-mordenite$^*_1$ (15.5% damaged) indicate that although a loss in sorptive capacity was observed, the sorption of krypton by the damaged zeolite still agreed best with the ideal model of localized sorption, with mutually sorbed molecule interactions.

4.1.15. Irradiation at liquid Nitrogen Temperature:-

Na-mordenite$^*_{13}$ and Na-mordenite$^*_{14}$ were irradiated to a fast neutron dose of 0.712×10^{18} n/cm^2 and 0.8×10^{19} n/cm^2 respectively at liquid nitrogen temperature. This experiment was carried out in order to find if any annealing of damage in Na-mordenite occurred during irradiation under normal reactor temperature of Ca. 80C$^\circ$ and also possibly during outgassing at 360C$^\circ$ under the standard treatment of samples prior to sorption measurements. Na-mordenite$^*_{13}$ was found to be 5.5% damaged by argon sorption run at liquid nitrogen temperature. Great care was taken in maintaining liquid nitrogen temperature throughout the irradiation and until the argon sorption run was completed. It was then allowed to warm up to room temperature and sorption run repeated. No change in the damage was observed. Heating of the sample even up to 360C$^\circ$ for 24 hours did not appear to anneal any damage. Plots of various sorption runs are shown in figure 26.

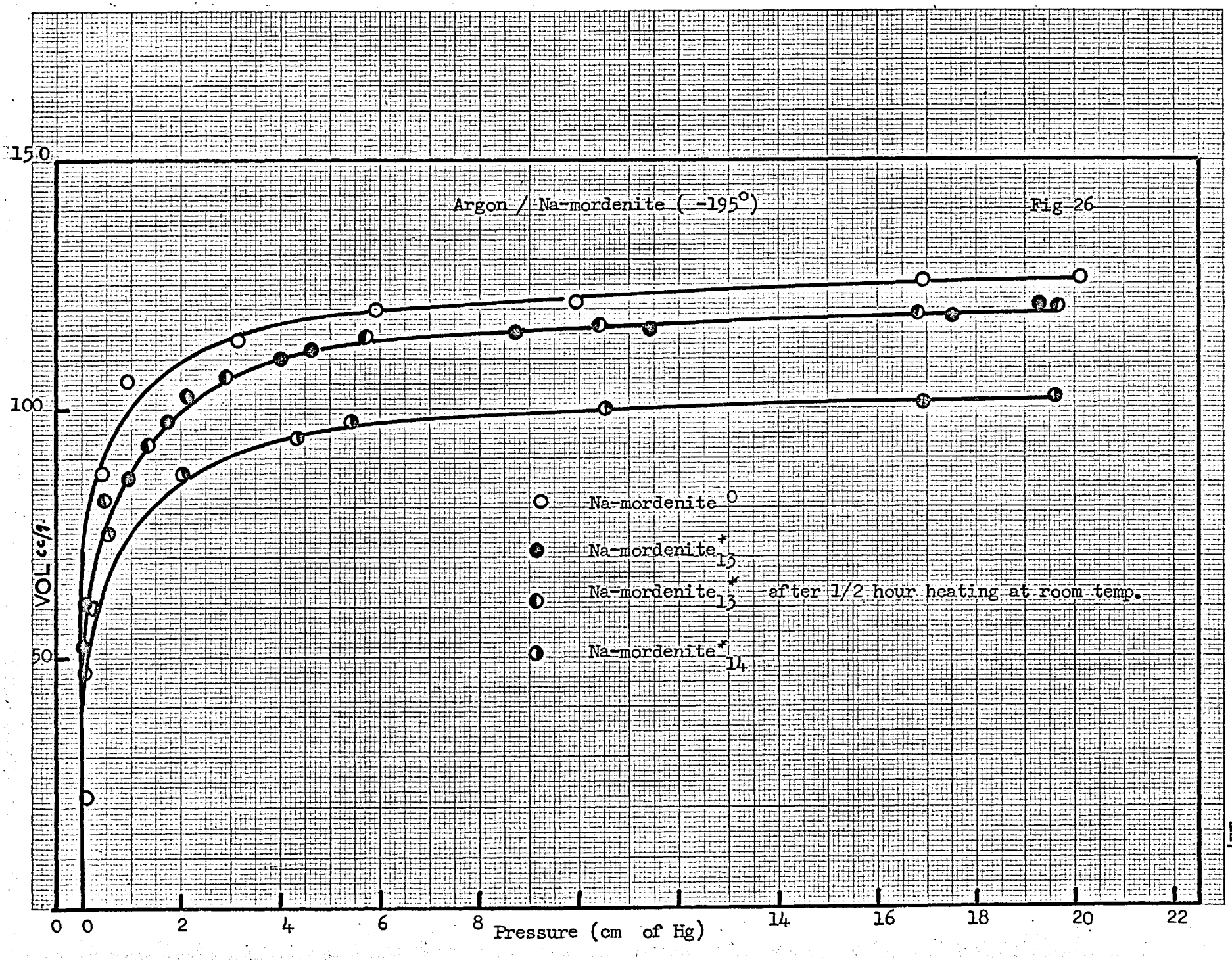
Argon / Na-mordenite (-195°)
Fig 26
150
100
50
VOL cc/g.
Na-mordenite 0
Na-mordenite* 13
Na-mordenite* 13 after 1/2 hour heating at room temp.
Na-mordenite* 14
0 0
2
4
6
8
14
16
18
20
22
Pressure (cm of Hg)

Na-mordenite$^{*}_{14}$ showed 19.2% damage. No annealing effect could be observed with this ample as well. It can be concluded, therefore, that Na-mordenite does show damage when irradiated to a fast neutron dose of 0.712 x 10^{18} n/cm^2 at liquid nitrogen temperature, and it appears not to have been annealed by heating the sample up to 360C^{o} for 24 hours. Therefore, it can be assumed that no damage has been annealed out while outgassing the samples after irradiation.

The damage is found to be less when Na-mordenite is irradiated at 80C^{o} under the same dose of fast neutron. This is probably due to the fact that at liquid nitrogen temperature, some of the atoms displaced by neutron bombardment do not have sufficient energy to recombine and also to move about and fill vacant sites, whereas at ambient temperature of reactor it is possible for the displaced atoms having comparatively more energy to occupy some of the vacancies created by irradiation and thus annealing out the damage.

4.2. Neutron Irradiation:-

The previous section dealt with the effects of neutron irradiation of Na-mordenite in respect of its krypton adsorption properties. This section includes some observation and some simple calculations for the damage arising from fast neutron bombardment and for the nuclear transmutations due to thermal neutrons.

Figure 27 shows a plot of % loss in capacity for sorption at -150C^{o} and 25C^{o} against neutron dose. The plot shows that Na-mordenite is completely damaged, when

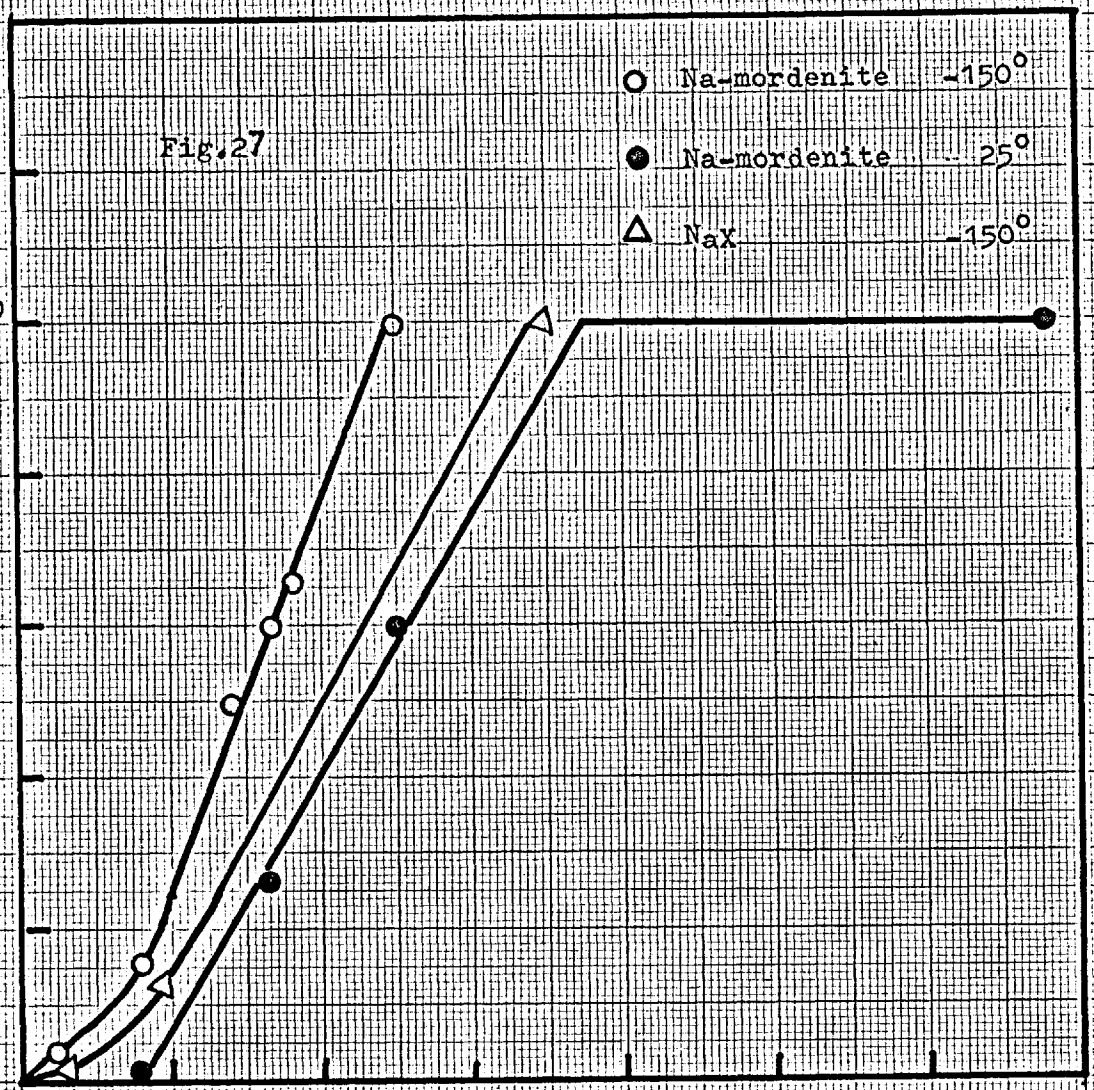
Na-mordenite -150°
Na-mordenite 25°
NaX -150°
100
80
60
40
20
0
% loss in capacity
2
4
6
8
10
12
x 10^19 n/cm^2

Fig. 27

the integrated neutron dose is 5.0×10^{19} n/cm^2 for -150 C$^\circ$ sorption, but at 250° the damage is 60% for the same neutron dose. On comparison with the plot for NaX, it is quite clear that Na-mordenite is more susceptible to damage than NaX.

4.2.1. Calculation of the Number of Atoms Displaced by Fast Neutron Irradiation:-

Neutrons obtained from fission of u ^{235} atom, range in energy from 0.5 to 15 Mev, the average for the purpose of calculations usually being taken between 1 - 2 Mev. In the present calculations value of 1 Mev will be used.

The maximum amount of energy in an elastic collision that may be transferred to an element of atomic mass M, by a neutron of mass N = 1, and energy E, is given by:-

$$E_{max} = {}^{4\,EMN}/_{(M+N)^2} \qquad (18)$$

which approximate to:-

$${}^{4\,EM}/_{(M+1)^2} \quad \text{or} \quad {}^{4\,E}/_{M} \qquad (19)$$

For a silicon atom it is one tenth of the incident neutron energy, i.e. 0.1 Mev. This is applicable to a direct head on collision between the neutron and lattice atom, in glancing collision, the energy transferred would be correspondingly less. The average energy transferred is $E = {}^{E\ max}/_{2} = 0.05$ Mev, which is considerably larger than the displacement energy of an atom, usually taken as 25 ev. It is, therefore, quite clear that as long as the bombarding neutron possesses energy in excess of ${}^{M}/_{2} \times 25$ ev,

it will continue to displace lattice atoms upon collision. The number of primary collision resulting in displacements due to each bombarding neutron, may therefore be expressed as:-

$$Nd = E_{max}/4\,Ed = E/2Ed = \frac{0.05 \text{ Mev.}}{2x25 \text{ ev.}} \qquad (22)$$

$$= 1000 \text{ displacements}$$

According to previous calculations (section 2.2.3. page 48 this estimate is of the order of five times too large, i.e. approx. 200 primary displacements occur per incident neutron. These 200 projectiles atoms resulting from every fast neutron, travel throughout the lattice causing ionization and excitation until they come to rest as interstitial atoms or fall into vacant site.

Dienes and Vineyard (51) showed that the number of primary atoms displaced per g. by a bombarding neutron is given by:-

$$Np = \phi . t . n . Cd.$$

where ϕ = instantaneous neutron flux

t = time

n = number of atoms per g. target and

Cd = the displacement cross-section of the lattice atom.

Since each primary "knock-on" produced many more displacements, Np corresponds to only a small fraction of the total number Nd of displacements. The following table gives the values of "n" for Na-mordenite, the cross-section of lattice atoms and the number of displacement corresponding to neutron doses of 3.3×10^{19} n/cm^2 and

5.0×10^{19} n/cm^2, (Na-mordenite$^*_2$ and Na-mordenite$^*_5$ respectively) calculated using the following formula as shown in section 2.2.3.

$$Nd = \frac{Np.\ E.\ M.\ f}{Ed.\ (M+N)^2} \qquad (27)$$

Table 6

Percentage of Atoms Displaced

Atom	No. of atoms lg. Na-mordenite ($\times 10^{21}$)	Cross-section (barns)	Nd ($\times 10^{20}$ corrected)		% No. of atoms displaced			
			3.3×10^{19} n/cm^2	5.0×10^{19} n/cm^2	1.6×10^{19} n/cm^2	3.3×10^{19} n/cm^2	5.0×10^{19} n/cm^2	1.36×10^{20} n/cm^2
Si	8.0	4.7	3.6	5.5	2.2%	4.3%	7.0%	18.7%
Al	0.80	2.6	0.21	3.1	1.3%	2.6%	3.9%	10.7%
Na^+	0.70	3.7	0.30	4.5	2.8%	4.7%	6.4%	17.1%
O	19.01	8.0	24.0	37.0	6.2%	12.8%	20.0%	53.0%

The calculated numbers of atoms displaced are too large. This is to be expected since the theory makes no allowance for "replacements", i.e. the exchange of roles between the moving atom and the stationary one. In practice, the ratios of theoretical to experimental figures for displacements range from 3 to 10, (21, 51) the ratio for quartz being 5. The ratio for Na-mordenite structure would probably be less and when a factor of 3 is taken, 53, 12, and 6.2% approximate

displacements of oxygen, the element mainly affected by the radiation, correspond to losses in sorption capacity of 100, 60, 15% respectively. Since silicon and aluminium atoms are bonded through oxygen bridges tetrahedrally, 53% displacement of oxygen would represent the breaking of two bonds per silicon or aluminium atom, and this should lead to lattice collapse with complete loss in sorption capacity. This also agrees with the experimental finding that % loss in capacity $\propto$ (dose)$^{5}/3$, as shown in fig. 28 which suggests that approximately two oxygen atoms have to be displaced from each silicon or aluminium before any loss in sorption capacity develops.

4.2.2. Calculation of Specific Activities resulting from the irradiation of Na-mordenite with slow neutrons

The yield or specific activity of an element is given by equation 27 page 53 . It has already been shown in section 2.2.4 that Al_{13}^{28}, Si_{14}^{31} and O_{8}^{19} atoms give specific activities which would completely decay within a few days, but the formation of Mg^{24} from Na^{23} could be of some interest.

$$Na_{11}^{23}\ (n, \gamma)\ Na_{11}^{24} \longrightarrow Mg_{12}^{24}$$

The actual weight of magnesium produced in a sample by the β-decay of the unstable Na^{24}, may be calculated as follows:-

$$\text{Mass (of Mg)} = 7.7 \times 10^{-9}\ \text{A.T.S.} \qquad (28)$$

where A, T and S are defined at page 54 , the mass of magnesium equals to 8.0×10^{-7} g / g of Na-mordenite

Fig.28

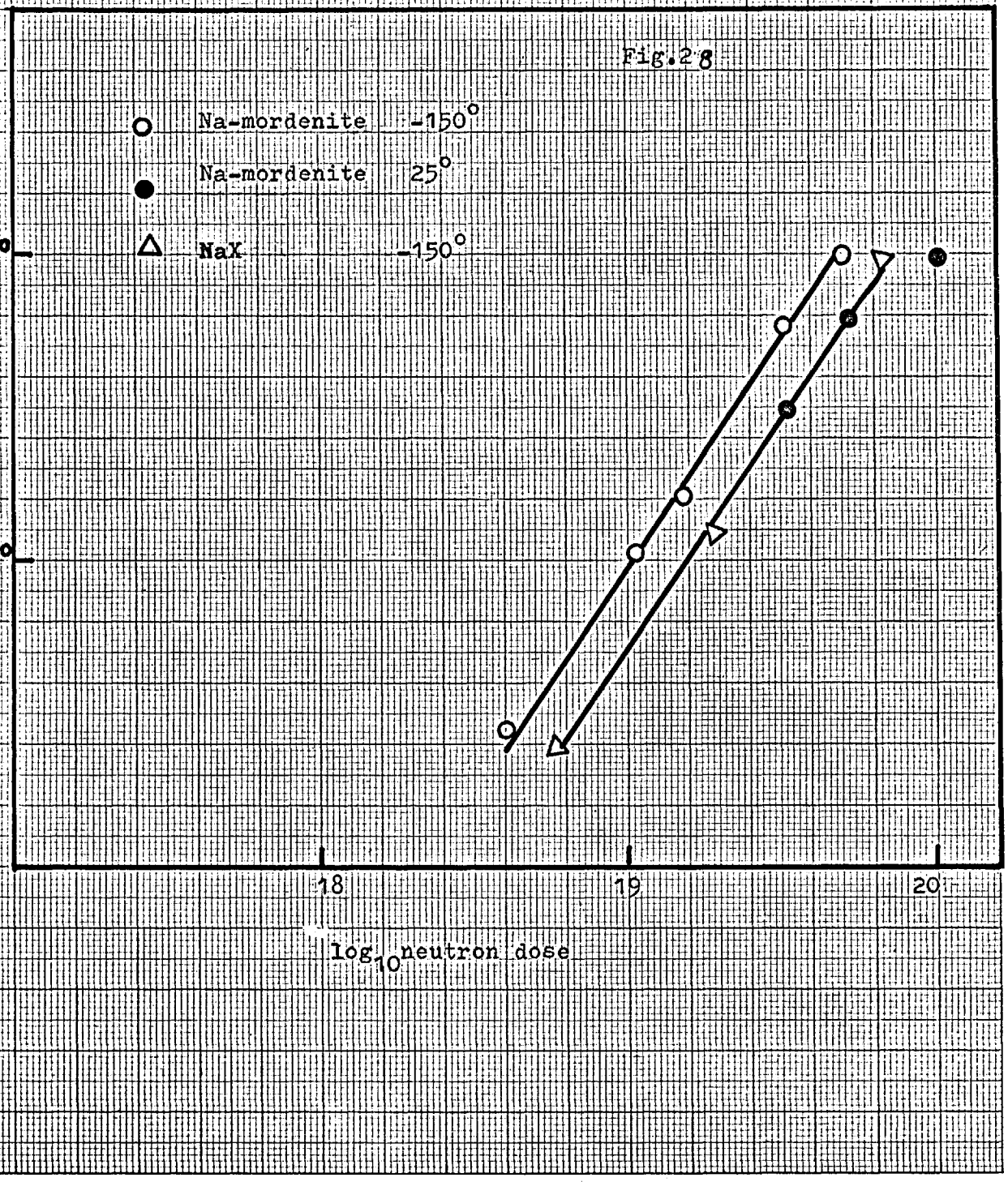
Na-mordenite -150°
Na-mordenite 25°
NaX -150°
2.0
1.0
0
log10 loss in capacity
18
19
20
log10 neutron dose

(anhydrous). Divalent Mg^{++} ions, are bound to affect the sorptive properties of the zeolite, however, the yield of magnesium is so small that it is extremely unlikely that the isosteric heat curves would show the slightest change. Much heavier thermal neutron doses would be necessary to produce any appreciable effect.

4.2.3. Discussion of Effects of Neutron Irradiation on a zeolite:-

It was assumed by Crawford and Wittels (16) that the lattice vacancies and interstitials resulting from the neutron irradiation of quartz, were almost entirely due to oxygen atoms. This assumption was made because the oxygen and silicon atoms have displacement cross sections of 8.0 and 4.7 barns respectively; because there are more O atoms than Si atoms per unit volume; also because more energy is required to displace a Si atom. The latter reason arises because each Si atom is covalently bonded to four O atoms, whereas each O atom is joined to only two neighbouring atoms. The same applies to the structure of Na-mordenite, the cross section of Al and Na^{+} being 2.6 and 3.7 barns respectively and the oxygen atoms outnumber the other atoms. It is, therefore, expected that a high percentage number of displaced oxygen atoms, will result in a collapse of the lattice.

Appreciable damage to Na-mordenite occurs at a slightly lower dose than for NaX, i.e. approximately $5.0 \times 10^{19} n/cm^2$ as opposed to $7.0 \times 10^{19} n/cm^2$; this might be expected because of high alumina and silica contents (10:1) of Na-mordenite as compared to NaX. Although oxygen having capture cross section for neutrons 8.0 barns are usually

responsible for damage in the zeolite but Si with greater cross section (4.7 barns) than Al (2.6 barns) can also be displaced and have some effect. Therefore, high silica contents of Na-mordenite is one of the factors in producing damage in it at a lower neutron dose than in NaX. Density measurements showed there to be a distinct increase in density for the completely damaged sample (5.0×10^{19} n/cm^2), from approximately 2.0 g/c.c. of hydrated Na-mordenite to 2.5 g/c.c., representing a 25% increase. This is of the same order as the density increase observed for vitreous silica. Primak (18) suggested that the displaced atoms in vitreous silica lodge in the cavities within the lattice, so permitting a general relaxation of the structure into a more compact arrangement, thus increasing the density.

Work by Levy and Kammerer (65) on the neutron irradiation of diamond, led Dienes and Vineyard (51) to make tentative conclusion that in diamond, a drastic collapse of the crystal lattice occurs rather suddenly at high exposures. This also might be the case with Na-mordenite, see figure 26.

It has been observed that annealing of damage is possible simply by heating the sample. Primak and Szymanski (19) found that vitreous silica could be gradually annealed at 300C° and Primak et al (18) found that diamond was annealed above 100C°. Two samples of Na-mordenite were irradiated and analysed at liquid nitrogen temperature. When these samples were heated to 360C° for 24 hours, no annealing out effect was observed. Therefore, it can be concluded that while outgassing the sample at 360C°, before sorption measurements were made, annealing of any structural damage did not take place.

4.3. Some Experiments with Cation Exchange in Na-mordenite

After determining the effects of neutron irradiation on the sorption properties of Na-mordenite, it was of interest to ascertain the effect of irradiation on the exchange properties. Therefore, a few cation exchange experiments with Cs^{+} and Ba^{++} were carried out.

Chemical analysis of two samples of Na-mordenite, expressed as % weight, gave

$Na_2O = 6.0\%$ $Al_2O_3 = 12.0\%$ $SiO_2 = 68.6\%$ $H_2O = 14.2\%$

The oxide formula may therefore be written as:-

$(3.50)\ Na_2O.\ (4.0)\ Al_2O_3.\ (39.5)\ SiO_2.\ (26.5)\ H_2O$

The cation deficiency was assumed to be counter-balanced by the presence of hydronium ions. The high silica to alumina ratio (10:1) is partly responsible for the high stability of Na-mordenite as compared with that of most other zeolites.

Only 4 out of 8 sodium ions per unit cell have been definitely located (3), the others being assumed to be distributed within the large channels. The four cations which have been located are in the centre of the windows (free diameter 2.8A°) in the channels of about 4.0A° diameter, which connect the wider channels (5.8A°). Complete ion exchange should therefore, be possible with any univalent cation of diameter not exceeding 4.0A°; cations larger than this may be unable to replace these 4 Na^{+} ions, thus imposing a maximum exchange of 50% on

systems involving such large ions.

4.3.1. Exchange Technique

A few gm. of Na-mordenite was labelled with active Na^{22} obtained from the Radiochemical Centre, Amersham. Na-mordenite was stirred overnight with a solution of $Na^{22}\dot{C}l$ of the required specific activity such that one gm. of Na-mordenite labelled with Na^{22}, when dissolved in a 30 ml solution of $Na\dot{C}l$ and counted in a halogen quenched liquid Gieger-Muller counter tube type M6H, gave approx. 2000 counts/min. The tagged Na-mordenite was then washed with distilled water, several times in order to remove $\bar{C}l$ and stored over a saturated solution of ammonium chloride at room temperature.

A definite amount of tagged Na-mordenite was weighed out into dry pyrex tubes which had already been boiled in distilled water for a few hours to remove alkali. 30 ml of exchange solutions of various strengths were added to the tubes, which were then sealed and rotated in an oven for 2-4 days at $25C^{o}$. This length of time was found to be sufficient for the systems studied for equilibrium to to attained. The solution was then centrifuged and the resultant Na^{+}ion concentration in solution was determined by the liquid counting technique.

4.3.2. Radioactive Counting Technique

The equipment employed consisted of a halogen quenched liquid Gieger-Muller counter tube, type M6H at an operating voltage of 400 volts. The counts were recorded on an automatic scalar unit in conjunction with a probe unit of dead time 300 u secs. The counter tube had a capacity of

10 ml and was filled to the same mark each time.

The number of counts recorded on this scalar unit were all corrected for the background (approx. 20 counts/min.), and also corrected for the dead time by means of equation:-

$$N_T = \frac{No}{1 - t\,No} \qquad (28)$$

where N_T = true count rate per min.

No = observed count rate per min.

t = dead time (minutes)

The solutions were usually counted for three successive periods of 300 seconds to obtain an average count. Between counting each solution, the G.M. tube was thoroughly washed to remove contamination. To show that all activity had been removed, a background count was made each time.

4.3.3. Na-mordenite/Ba^{++} Exchange System

Figure 29 (a) shows the exchange isotherm constructed for the standard sample. Complete exchange could not be accomplished and the maximum achieved after rotation with several fresh Ba^{++} solutions was approx. 72% The isotherm obtained for Na-mordenite$^*_2$ (60% loss in sorptive capacity) showed the decrease in exchange capacity, shown in fig. 29 (a).

4.3.4. Na-mordenite/Cs^+ Exchange System

The exchange isotherm constructed for the standard sample is shown in fig 29 (b). Complete exchange of Cs^+

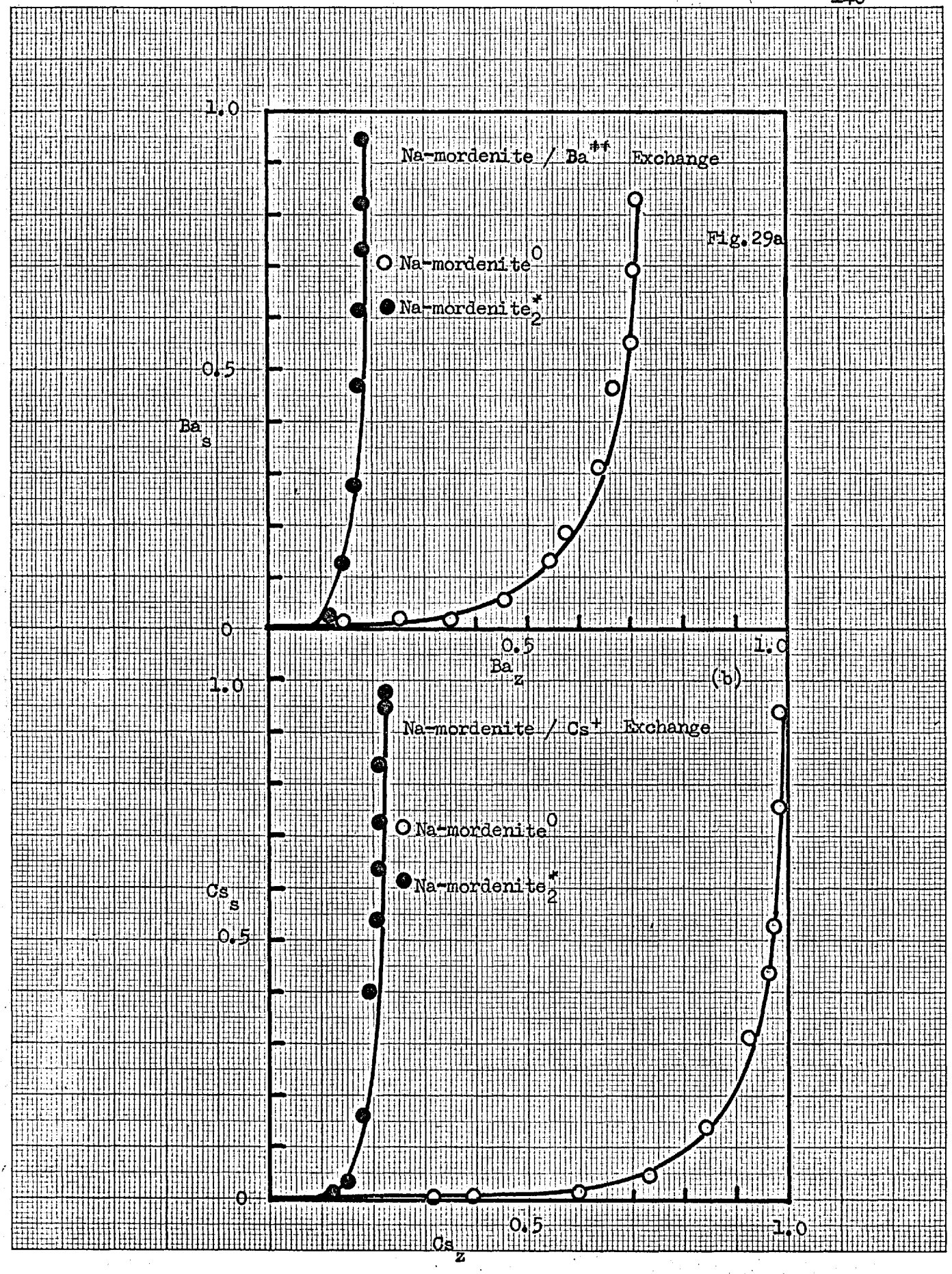
Na-mordenite / Ba++ Exchange
Na-mordenite 0
Na-mordenite* 2
1.0
0.5
0
Ba s
0.5
1.0
Ba z
(b)
Na-mordenite / Cs+ Exchange
Na-mordenite 0
Na-mordenite* 2
1.0
Cs s
0.5
0
0.5
1.0
Cs z

Fig. 29a

ion for Na^+ is possible, and from the shape of the curve, it is obvious that mordenite exhibits a very strong selectivity for Cs^+ ion. When a similar isotherm was constructed for Na-mordenite$_2^*$, a distinct decrease in exchange capacity was observed as shown in fig. 29 (b).

4.3.5. Effects of Neutron Irradiation on the Cation Exchange Properties of Na-mordenite

Four of the eight Na^+ ions per unit cell, which have been definitely located (3), lie in the 2.8A° windows in the 4.0A° channels, while the other 4 Na^+ are distributed within the channel, these can be easily replaced by any ion small enough to diffuse through the same channels. They should all, therefore, be replaceable by the Cs^+ ion, to give 100% exchange, as was observed. Ba^{++} exchange on the other hand, leads to the problem as to how one Ba^{++} ion can replace 2 Na^+ ions which effectively lie in neighbouring channels. If Ba^{++} ions are assumed to occupy the same sites as do the Na^+ ions, then a redistribution of the anionic charge on the frame-work must occur. However, if Ba^{++} ions are assumed to be located in between the two sites previously occupied by Na^+ ions, then 100% exchange should be possible; (as the distance between the two sites is of the order of 3A°). However, the maximum exchange observed experimentally was only 72%, suggesting that the Ba^{++} ions might well occupy different sites altogether, or that stacking fault (see page 15) might lead to trap the individual cations, thus restricting exchange by the Ba^{++} ions, but at the same time allowing complete exchange by the Cs^+ ions.

Several exchange experiments were conducted with

Na-mordenite$^*_1$, Na-mordenite$^*_2$ and Na-mordenite$^*_5$. Isotherm for Na-mordenite$^*_1$ lie on the plots for the standard sample. It may be either that the cation exchange properties of Na-mordenite$^*_1$ are unaffected by a neutron dose of 1.6×10^{19} n/cm^2 or that any effect lies within the experimental error. On the other hand Na-mordenite$^*_2$ showed a distinct decrease in exchange capacity for Cs^+ and Ba^{++}. It has already been shown that Na-mordenite$^*_2$ sustained a 60% loss in sorption capacity (see page 85,86). Analysis of cation exchange isotherms show a 73% and 77% loss in exchange capacity for Ba^{++} and Cs^+ respectively. We know from sorption results that there is a 30% loss in sorption capacity at high temperatures and 60% loss at low temperatures, suggesting that there is a considerable degree of complete collapse of lattice (30%) accompanying a general contraction of 30% (see page 94,95 for discussion on this subject). However, ion exchange results show a much higher loss in exchange capacity indicating that this contraction and complete damage is locking up the higher percentage of the exchangeable Na^+ than one would expect from a random distribution of the cations. Exchange with Na^{22} in Na-mordenite shows that 25% of the cations are available for exchange.

In case of Na-mordenite$^*_5$ (100% loss in sorption capacity) exchange with Cs^+ and Ba^{++} was found to be practically non-existant, which was expected as this sample was found to be completely amorphous by x-ray studies and to have sustained a complete loss in sorption capacity.

It can be concluded that there is no definite effect

to the zeolite up to and including a neutron dose of 1.6×10^{19} n/cm^2. Only a dose of 5.0×10^{19} n/cm^2 would render the zeolite useless for the purpose of cation exchange. Therefore, in conclusion Na-mordenite is quite resistant towards the damaging effects of radiation as compared with other cation exchangers.

REFERENCES

1.	Rees and Williams	Trans. Fara. Soc. 1964, 60, 1973.
2.	Loewenstein	Amer. Mineralog. 1954, 39, 92.
3.	Meier	Z. krist. 1961, 115, 439.
4.	Zoltai and Buerger	Z. krist. 1960, 114, 1.
5.	Vogel	"Quantitative Inorganic Analysis" Longman Ed. 2. 1957.
6.	Breck and Smith	Scientific American, 200, 85, 1959.
7.	Breck, Eversole, Milton Reed, Thomas	J. Amer. Chem. Soc. 1956, 78, 5963.
8.	Barrer and Rees	Trans. Fara. Soc. 1959, 55, 992
9.	Brunauer	"The adsorption of gases and vapours" Oxford, 1945.
10.	Barrer and Wasilewski	Trans. Fara. Soc. 1961, 57, 1153
11.	Barrer and Gibbons	Trans. Fara. Soc. 1963, 59
12.	Kiselev	Russ. J. Phys. Chem. 1961, 35 892.
13.	Tompkins	Trans. Fara. Soc. 1950, 46, 569
14.	Seitz	Faraday Disc. 1949, 5, 271
15.	Primak, Fuchs & Day	Phys. Rev. 1953, 92, 1064
16.	Crawford & Wittles	Proc. Insternt. Conf. on Peaceful uses of A.E. 1955, paper.
17.	Wittles and Sherrill	Phys. Rev. 1954, 93, 1117.
18.	Primak	J. Amer. Chem. Soc. 1955, 38, 135.
19.	Primak, Szymanskis	Phys. Rev. 1956, 101, 1268.
20.	Simon	Phys. Rev. 1956, 103, 1587
21.	Billington & Crawford	"Radiation Damage in Solids" Oxford 1961.
22.	Young	J. Phys. & Chem. of Solids, 1960, 15, 119.

23.	Garden and Kington	Proc. Roy. Soc. 1956, A234, 35.
24.	Rees and Williams	Trans. Fara. Soc. 1965, 61, 1481
25.	Hill	J. Chem. Phys. 1949, 17, 762.
26.	Hill	J. Chem. Phys. 1950, 18, 246.
27.	Everett	Trans. Fara. Soc. 1950, 46, 453
28.	Hill	Adv. Catalysis. 1952, 4, 211
29.	Drain	Sci. Progr. 1954, 42, 408
30.	Garden, Kington & Liang	Trans. Fara. Soc. 1955, 51, 1558.
31.	Tykodi	J. Chem. Phys. 1954, 22, 1647.
32.	Amphlett	Endeavour 1958, 17, 149.
33.	Grover	J. Brit. Nucl. Energy Conf. 1958, 3 (1), 80.
34.	Amphlett	J. Inorg. Nuclear Chem. 1958, 6, 220.
35.	Ahrland	Acta. Chem. Scand. 1960, 14,1077.
36.	Garden, Kington & Laing	Trans. Fara. Soc. 1955, 51, 1558.
37.	Barrer & Sunderland	Proc. Roy. Soc. 1956, A237, 439.
38.	Hill	J. Chem. Phys. 1946, 14, 441.
39.	Morrison, Los, Drain	Trans. Fara. Soc. 1951, 47, 1023.
40.	Langmuir	J. Amer. Chem. Soc. 1918, 40,1361.
41.	Fowler	Proc. Cambridge Phil. Soc. 1936, 32, 144.
42.	Fowler	Proc. Cambridge Phil. Soc. 1935, 31, 260.
43.	Fowler & Guggenheim	"Statistical Thermodynamics" C.U.P. 1935.
44.	Lacher	Proc. Roy. Soc. 1937, A161, 525.
45.	Rees	Trans. Fara. Soc. 1954, 50, 335.

46.	Kemball	Adv. Catalysis. 1950, 27, 233.
47.	Lucchesi, Baeder, Longwell & Schroeder	J. Chem. Phys. 1959, 31, 558.
48.	Broussard & Shoemaker	J. Amer. Chem. Soc. 1960, 82, 1041.
49.	Cockelbergs	Adv. Catalysis, 1950, 2, 233.
50.	Kinchin & Pease	Reports Progr. Phys. 1955, 18,1.
51.	Dienes & Vineyard	"Radiation Effects in Solids" Intersc. Monographs. 1957. Vol.2.
52.	"The Radiochemical Manual" Part 1. Physical data. The Radiochemical Centre, Amersham 1962.	
53.	"Radiochemical Materials and Stable Isotopes" Cat.No.4 A.E.R.E. Harwell, 1957.	
54.	L.T. Chadderton	"Radiation Damage in Crystals"
55.	R. Strumene, J. Nikoul R. Gevers	"The Interaction of Radiation with Solids"
56.	Kaye and Laby	Tables of Physical & Chemical Constants 1956.
57.	Cook	Argon, Helium and the rare gases interscience.
58.	Jnanananda	"High Vacua" Van Nostrand 1947.
59.	Liang	J. Phys. Chem. 1953, 57, 910.
60.	Farkas & Melville	"Experimental methods in gas reactions" Macmillan 1939.
61.	Barrer & Reucroft	Proc. Roy. Soc. 1960, 258A, 431.
62.	Barrer & Stuart	Proc. Roy. Soc. 1959, 249A, 484.
63.	P.R. Natarajan	Ph.D. Thesis London University 1962.
64.	Barrer	Colston Papers, 10th Symp. 1958, 10.
65.	Levy & Kammerer	Phys. Rev. 1955, 100, 1787.

APPENDIX

ISOTHERM DATA

P = equilibrium pressure (cm. Hg.)
V = volume of gas adsorbed at equilibrium (cc. N.T.P./g anhydrous Na-mordenite)

Na-mordenite^{o}/Argon
90 K^{o}

P	V
0.551	90.732
0.832	98.461
1.672	103.331
2.014	105.512
2.571	108.312
4.141	110.301
5.341	111.401
7.561	112.132
10.067	114.731
12.501	115.612
14.786	116.220
19.833	116.861
23.513	117.334
27.563	118.413
35.343	119.431
42.531	120.181
50.651	120.913

Na-mordenite$_1^{*}$/Argon
90 K^{o}

0.601	70.512
1.331	78.781
2.561	85.319
4.991	88.642
6.431	92.320
8.101	95.455

Na-mordenite$_1^{*}$/Argon
90 K^{o}

P	V
10.301	96.461
13.331	99.631
17.551	100.361
22.551	101.450
32.001	102.981
37.516	103.312
45.112	104.031
52.512	104.512

Na-mordenite$_2^{*}$/Argon
90 K^{o}

0.321	28.321
0.461	33.321
0.552	37.771
0.751	40.561
1.144	44.506
2.307	47.366
5.033	50.103
8.661	51.672
10.571	52.891
14.671	53.723
18.532	54.013
32.101	54.833
46.342	53.455
52.481	56.321

Na-mordenite°/Krypton

-150C°		-150C°	
P	V	P	V
0.002	35.501	12.884	98.337
0.009	48.718	19.123	99.620
0.012	51.336	29.011	100.121
0.015	54.312	36.512	101.313
0.022	58.616	53.410	102.231
0.028	60.343		
0.040	63.712	-140C°	
0.051	65.344		
0.070	68.131	0.010	36.931
0.085	71.012	0.040	39.532
0.101	73.121	0.051	42.103
0.175	75.512	0.065	45.510
0.280	77.601	0.075	47.101
0.565	82.101	0.088	49.733
0.806	84.532	0.118	51.001
1.023	86.731	0.133	53.345
1.266	87.311	0.235	56.661
1.588	87.912	0.291	58.903
1.853	88.202	0.440	64.332
2.393	89.713	0.779	70.771
2.931	90.113	1.244	72.206
3.639	92.544	1.481	73.671
4.907	95.033	3.436	86.103
6.663	96.112	4.261	88.761
8.003	97.818	5.339	89.931

-140C°

P	V
6.663	90.561
8.275	91.343
10.001	92.531
12.251	93.230
15.233	94.731
20.302	95.100
27.510	95.832
33.012	96.003
43.570	96.691
50.220	97.410

-130C°

0.032	33.301
0.181	39.510
0.209	41.312
0.245	44.543
0.305	46.123
0.357	48.001
0.437	50.501
0.575	58.103
0.789	63.771
1.012	69.584
2.109	73.382
2.755	76.582
4.875	79.532
8.459	83.530
11.913	86.511
14.132	87.032

-130C°

P	V
18.151	88.441
22.628	89.109
28.564	89.931
34.209	90.012
41.657	90.630
51.382	90.891

-120C°

0.094	32.480
0.407	40.103
0.708	43.344
0.754	46.406
0.807	48.811
0.897	49.513
0.912	52.321
1.321	57.381
1.766	61.374
2.230	65.131
4.312	72.655
7.568	75.850
14.750	81.334
24.738	83.362
34.012	84.071
41.512	84.558
52.811	85.214

-100C°

0.147	24.466

-100C°

P	V
0.295	28.401
0.454	32.312
0.723	34.221
0.793	34.512
0.910	36.321
1.003	37.617
1.755	40.509
2.133	43.366
3.467	46.178
4.095	48.536
4.744	51.331
8.019	56.501
10.137	58.881
13.121	61.407
16.178	63.443
19.976	64.327
23.131	65.113
32.086	67.662
38.064	68.551
53.305	71.319

-90C°

0.321	20.501
0.645	23.561
0.958	25.311
1.581	28.032
1.688	29.781

-90C°

P	V
1.937	31.505
2.494	35.871
3.680	41.629
4.494	44.707
5.199	47.282
7.531	50.534
9.787	54.415
16.838	60.491
21.964	62.382
26.656	64.162
35.956	65.657
40.541	66.123
50.705	67.794

-70C°

0.661	14.731
0.876	17.621
1.191	21.371
1.533	23.366
2.446	30.434
4.121	37.771
5.013	40.612
8.551	47.544
10.632	49.301
13.761	52.410
15.981	53.661
24.532	57.471

-70C°

P	V
34.991	60.441
50.321	62.537

-40C°

1.071	8.823
1.206	9.731
2.321	12.511
3.017	16.633
5.010	22.655
6.761	26.113
13.131	35.761
22.561	41.732
29.998	45.066
36.430	47.511
42.006	49.326
53.610	51.501

0C°

2.175	2.951
2.877	3.919
3.901	4.632
4.593	5.442
7.845	9.202
12.551	13.202
16.301	16.529
22.120	19.090
28.207	23.193
33.930	26.016

0C°

P	V
43.028	29.662
45.728	30.532

+25C°

4.660	2.029
6.143	3.228
8.352	3.945
11.957	5.873
15.015	7.409
18.262	8.600
22.049	10.000
28.398	12.359
37.798	15.504
51.967	19.839

Na-mordenite*$_1$/Krypton

-150C°

0.010	20.515
0.012	22.321
0.018	25.122
0.023	28.701
0.031	30.712
0.040	32.432
0.051	35.012
0.081	38.772
0.095	40.712
0.126	42.321

-150C°

P	V
0.266	46.203
0.493	50.661
0.699	55.721
0.756	58.662
0.936	60.771
1.211	62.612
2.166	69.321
2.376	70.832
2.473	71.401
3.681	74.551
5.199	77.161
7.802	82.331
10.101	84.401
16.501	87.490
25.012	89.133
32.016	90.361
38.010	91.032
52.551	92.356

-140C°

P	V
0.049	26.662
0.072	28.112
0.091	30.321
0.105	35.717
0.164	40.090
0.185	41.311
0.225	45.012
0.306	50.134
0.668	53.312

-140C°

P	V
1.055	58.512
1.159	60.712
2.407	63.338
2.977	64.191
3.258	67.812
4.006	69.122
5.195	71.496
7.233	75.112
9.881	77.414
12.543	79.541
16.321	82.331
21.563	83.817
32.493	85.012
40.712	85.612
53.312	86.513

-130C°

P	V
0.116	22.101
0.187	26.461
0.269	28.801
0.311	34.443
0.381	36.712
0.455	40.321
0.570	42.201
1.305	49.441
1.426	50.317
1.657	52.223
2.715	56.314
3.233	59.881

-130C°

P	V
4.605	64.551
8.304	70.432
14.733	74.632
18.230	76.513
20.531	77.307
33.932	79.013
42.531	79.633
51.630	80.706

-120C°

0.363	25.512
0.562	30.132
0.612	33.321
0.713	36.910
0.857	38.719
0.985	41.514
2.161	47.617
3.253	52.881
4.907	58.013
8.124	63.123
10.793	65.471
14.480	68.414
22.448	71.773
29.456	72.911
35.566	73.616
41.080	74.501
52.608	75.557

-100C°

P	V
0.061	9.355
0.134	12.771
0.295	18.120
0.562	26.612
1.133	33.871
1.323	35.501
2.301	43.441
2.525	44.931
2.951	45.301
4.577	50.140
5.410	51.334
7.055	55.121
10.201	58.061
11.032	58.816
12.101	60.371
17.513	63.441
21.018	64.512
26.171	66.311
36.102	67.012
44.012	67.701
52.321	68.912

-90C°

0.132	8.322
0.294	12.591
0.643	16.321
1.225	26.322

-90C°

P	V
2.458	34.316
2.841	40.232
4.949	44.123
5.393	45.412
6.294	46.987
9.687	53.532
11.437	55.701
12.781	57.321
14.149	58.621
20.056	61.890
26.299	63.023
31.393	63.891
36.202	64.871
43.250	65.821
52.519	67.321

-70C°

0.455	7.430
0.981	13.321
1.121	15.012
2.012	26.132
3.321	33.512
6.347	43.321
12.553	50.401
21.367	56.012
30.712	58.532
39.891	60.121
52.512	62.321

-40C°

P	V
1.212	8.321
2.433	12.512
4.451	20.012
6.123	24.932
9.532	30.129
16.713	37.343
26.124	43.512
31.610	45.523
43.612	49.321
51.321	51.321

0C°

2.118	2.587
2.723	3.603
3.193	4.013
3.671	4.631
5.530	5.671
6.541	7.210
9.605	10.413
13.616	14.124
15.625	15.212
23.513	20.593
30.633	24.012
36.534	27.412
43.321	29.512

+25C°

4.829	2.031

+25C°

P	V
5.812	3.941
6.442	3.221
8.693	3.601
11.960	5.453
15.606	7.030
18.294	8.431
22.511	9.670
28.162	12.200
37.231	15.636
53.088	19.897

-150C°

P	V
2.768	33.344
3.509	34.710
5.173	37.099
6.961	39.322
9.006	41.377
10.331	41.910
12.156	42.887
17.384	43.577
27.391	44.981
38.116	45.533
52.517	46.322

Na-mordenite*/ CO_2 Krypton

-150C°

0.012	10.201
0.017	11.351
0.026	13.422
0.049	15.313
0.070	18.501
0.098	20.601
0.181	21.322
0.239	23.211
0.373	24.522
0.548	25.740
0.756	26.423
0.928	27.711
1.127	28.412
1.665	29.630
2.197	31.424

-140C°

0.055	7.610
0.078	8.155
0.118	9.338
0.224	11.501
0.316	13.736
0.444	15.515
0.810	17.727
1.076	20.491
1.487	24.466
2.448	28.883
3.345	30.555
4.099	31.670
4.947	34.131
7.261	37.510
9.572	39.011

-140C°

P	V
12.001	40.483
15.206	41.335
22.375	42.531
29.991	43.101
38.563	43.616
51.731	44.193

-130C°

P	V
0.206	12.113
0.288	14.660
0.436	16.334
0.813	19.450
1.153	20.322
1.614	22.313
2.911	25.717
3.822	28.113
5.274	31.730
8.637	35.808
11.854	37.622
14.578	39.019
17.336	39.445
25.754	40.531
33.370	40.882
41.701	41.133
52.605	41.602

-120C°

P	V
0.543	10.501
0.659	11.341
0.917	12.712
0.995	13.011
1.351	15.773
2.501	21.454
3.595	24.716
4.892	27.610
8.893	31.813
11.643	34.011
15.919	35.476
26.007	37.212
35.680	38.030
43.131	38.939
51.181	39.531

-100C°

P	V
0.155	4.322
0.202	5.892
0.773	8.321
1.554	11.000
3.554	15.266
4.943	18.501
5.632	20.544
9.559	24.632
12.209	26.311
17.455	28.677
32.374	32.491
45.338	34.901
53.853	36.661

-90C°	
P	V
0.532	3.732
0.853	6.322
1.682	10.172
3.157	12.511
4.762	16.517
8.913	22.930
11.997	24.190
14.314	25.055
16.360	26.100
26.230	29.854
36.215	31.153
45.280	33.111
52.686	34.733

-70C°	
1.503	5.011
3.133	12.220
6.341	16.123
9.934	19.532
12.506	20.432
17.544	22.610
25.163	25.491
34.311	28.600
42.515	30.233
52.165	31.988

-40C°	
3.531	7.503
7.607	12.122
12.553	15.010
19.973	18.507
27.533	20.616
37.501	23.500
47.551	24.433
53.122	25.506

0C°	
3.361	2.987
5.681	4.231
7.334	5.983
15.019	10.212
23.543	12.897
30.101	16.301
40.096	20.011
51.781	22.443

+25C°	
7.247	2.108
12.234	3.512
15.760	4.631
21.619	6.080
31.963	8.135
36.339	9.708
49.650	12.443
52.321	13.112

Na-mordenite$^{*}_{11}$/Krypton

-150C°

P	V
0.010	14.200
0.020	15.351
0.029	18.402
0.051	20.323
0.073	25.611
0.121	26.223
0.210	28.112
0.403	29.252
0.578	30.740
0.786	31.243
0.958	32.701
1.157	33.124
1.695	34.360
2.227	36.244
3.539	38.434
5.203	39.710
6.991	42.099
9.036	46.307
10.361	47.410
12.186	47.809
17.414	48.891
27.431	50.125
38.146	51.533
52.547	52.432

-140C°

P	V
0.053	13.106
0.081	14.032
0.148	14.891
0.254	16.801
0.346	19.236
0.474	21.015
0.840	23.301
1.106	26.491
1.517	30.466
2.478	34.313
3.375	36.505
4.129	37.076
4.977	39.891
7.291	43.343
9.602	45.101
11.987	46.438
15.336	47.533
23.475	48.351
29.199	49.100
37.563	49.661
51.813	50.193

-140C°

P	V
0.148	14.891
0.254	16.801
0.346	19.236
0.474	21.015
0.840	23.301
1.106	26.491
1.517	30.466
2.478	34.313
3.375	36.505
4.129	37.076
4.977	39.891
7.291	43.343
9.602	45.101
11.987	46.438
15.336	47.533
23.475	48.351
29.199	49.100
37.563	49.661
51.813	50.193

-130C°

P	V
0.301	18.131
0.388	19.606
0.401	22.344
0.913	25.405
1.513	26.223
1.714	28.133

-130C°		-120C°	
P	V	P	V
2.119	31.717	0.551	16.105
4.822	34.133	0.697	17.341
6.271	37.307	0.971	18.127
8.730	41.818	1.037	19.110
11.548	43.262	2.015	21.377
13.987	45.109	3.796	27.445
18.036	45.545	5.013	29.998
26.054	46.351	8.197	33.106
33.703	46.872	10.771	37.318
40.981	47.132	15.900	39.899
51.056	47.781	25.775	40.876
		34.780	43.122
		42.762	44.011
		52.012	45.451